



12-2001

**Geology of the Scaly Mountain quadrangle, emphasizing the structures, timing and emplacement mechanisms for the Rabun Granodiorites, eastern Blue Ridge, southwestern North Carolina**

Dwight D. Lamb

Follow this and additional works at: [https://trace.tennessee.edu/utk\\_gradthes](https://trace.tennessee.edu/utk_gradthes)

---

**Recommended Citation**

Lamb, Dwight D., "Geology of the Scaly Mountain quadrangle, emphasizing the structures, timing and emplacement mechanisms for the Rabun Granodiorites, eastern Blue Ridge, southwestern North Carolina." Master's Thesis, University of Tennessee, 2001.  
[https://trace.tennessee.edu/utk\\_gradthes/9667](https://trace.tennessee.edu/utk_gradthes/9667)

This Thesis is brought to you for free and open access by the Graduate School at TRACE: Tennessee Research and Creative Exchange. It has been accepted for inclusion in Masters Theses by an authorized administrator of TRACE: Tennessee Research and Creative Exchange. For more information, please contact [trace@utk.edu](mailto:trace@utk.edu).

To the Graduate Council:

I am submitting herewith a thesis written by Dwight D. Lamb entitled "Geology of the Scaly Mountain quadrangle, emphasizing the structures, timing and emplacement mechanisms for the Rabun Granodiorites, eastern Blue Ridge, southwestern North Carolina." I have examined the final electronic copy of this thesis for form and content and recommend that it be accepted in partial fulfillment of the requirements for the degree of Master of Science, with a major in Geology.

Robert D. Hatcher, Major Professor

We have read this thesis and recommend its acceptance:

Hap McSween, Mike Clark

Accepted for the Council:

Carolyn R. Hodges

Vice Provost and Dean of the Graduate School

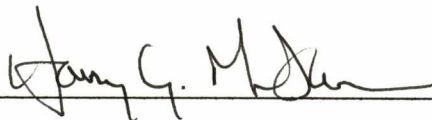
(Original signatures are on file with official student records.)


To the Graduate Council

I am submitting herewith a thesis written by Dwight D. Lamb entitled "Geology of the Scaly Mountain quadrangle, emphasizing the structures, timing, and emplacement mechanisms for the Rabun granodiorite, eastern Blue Ridge, southwestern North Carolina." I have examined the final copy of this thesis for form and content and recommend that it be accepted in partial fulfillment of the requirements for the degree of Master of Science, with a major in Geology.

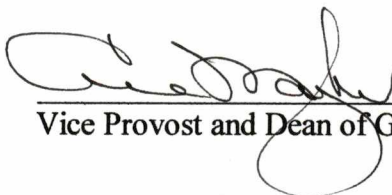
  
Robert D. Hatcher, Major Professor

We have read this thesis  
and recommend its acceptance:

  
\_\_\_\_\_

  
\_\_\_\_\_

Accepted for the Council:

  
Vice Provost and Dean of Graduate Studies

**GEOLOGY OF THE SCALY MOUNTAIN QUADRANGLE,  
EMPHASIZING THE STRUCTURES, TIMING AND  
EMPLACEMENT MECHANISMS FOR THE RABUN  
GRANODIORITE, EASTERN BLUE RIDGE, SOUTHWESTERN  
NORTH CAROLINA**

A Thesis  
Presented for the  
Master of Science  
Degree  
The University of Tennessee, Knoxville

Dwight D. Lamb  
December, 2001

*This thesis is dedicated to the memory of my father,  
William R. Lamb*

## ACKNOWLEDGEMENTS

I would first like to thank my advisor, Dr. Robert D. Hatcher, Jr., whose patience and direction has helped throughout this endeavor. I also wish to thank Dr. Hatcher for allowing me to return to school under his tutelage to finish my thesis after so many years away. Along this same line I feel that I should extend my thanks to Dr. Bill Dunne and the members of the Graduate Committee for supporting my return to the university. My other committee members, Drs. Hap McSween and Mike Clark, have provided a generous amount of time, assistance, and guidance. I have also benefited from the insights and help of present and past members of the North and South Carolina Geological Surveys: Leonard Weiner and Carl Merschat. Funding for my work at UT was provided by the Science Alliance Center of Excellence Distinguished Scientist stipend.

The many geologists at the IT Corporation who have stopped me in the hallway to ask how my thesis is coming along and just showing interest in what I am doing. I would also like to thank my supervisors, Bill Hedberg, Mark Maki, Scott Logan, and Belinda Price for helping me obtain funding to return to school. I would like to thank IT Corporation for the funding that allowed me to return to school.

The "Hatchery" group, past and present, deserve a thank you. Steve Martin, Don Geddes, Mark Carter were all there when I started many years ago and provided me with excellent advice and opinions on geology and mapping. Camillo Montes and Doug Curl who came into the "Hatchery" after I for helping me with various classes and computer programs. Brendan Bream and Dave Settles who have willingly helped me with advice and their time while working with computerized mapping. They have patiently listened to me complain and have on occasion explained the same process more than once. Marvin Bennett, has always been willing to help and offer friendly advice. Most importantly, Nancy Meadows deserves my utmost gratitude for reading every draft of my thesis, providing fresh coffee and candy, and listening to my problems whether those problems were occurring at school or work.

Each member of my family and all of my friends also need to be thanked. My father and mother in particular demonstrated an unsurpassed devotion, love, and strength. It was my father's last wish that I

finish my studies and that has been my driving force to finish. I would also like to thank everyone (staff, students, and faculty, past and present) in the UT Geology Department who have made my stay here unforgettable and enjoyable.

My final thank you, and most important one, is to my loving and beautiful wife Jennifer and my wonderful daughter Alex, who have put up with my sleep deprivation, grouchy moods, and lack of patience at times. None of this would have been possible without their understanding and support. They have stood by me even when I thought this was an impossible task.

## ABSTRACT

This thesis examines the geology of the Scaly Mountain quadrangle in the eastern Blue Ridge of southwestern North Carolina. Particular emphasis was placed on determining the structures, timing, and emplacement mechanisms of the Rabun granodiorite pluton. The Scaly Mountain quadrangle was mapped in detail (1:12,000 scale). The mapping effort included collection of structural data from 1,333 data stations using a Brunton compass. Particular attention was paid to structural measurements that were taken within the Rabun pluton, including measurements of what are interpreted to be both magmatic flow foliations and tectonic foliations (two distinct foliations); folds, and the orientations of the folds and other linear structures; faults along the edge of the pluton in some areas; fractures; contacts with the surrounding country rock; and crosscutting dikes in the area. After the mapping was completed, the structural data were compiled at 1:24,000 scale and analyzed to determine deformation events, average orientations of folds and other linear structures, interrelationships of the tectonic units, and, perhaps most importantly for this study, different fabric relationships that will provide clues about the emplacement history of the Rabun granodiorite. Conclusions drawn from this study are: (1) The Scaly Mountain quadrangle contains three tectonic units: the Chattahoochee thrust sheet, the Dahlonega gold belt, and the Shope Fork thrust sheet. (2) The rocks present in the Scaly Mountain quadrangle are: the Tallulah Falls Formation (graywacke-schist member), the Rabun granodiorite, the Otto Formation, the Coweeta Group (Coleman River Formation), calc-silicate rocks, amphibolites, and pegmatites. In addition there are surficial deposits of colluvium, alluvium, and ancient landslides. (3) There are six to seven deformation events represented in the rocks in the Scaly Mountain quadrangle. (4) Evidence for multiple deformation events can be seen along the trace of the Chattahoochee fault. The fault deforms the Rabun granodiorite, truncates structures in the surrounding country rock, and is itself folded. Evidence for multiple deformation events can also be seen in the surrounding country rock. There is an early foliation that is preserved in boudins. There are at least two generations of folding as well. (5) The Chattahoochee fault postdates the Rabun granodiorite. Evidence for this is the truncation of the Rabun pluton by the Chattahoochee fault. (6) The Rabun granodiorite consists of a medium-grained phase and a megacrystic



phase. (7) The Rabun granodiorite contains a magmatic flow foliation and an overprinting tectonic foliation. (8) The Rabun granodiorite was emplaced by a combination of mechanisms either operating together or at different times during the pluton emplacement. These are: stoping, diapirism, outward displacement of the Earth's surface, the principle of effective stress, and dike-feeding of the pluton.

## TABLE OF CONTENTS

CHAPTER	PAGE
1. INTRODUCTION .....	1
Previous Work.....	5
Methodology.....	9
2. REGIONAL GEOLOGIC AND TECTONIC SETTING .....	10
Stratigraphic Succession .....	10
Rock Units.....	10
Chattahoochee Thrust Sheet.....	10
Tallulah Falls Formation .....	10
Dahlongega Gold Belt.....	17
Otto Formation.....	17
Soque River Thrust Sheet.....	17
Coweeta Group.....	17
Rabun Granodiorite.....	21
Pegmatite Bodies.....	27
Calc-Silicate Bodies .....	27
Amphibolite.....	27
Quaternary Deposits.....	28
3. STRUCTURES WITHIN THE SCALY MOUNTAIN QUADRANGLE .....	29
Mesoscopic Structures .....	29
Map Scale Structures.....	30
Tectonic Boundaries .....	36
Chattahoochee Fault.....	37
Shope Fork Fault.....	38
Soque River Fault.....	38
Metamorphism .....	39
Geomorphic Expression of the Rabun Granodiorite.....	40
4. THE RABUN GRANODIORITE.....	42
Geology of the Rabun Granodiorite.....	42
Magmatic Flow Structures Versus Tectonic Structures.....	42
Contacts of the Rabun Granodiorite with the Surrounding Country Rock .....	44
Relationship of the Rabun Granodiorite with Surrounding Country Rock.....	44
Description and Possible Relationship of the Pluton Facies .....	45
Chemistry of the Rabun Granodiorite.....	45
Timing and Possible Modes of Emplacement of the Rabun Granodiorite.....	49
Emplacement of the Pluton along the Chattahoochee Fault .....	51
Stooping .....	51
Diapirism.....	51
Outward Displacement of the Earth's Surface .....	52
Principle of Effective Stress.....	52
Dike-Feeding of the Pluton.....	52
5. CONCLUSIONS .....	54
REFERENCES CITED.....	56
APPENDICES.....	61
APPENDIX A. STRUCTURAL DATA FROM THE SCALY MOUNTAIN QUADRANGLE.....	62
VITA.....	86

## LIST OF TABLES

<b>TABLE</b>	<b>PAGE</b>
1. Summary of Rock Units, Rock Types, and Tectonic Affinities, Scaly Mountain Quadrangle, southwestern North Carolina .....	6
2. Tectonic Boundaries of the eastern Blue Ridge Province.....	7
3. Modal Analyses, Scaly Mountain Quadrangle, North Carolina .....	16
4. Elemental and Isotopic Data for Representative Samples from the Rabun Granodiorite .....	47
5. Pluton Emplacement Mechanisms Proposed by Others .....	50

## LIST OF FIGURES

FIGURE	PAGE
1. Location of the Scaly Mountain 7.5 minute quadrangle in western North Carolina .....	2
2. Geology of a portion of the western and eastern Blue Ridge in Georgia, North Carolina, and South Carolina .....	3
3. Major boundaries and thrust sheets occurring in the Scaly Mountain 7.5minute quadrangle, North Carolina.....	11
4. Photograph of a typical outcrop of biotite gneiss and schist in the Tallulah Falls Formation containing ptygmatic folds of quartz-feldspar veins, at the Cat Stairs on Highway 106.....	13
5. Photograph of a typical outcrop of Tallulah Falls Formation from along Highway 64 near Cullasaja Falls.....	13
6. Photomicrograph of Tallulah Falls Formation biotite gneiss from near Scaly Mountain .....	14
7. Photomicrograph of amphibolite occurring within the Tallulah Falls Formation from near the Cat Stairs on Highway 106.....	14
8. Photomicrograph of calc-silicate quartzite occurring within the Tallulah Falls Formation.....	15
9. Photograph of a typical outcrop of Otto Formation graywacke and pelitic schist.....	18
10. Photograph of a typical outcrop of Otto Formation schist from Sill Vinson's rock near Otto, North Carolina .....	19
11. Photomicrograph of garnetiferous muscovite-biotite schist from the Otto Formation .....	20
12. Photomicrograph of muscovite-biotite schist interlayered with metasandstone from the Otto Formation .....	20
13. Photograph of the megacrystic phase of the Rabun granodiorite showing feldspar alignment and weak tectonic overprinting.....	22
14. Photograph of the megacrystic phase of the Rabun granodiorite showing feldspar alignment and tectonic overprinting.....	22
15. Photograph of the megacrystic phase of the Rabun granodiorite showing feldspar alignment and weak tectonic overprinting.....	23
16. Photomicrograph of the megacrystic phase of the Rabun granodiorite .....	24
17. Photomicrograph of the megacrystic phase of the Rabun granodiorite .....	24
18. Photomicrograph of the equigranular phase of the Rabun granodiorite.....	25
19. Photomicrograph of a calc-silicate quartzite from the Rabun granodiorite.....	26
20. Scatter plot and fabric diagrams for all foliation measurements obtained in the study area .....	31
21. Scatter plot and fabric diagrams for foliation measurements obtained in the study area from the Otto Formation.....	32
22. Scatter plot and fabric diagrams for foliation measurements obtained from the Tallulah Falls Formation in the study area .....	33
23. Scatter plot and fabric diagrams for foliation measurements obtained in the Rabun granodiorite in the study area.....	34
24. Scatter plot and fabric diagrams for lineation measurements obtained in the Rabun granodiorite in the study area.....	35

## LIST OF PLATES

<u>PLATE</u>	<u>PAGE</u>
I. Geologic map and cross sections, Scaly Mountain 7.5' quadrangle, North Carolina .....	in pocket
II. Station map of the Scaly Mountain 7.5' quadrangle, North Carolina.....	in pocket
III. Quaternary surficial deposit map, Scaly Mountain 7.5' quadrangle, North Carolina .....	in pocket

## CHAPTER 1

### Introduction

The geology of the southern Appalachian eastern Blue Ridge is complex and varied. It consists primarily of polydeformed metamorphic and igneous rocks. Perhaps the most challenging part of unraveling the geologic history of the eastern Blue Ridge is in trying to determine the timing and emplacement history of the various plutons that occur within this province. Diapirism, ballooning, emplacement along faults, stoping, and magma fracturing are a few examples of emplacement mechanisms that have been proposed to explain emplacement of granitic plutons.

The primary focus of this research is the Rabun granodiorite, located in the hanging wall of the Chattahoochee thrust sheet in southwestern North Carolina and northeastern Georgia (Fig. 1). The primary study area is the Scaly Mountain quadrangle located in the eastern Blue Ridge of southwestern North Carolina (Fig. 2). Rock units that exist within the study area are the Rabun granodiorite, the Otto Formation, the Tallulah Falls Formation, and the Coweeta Group. The Otto Formation is a sequence of quartz-rich, two-mica (muscovite and biotite), feldspathic metasandstone interlayered with aluminous schist. The Tallulah Falls Formation in the study area consists entirely of the upper member, a migmatitic metagraywacke and muscovite-biotite schist. The Rabun granodiorite is best described as a coarse-grained, megacrystic, microcline-plagioclase granitoid, but also contains mappable fine-grained leucocratic granitic gneiss (Hopson et al., 1989; Miller et al., 1997). While only a portion of the Rabun granodiorite occurs within the boundaries of the Scaly Mountain quadrangle, data from several other mapped quadrangles were incorporated into the analysis. The Coweeta Group rocks in the study

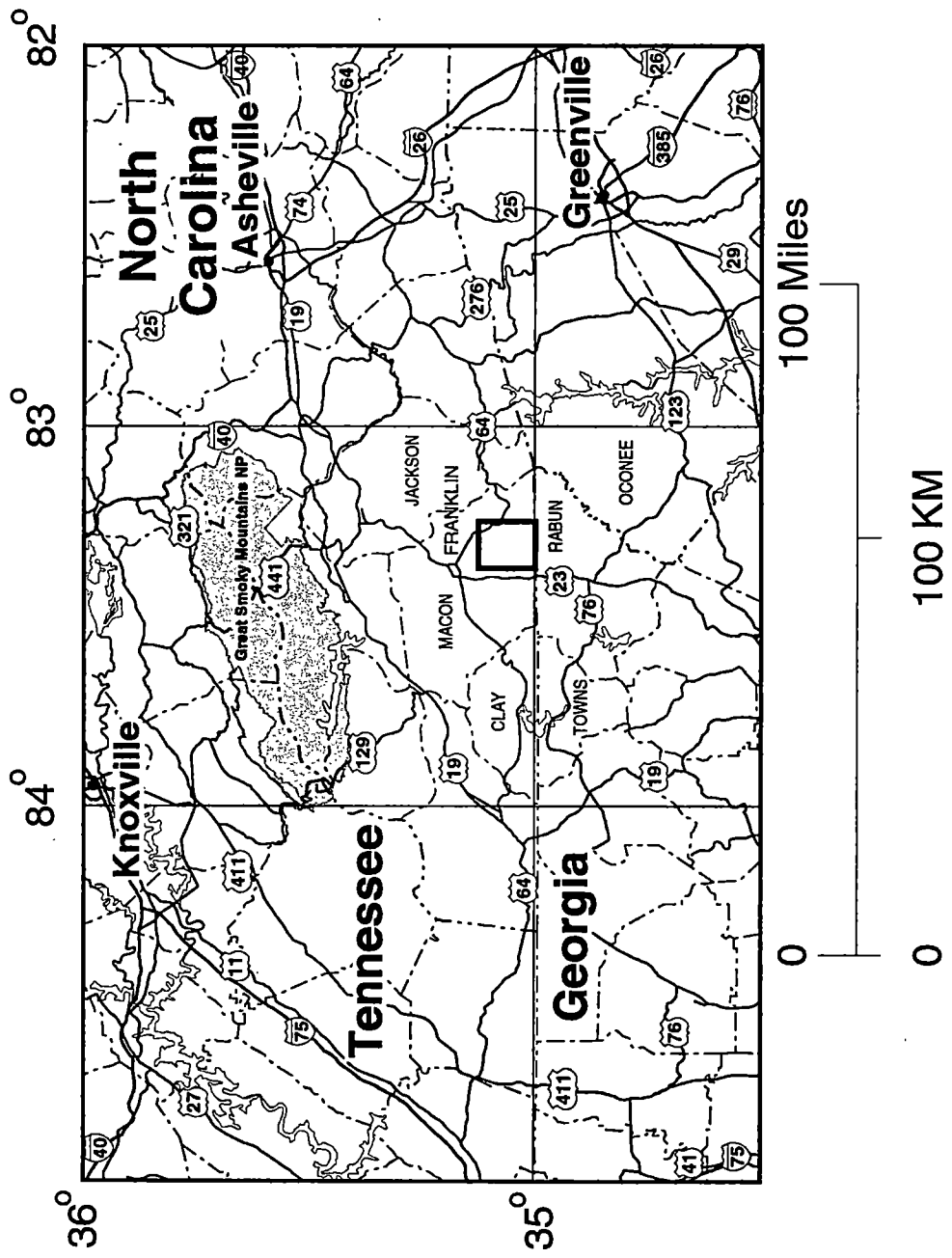
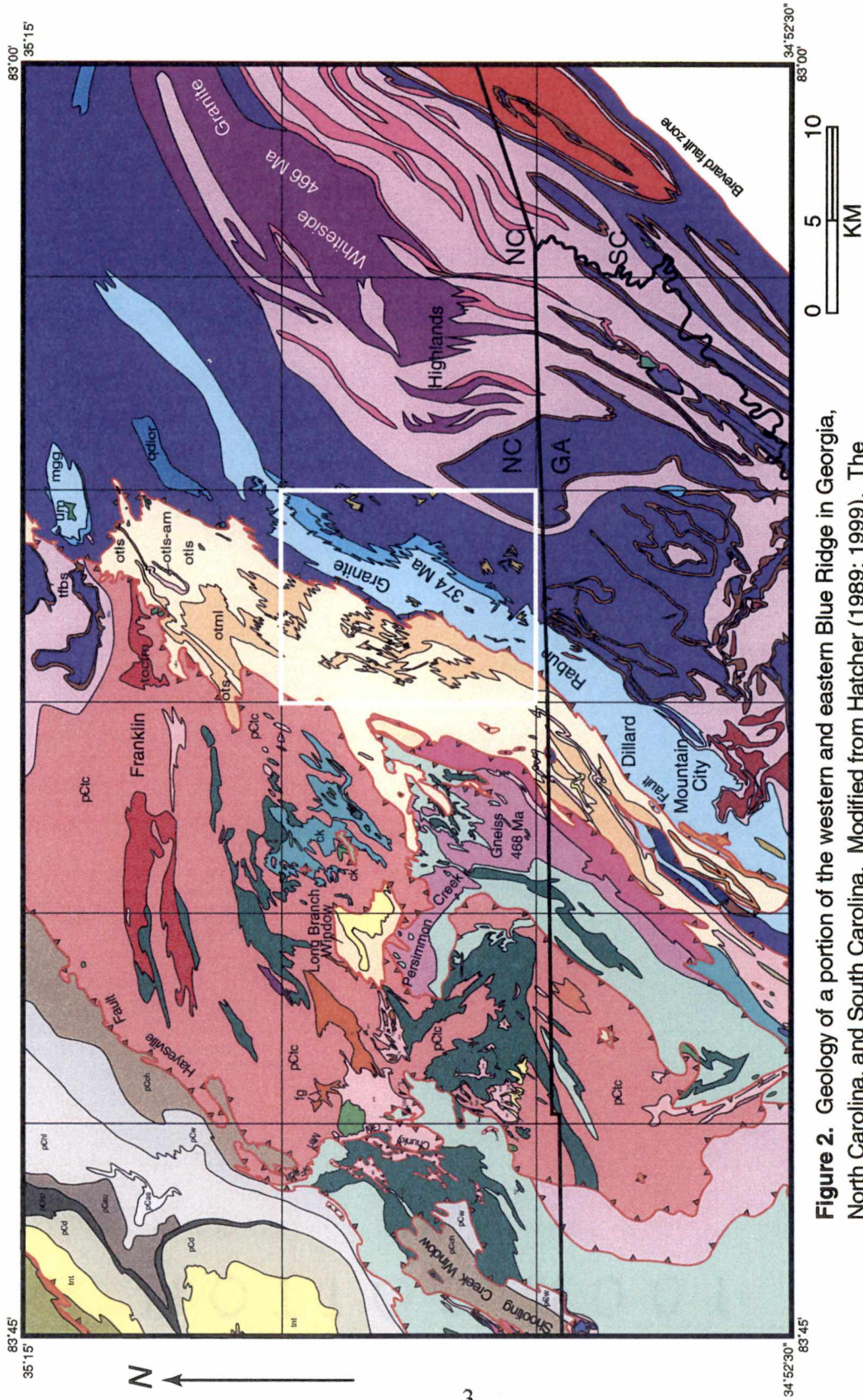


Figure 1. Location of the Scaly Mountain 7.5-minute quadrangle in western North Carolina.







**Figure 2.** Geology of a portion of the western and eastern Blue Ridge in Georgia, North Carolina, and South Carolina. Modified from Hatcher (1989; 1999). The Scaly Mountain quadrangle is outlined by the white box.



Mesozoic diabase


### Soque River-Hayesville Thrust Sheet

#### Coweeta Group

-  Ridgepole Mountain Formation
-  Coleman River Formation
-  Upper Persimmon Creek Gneiss (quartz diorite + metasandstone)
-  Lower Persimmon Creek Gneiss (quartz diorite, 468 Ma Pb/U)

### Western Blue Ridge

#### Great Smoky Group



-  Great Smoky (Undivided)
-  Dean Formation
-  Ammons Formation
-  Wehatty Formation
-  Copperhill Formation

#### Murphy Belt

-  Mineral Bluff Formation
-  Murphy Marble & Andrews Fm.
-  Brassstown Formation
-  Nantahala/Tusquittee Fm.

### Shope Fork-Chunky Gal Mountain Thrust Sheet



#### Coweeta Group

-  Ridgepole Mountain Formation
-  Coleman River Formation

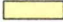

#### Coweeta Group-Tallulah Falls Formation, undivided

-  Metasandstone, pelitic schist




#### Basement (?) Orthogneisses

-  Intermediate to anorthositic orthogneiss
-  Foliated massive felsic orthogneiss

#### Long Branch Window





-  Muscovite Quartzite
-  Metasandstone (Otto Formation?)

#### Plutonic and Metavolcanic Rocks

-  Amphibolite
-  Ultramafic bodies
-  Metagabbro

### Dahlonaga Gold Belt





#### Otto Formation

-  Otto Formation, metasandstone & two-mica schist
-  Otto Formation, two-mica schist & metasandstone
-  Calcsilicate quartzite
-  Aluminous schist

#### Basement (?)


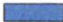





-  Augen gneiss (altered)

#### Lake Burton Mafic-Ultramafic Complex & Related Rocks






-  Amphibolite
-  Metagabbro + amphibolite
-  Felsic tuff
-  Ultramafic rocks

### Chattahoochee Thrust Sheet

#### Plutonic Rocks

-  Rabun Granodiorite (374 Ma Pb/U)  
Light blue-megacrystic phase; medium blue-fine-grained phase
-  Looking Glass Granite (380 Ma Pb/U)
-  Pink Beds Granite (383 Ma Pb/U)
-  Whiteside Granite (Quartz diorite; 466 Ma Pb/U)
-  Quartz diorite, age unknown
-  Pegmatite
-  Calcsilicate quartzite

#### Tallulah Falls Formation

-  Tallulah Falls Quartzite
-  Upper Tallulah Falls Formation  
Metagraywacke (migmatitic) & pelitic schist member
-  Tallulah Falls Formation  
Aluminous schist (sillimanite- or kyanite-bearing) member
-  Lower Tallulah Falls Formation  
(Migmatitic metagraywacke, schist, and amphibolite) member
-  Migmatite
-  Amphibolite
-  Ultramafic bodies

#### Basement Rocks

-  Sutton Creek & Wolf Creek Gneisses (1.103 Ga Rb/Sr)
-  Wiley Gneiss (1.169 Ga Rb/Sr)
-  Toxaway Gneiss (~1.2 Ga)

Figure 2. cont.

area are primarily metasandstones. Table 1 consists of a summary of the various rock units and Table 2 summarizes the tectonic boundaries.

The purpose of the study is to determine the emplacement history of the mapped portions of the Rabun granodiorite in North Carolina and Georgia. With this in mind, the primary objectives of this study were to collect structural and lithologic data needed to construct a detailed geologic map of the Scaly Mountain quadrangle in southwestern North Carolina. These data have been employed to attempt to determine the timing and emplacement mechanism of the Rabun granodiorite, present structural data to separate magmatic flow structures from tectonic structures within the pluton, explain the relationships of the Rabun granodiorite to the surrounding country rock, and employ published geochemical data to further constrain the emplacement history of the Rabun granodiorite.

Using the U-Pb ion microprobe technique, the Rabun granodiorite has been dated at 375 Ma (Miller et al., 2000), which would make it one of the younger granitic plutons in the eastern Blue Ridge. The Rabun is one of a series of Acadian plutons; the Pink Beds (390 Ma) and Looking Glass plutons (380 Ma) are other plutons occurring nearby in the eastern Blue Ridge that are approximately the same age (Miller et al., 2000).

### **Previous Work**

There have been several studies conducted near the Scaly Mountain quadrangle in the eastern Blue Ridge. The adjacent Prentiss quadrangle (Hatcher, 1980) to the west and the Rabun Bald and Dillard quadrangles (Acker and Hatcher, unpublished) to the south and southwest have also been mapped in detail. The Corbin Knob and Franklin

Table 1

Summary of Rock Units, Rock Types, and Tectonic Affinities,  
Scully Mountain Quadrangle, southwestern North Carolina

Unit Name	Rock Type(s)	Thrust Sheet	Associated (minor) Rock Type(s)
Tallulah Falls Formation	Migmatitic graywacke and muscovite-biotite schist.	Chattahoochee	Amphibolites, pegmatites, some calc-silicates
Otto Formation	Metasandstones and muscovite-biotite schist.	Great Smoky	Altered basement
Coweeta Group (Coleman River Formation)	Metasandstone.	Shope Fork	
Rabun Granodiorite	Coarse-grained, megacrystic, microcline-plagioclase granodiorite that also contains a fine-grained, leucocratic granitic gneiss.	Chattahoochee	Calc-silicates (enclaves), some pegmatites

Table 2

Tectonic Boundaries of the eastern Blue Ridge Province

Fault	Bounds
Hayesville	Western Blue Ridge from the eastern Blue Ridge
Brevard Fault Zone	Eastern Blue Ridge from the Inner Piedmont
Chattahoochee	Dahlonega gold belt from Tallulah Falls Formation
Soque River	Dahlonega gold belt from Hayesville thrust sheet
Shope Fork	Coweeta Group from amphibolite-rich biotite gneisses and schists to the northwest

quadrangles (Eckert and Yurkovich, unpublished), the Hightower and Lake Burton quadrangles (Hopson, unpublished) and a portion of the Tallulah Falls dome (Stieve, unpublished) have been mapped in detail also. Speer et al. (1994) described emplacement mechanisms of some plutons in the southern Appalachians. Hatcher (1971, 1974, 1976, 1978, 1989) and Hatcher and Goldberg (1991) have conducted numerous geological investigations in the southern Appalachians, particularly in the eastern Blue Ridge (Hatcher, 1971, 1974, 1976, 1978, 1979, 1989). Teague and Furcron (1948) described the geology of part of northern Georgia (particularly Rabun and Habersham Counties) and produced a geologic map of the area. Fullagar et al. (1979) dated the Toxaway and basement gneisses in the Blue Ridge in North Carolina. Fullagar et al. (1997) performed Nd and Sr characterization of some crystalline rocks from the Blue Ridge of North Carolina. They concluded that the plutonic rocks of the western Blue Ridge are recycled Laurentian Middle Proterozoic crust with no evidence of a juvenile Late Proterozoic source component. They also indicated that all lithotectonic belts east of the western Blue Ridge appear to contain one or more crustal components derived from a non-Laurentian terrane. Miller et al. (1990; 1997; 2000) conducted geochemical analyses and age dating of the Rabun granodiorite and other plutons in the area. They concluded that there were two distinct ages of magmatism during which all of the plutons were intruded. The first age group is ~ 370 to 395 Ma and were emplaced during the Acadian orogeny. The Rabun granodiorite was emplaced during this time frame. The second age group is ~ 465 to 480 Ma and were emplaced during the Taconian orogeny.

Paterson et al. (1989) presented techniques and criteria for the differentiation of tectonic and magmatic flow foliations in plutonic rocks. Paterson and Fowler (1993) also

presented explanations for pluton emplacement mechanisms. Fernandez et al. (1997), Hutton (1997), John and Stunitz (1997), and Ramsay (1989), are a few of the numerous other researchers who have studied and provided data for mechanisms of pluton emplacement from around the world. All of this previous work has been helpful in gaining insight on the history of the Rabun granodiorite.

### **Methodology**

The Scaly Mountain quadrangle has been mapped in detail (1:12,000 scale) in the field. A geologic map was produced for the Scaly Mountain quadrangle from these data (Plate 1). The folding depicted at depth on the cross sections is projected down dip from surface folding and assumes that the folding at depth is not disharmonic. All plates are located in the map pocket. The mapping effort included collection of structural data from 1,333 data stations (Plate 2) using a Brunton compass. Particular attention was paid to structural measurements that were taken within the Rabun pluton, including measurements of what are interpreted to be both magmatic flow foliations and tectonic foliations (two distinct foliations); folds, and the orientations of the folds and other linear structures; faults along the edge of the pluton in some areas; fractures; contacts with the surrounding country rock; and crosscutting dikes in the area. After the mapping was completed, the structural data were compiled at 1:24,000 scale and analyzed to determine deformation events, average orientations of folds and other linear structures, interrelationships of the tectonic units, and, perhaps most importantly for this study, different fabric relationships that will provide clues about the emplacement history of the Rabun granodiorite.

## CHAPTER 2

### Regional Geologic and Tectonic Setting

The Scaly Mountain quadrangle rock units are polydeformed on all scales (Plate 1). Two major faults were traced across the quadrangle. The Chattahoochee fault separates the Tallulah Falls Formation and the Rabun granodiorite from the Otto Formation; and the Soque River fault separates the Otto Formation from the Coweeta Group (Fig. 3 and Plate 1).

### Stratigraphic Succession

The oldest rocks in the study area are the Tallulah Falls and Otto Formations; they are thought to be approximately the same age (Hopson et al., 1989; Hatcher and Goldberg 1991). The Coweeta Group rocks in the northwest corner of the area may be slightly younger (Hopson et al., 1989; Hatcher and Goldberg 1991). The calc-silicate bodies in the study area are most likely part of the Tallulah Falls Formation. Since they are primarily contained as enclaves within the Rabun granodiorite pluton, they are older than the pluton and probably were derived from the Tallulah Falls Formation. The Rabun granodiorite is the next youngest rock unit in the study area. The youngest rocks in the study area are the pegmatite dikes that crosscut most of the other rock units and are relatively undeformed.

### *Rock Units*

#### *Chattahoochee Thrust Sheet*

*Tallulah Falls Formation.* The Tallulah Falls Formation consists of a series of kyanite to sillimanite grade biotite paragneiss (metagraywacke), feldspathic quartzite, pelitic schist,

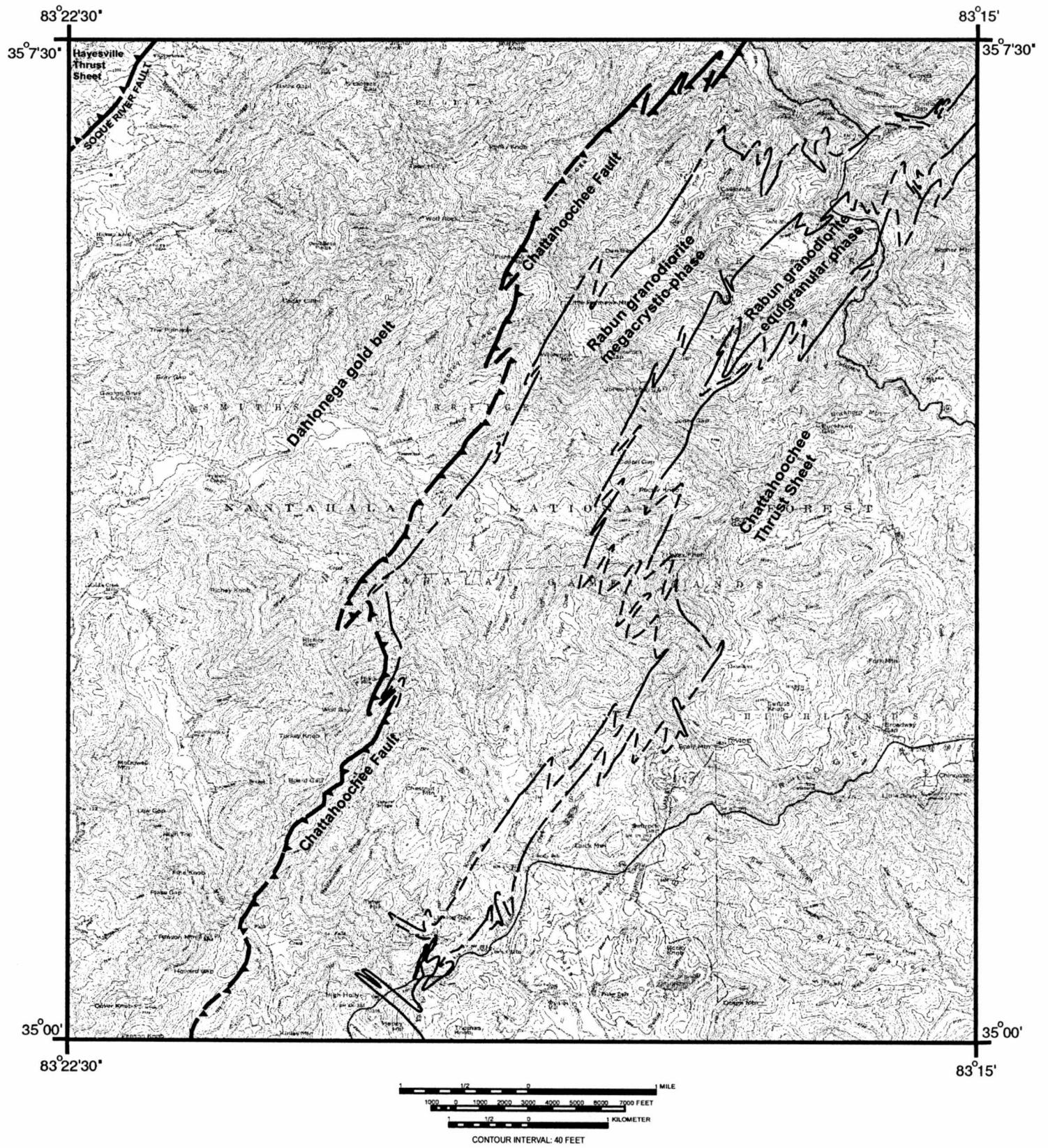


Figure 3. Major boundaries and thrust sheets occurring in the Scaly Mountain 7.5' quadrangle, North Carolina.



calc-silicate, and subordinate amphibolite (Hopson et al., 1989). Hatcher (1971) defined four members of the Tallulah Falls Formation: 1) Quartzite-schist member; 2) Graywacke-schist member; 3) Garnet-aluminous schist member; and 4) Graywacke-schist-amphibolite member. In the Scaly Mountain quadrangle the Tallulah Falls Formation is represented by biotite gneiss and metagraywacke that belong to the graywacke-schist member. Sillimanite-bearing aluminous schist occurs just to the south on the Rabun Bald quadrangle (Acker and Hatcher, Unpublished map). Typical exposures are shown in Figures 4 and 5. There are also some small amphibolite and calc-silicate bodies present within the Tallulah Falls Formation. The composition of the Tallulah Falls Formation rocks are quartz-plagioclase ( $An_{0-10}$ )-biotite-muscovite with minor microcline, garnet, epidote/clinozoisite, sphene, zircon, and opaque minerals (Fig. 6). Table 3 presents modal analyses for biotite gneiss samples taken from the Tallulah Falls Formation. Plagioclase composition was determined for all rocks by a combination of the Michel-Levy technique and by obtaining the optic sign of untwinned plagioclase crystals.

The major components of the Tallulah Falls amphibolites are hornblende-plagioclase ( $An_{10-20}$ )-quartz-biotite with minor garnet, sphene, epidote/clinozoisite, zircon, and opaques. Another mineral assemblage is hornblende-plagioclase ( $An_{10-20}$ )-quartz with minor constituents of garnet, calcite, epidote/clinozoisite, sphene, and opaques (Fig. 7). Table 3 presents modal analyses for amphibolites from the area.

The calc-silicates in the area are primarily epidote/clinozoisite-hornblende-quartz-calcite with minor amounts of plagioclase ( $An_{10-20}$ ), sphene, garnet, and opaques (Fig. 8). Table 3 presents modal analyses for calc-silicate rocks collected within the Scaly



Figure 4. Photograph of a typical outcrop of biotite gneiss and schist in the Tallulah Falls Formation containing pygmatic folds of quartz-feldspar veins, at the Cat Stairs on Highway 106.



Figure 5. Photograph of a typical outcrop of the Tallulah Falls Formation from along Highway 64 near Cullasaja Falls.

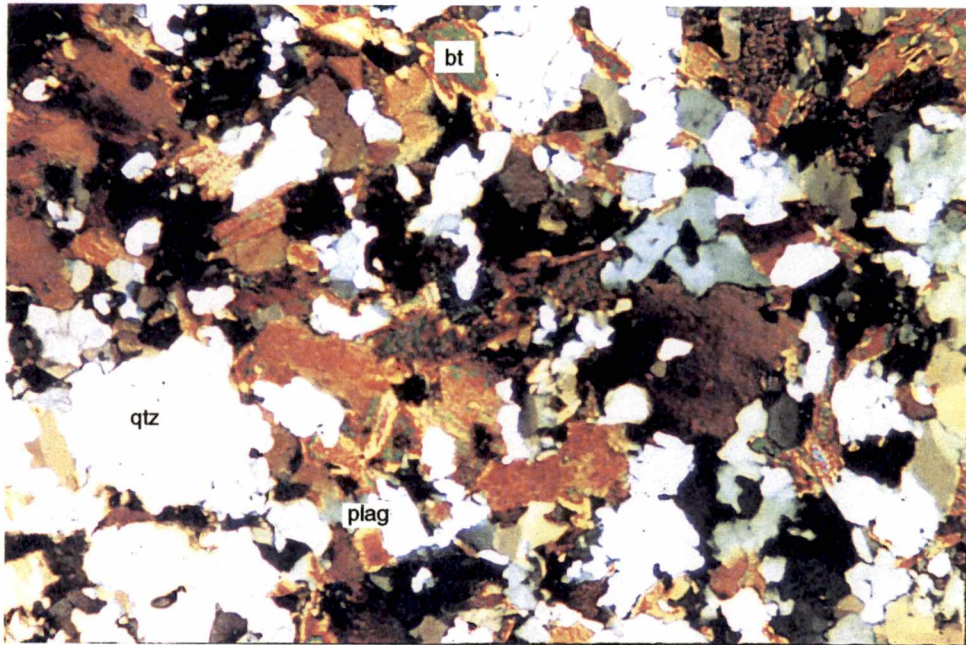


Figure 6. Photomicrograph of Tallulah Falls Formation biotite gneiss from near Scaly Mountain. Field of view is 4.25 mm. bt-biotite, qtz-quartz, plag-plagioclase.

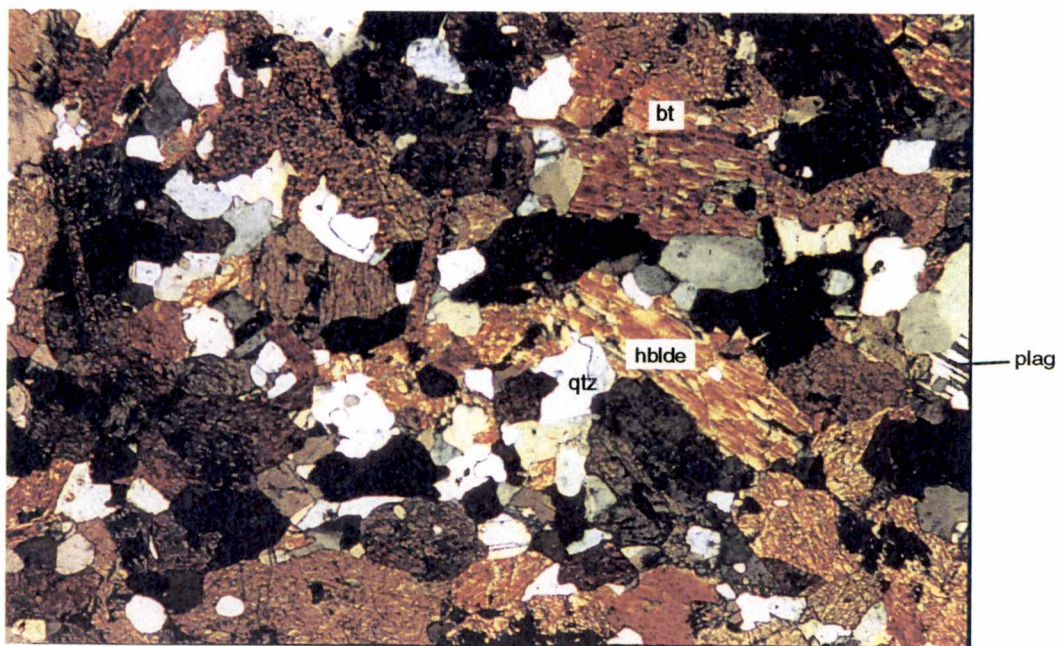


Figure 7. Photomicrograph of amphibolite occurring within the Tallulah Falls Formation from near the Cat Stairs on Highway 106. Field of view is 4.25 mm. bt-biotite, qtz-quartz, plag-plagioclase, hbldc-hornblende.

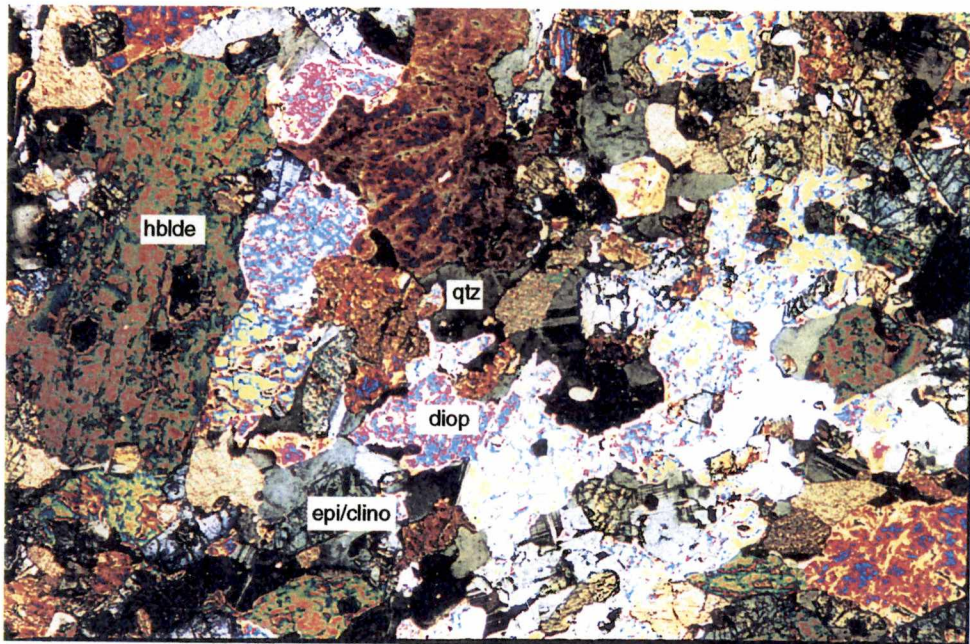


Figure 8. Photomicrograph of calc-silicate quartzite occurring within the Tallulah Falls Formation. Field of view is 4.25 mm. qtz-quartz, hblde-hornblende, diop-diopside, epi/clino-epidote/clinozoisite.

Table 3  
 Modal Analyses  
 Scaly Mountain Quadrangle  
 North Carolina

Mineral	Tallulah Falls Formation		Otto Formation		Rabun Granodiorite		Amphibolites		Calc-Silicates		
	SM1 1015 Points	SM11 1029 Points	SM81 1009 Points	SM248 1031 Points	Q6A 1061 Points	Q8B 1035 Points	SM19 (Medium-grained) 1019 Points	SM142 1024 Points	SM259 1011 Points	SM217 1007 Points	SM316 1017 Points
Quartz	27.3	30.5	2.2	37.5	22.4	15.6	29.7	14.6	15.1	19.7	23.0
Plagioclase	25.5	28.4	1.1	11.8	31.0	33	32.1	23.1	18.4	5.0	4.1
Microcline	14.3	2.1	0.4	11.6	28.5	29.5	23.6				10.0
Muscovite	10.9	4.9	42.9	15.4	5.1	6.1	9.4				
Biotite	18.1	30.5	20.5	23.6	8.8	13.4	3.9	13.9			
Garnet	2.7		12.7	Trace	Trace	Trace	Trace	2.4	2.2	0.5	1.4
Zircon		0.3	Trace	Trace	2.0	2.1	Trace	0.4			
Calcite		1.7	7.3	Trace	Trace	Trace	Trace		Trace	17.6	10.5
Epidote/Clinozoisite		1.1			Trace	Trace	Trace	1.0	3.9	31.6	24.7
Sphene			10.1					1.3	1.4	1.9	3.9
Staurolite			0.8								
Tourmaline			Trace								
Chlorite											
Hornblende								42.7	58.1	10.2	20.3
Dioptside											
Kyanite											
Opagues	Trace	0.5	1.8	Trace	Trace	Trace	1.0	0.6	0.8	0.5	2.1
Total	99.8	100.0	99.8	99.9	99.8	99.7	99.7	100.0	99.9	100.0	100.0

Mountain quadrangle. Tallulah Falls schist in the study area are composed of muscovite-biotite-quartz±plagioclase-opaque minerals.

### *Dahlonge Gold Belt*

*Otto Formation.* The Otto Formation is a sequence of quartz-rich, two-mica, feldspathic metasandstone interlayered with aluminous schist (Hatcher, 1979; 1980). In the Scaly Mountain quadrangle the Otto Formation is divided into two separate mappable units: a metasandstone unit and a schist unit (Plate 1). Photographs of typical metasandstone is presented in Figure 9 and of typical schist is presented in Figure 10. The metasandstone unit occurs primarily adjacent to the Chattahoochee fault and makes up approximately 50 percent of the mappable Otto Formation. The metasandstone is composed of quartz-biotite-muscovite-plagioclase (An<sub>0-10</sub>)-microcline with minor garnet, zircon, and opaques. The schist unit has major constituents of muscovite-biotite-quartz-garnet-staurolite with minor plagioclase (An<sub>0-10</sub>), epidote/clinozoisite, kyanite, tourmaline, zircon, microcline, chlorite (retrograde) and opaques. Photomicrographs of the Otto Formation muscovite-biotite schist and schist interlayered with metagraywacke are presented in Figures 11 and 12. Table 3 presents modal analyses of samples from the Otto Formation.

### *Soque River Thrust Sheet*

*Coweeta Group.* The Coweeta Group consists of three formations; 1) Persimmon Creek Gneiss; 2) Coleman River Formation; and 3) Ridgepole Mountain Formation (Hatcher, 1979). In the study area the Coweeta Group occurs in the extreme northwest corner and consists of soils derived from high-grade metasandstone that probably belongs to the



Figure 9. Photograph of a typical outcrop of the Otto Formation graywacke and pelitic schist. Photo from Sill Vinson's Rock in the Prentiss quadrangle near Otto, North Carolina. Photo by Robert D. Hatcher Jr. Knife is approximately 10 cm long.



Figure 10. Photograph of a typical outcrop of the Otto Formation schist from Sill Vinson's Rock near Otto, North Carolina. Coin is a U.S. quarter. Crenulation axial surfaces dip southeast. Photo by Robert D. Hatcher Jr.



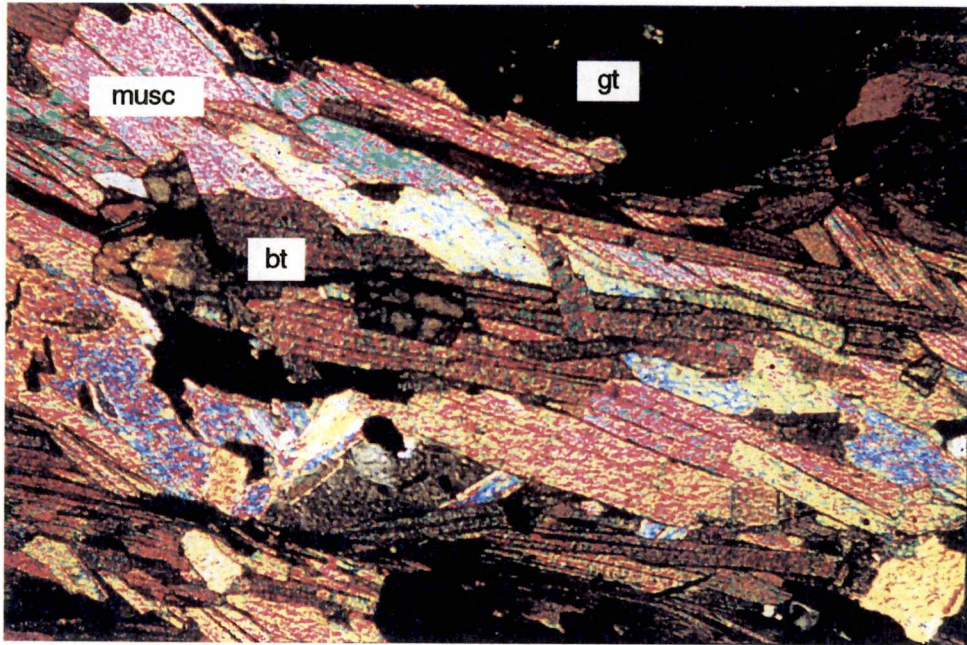


Figure 11. Photomicrograph of garnetiferous muscovite-biotite schist from the Otto Formation. Field of view is 4.25 mm. bt-biotite, musc-muscovite, gt-garnet.

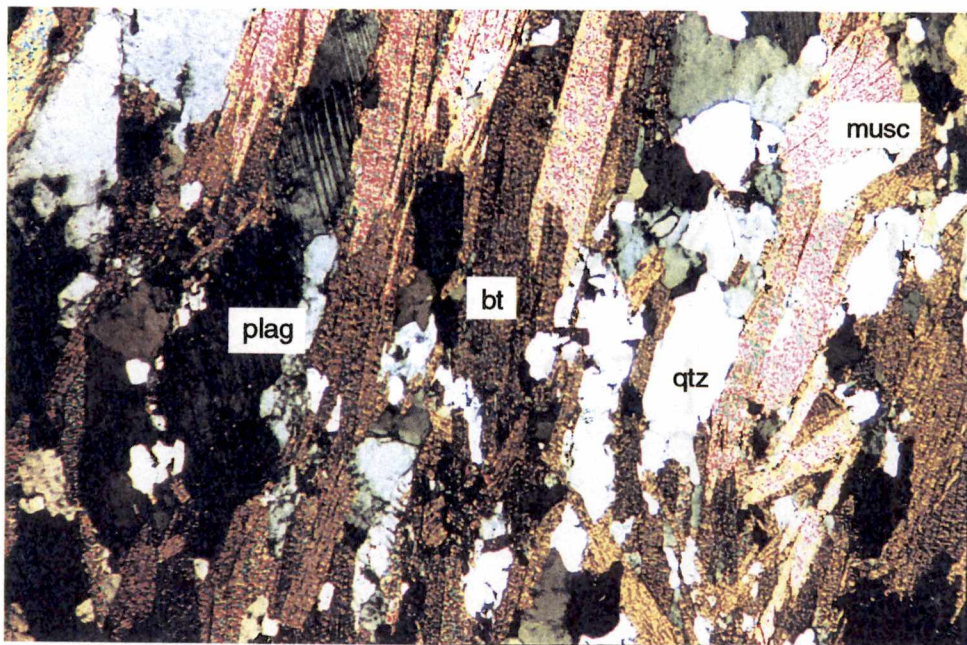


Figure 12. Photomicrograph of muscovite-biotite schist interlayered with metasandstone from the Otto Formation. Field of view is 4.25 mm. bt-biotite, qtz-quartz, musc-muscovite, plag-plagioclase.

Coleman River Formation. Coleman River metasandstone is composed of quartz plagioclase( $An_{20-30}$ )-biotite-epidote-chlorite-garnet with minor zircon and magnetite (Hatcher, 1980).

*Rabun Granodiorite.*

The Rabun granodiorite is a coarse-grained,  $\pm$  megacrystic, microcline-plagioclase granitoid that ranges from poorly foliated megacrystic granodiorite to fine-grained leucocratic granitic gneiss (Hopson et al., 1989; Miller et al., 1997).

In the study area it was possible to map the two distinct phases of the Rabun granodiorite: megacrystic granodiorite dominated by 1-to 4-centimeter phenocrysts of microcline (Figs. 13, 14, and 15), and medium-grained equigranular granitoid. The megacrystic phase of the granodiorite is primarily composed of plagioclase ( $An_{10-20}$ )-microcline-quartz with minor biotite, muscovite, zircon, garnet, epidote/clinozoisite, calcite, and opaques (Figs. 16 and 17). The medium-grained phase is composed of plagioclase ( $An_{10-20}$ )-quartz-microcline with minor muscovite, biotite, garnet, calcite, and opaques (Fig. 18). The two phases are easily separated within the study area by the presence or absence of microcline phenocrysts.

Also occurring within the pluton are calc-silicate rocks (presumably xenoliths). The calc-silicate rocks have major components of epidote/clinozoisite-quartz-diopside-calcite-hornblende with minor plagioclase ( $An_{10-20}$ ), sphene, and opaques (Fig. 19).

Table 3 presents modal analyses of the rock samples taken from the Rabun granodiorite.

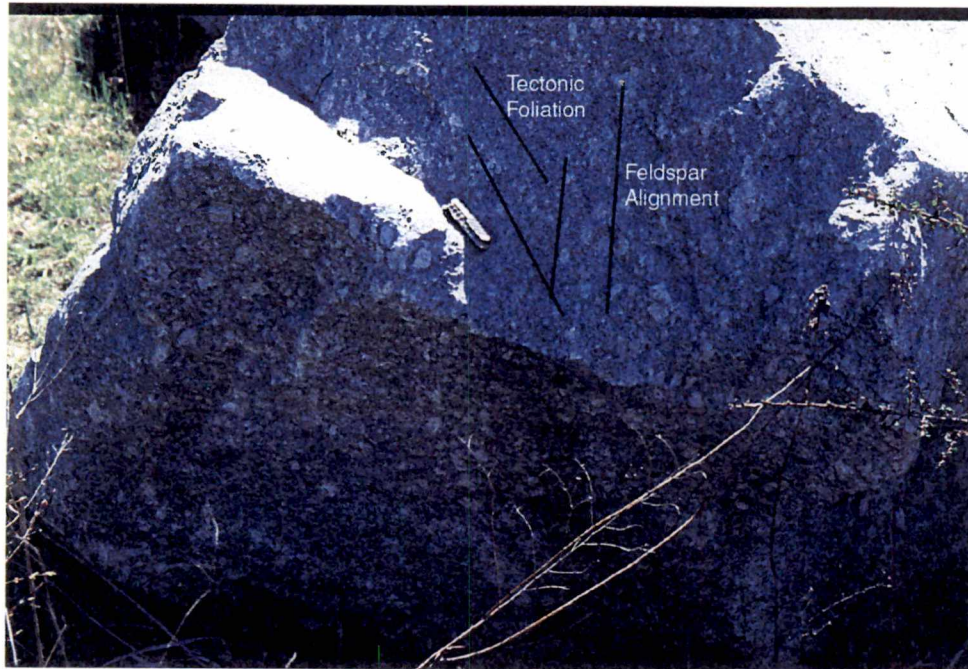


Figure 13. Photograph of the megacrystic phase of the Rabun granodiorite showing feldspar alignment and weak tectonic overprinting. Photograph from the Rabun Gap Quarry on the Rabun Bald quadrangle.



Figure 14. Photograph of the megacrystic phase of the Rabun granodiorite showing feldspar alignment and tectonic overprinting. Photograph from the Rabun Gap Quarry, on the Rabun Bald quadrangle.

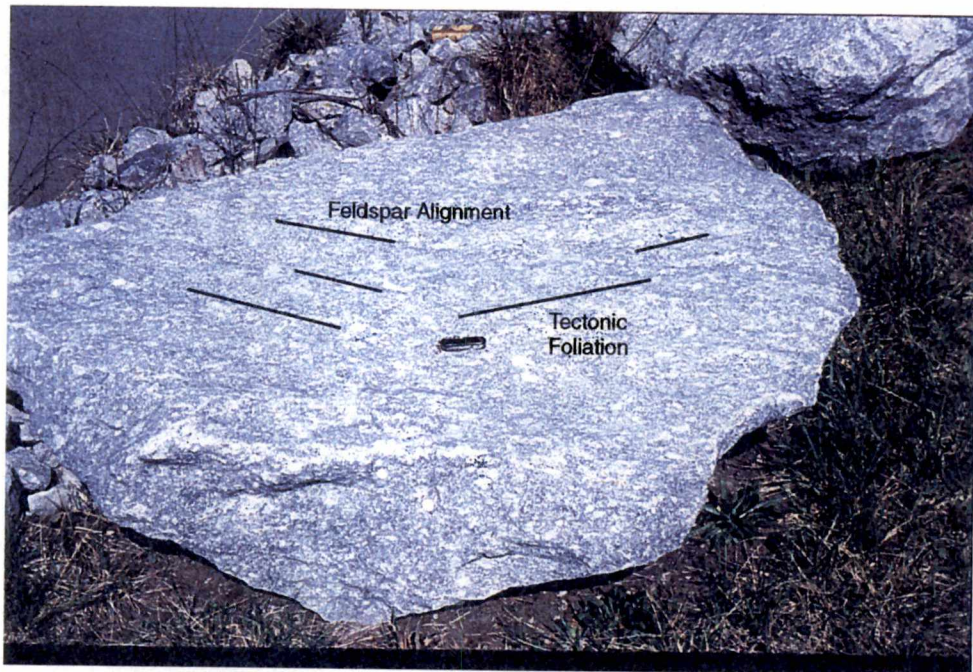


Figure 15. Photograph of the megacrystic phase of the Rabun granodiorite showing feldspar alignment and weak tectonic overprinting. Photograph from the Rabun Gap Quarry, on the Rabun Bald quadrangle.

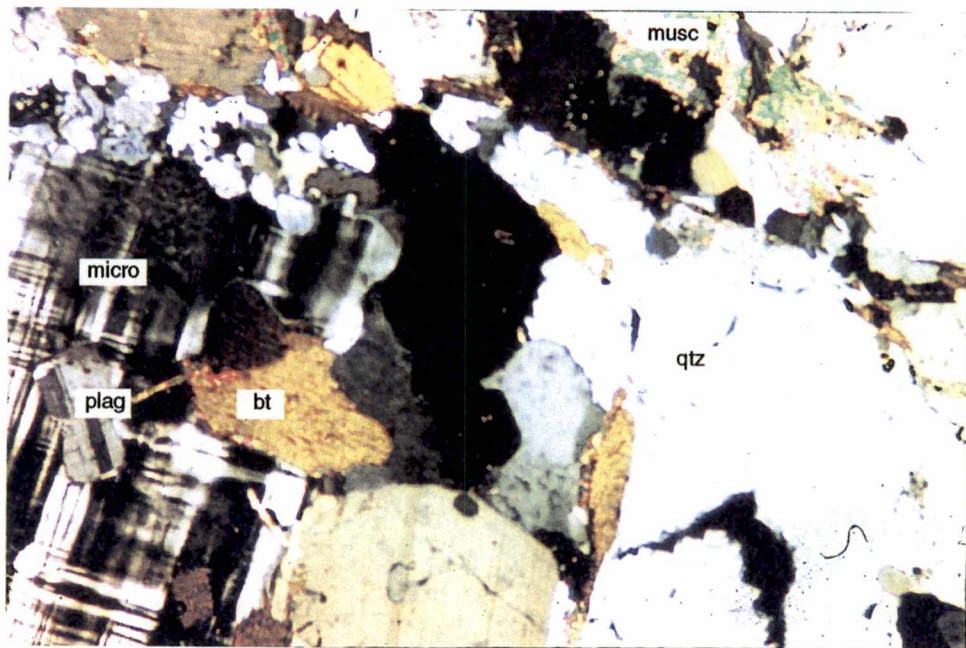


Figure 16. Photomicrograph of the megacrystic phase of the Rabun granodiorite. Field of view is 4.25 mm. From the Rabun Gap Quarry, Rabun Bald quadrangle. bt-biotite, qtz-quartz, musc-muscovite, plag-plagioclase, micro-microcline.

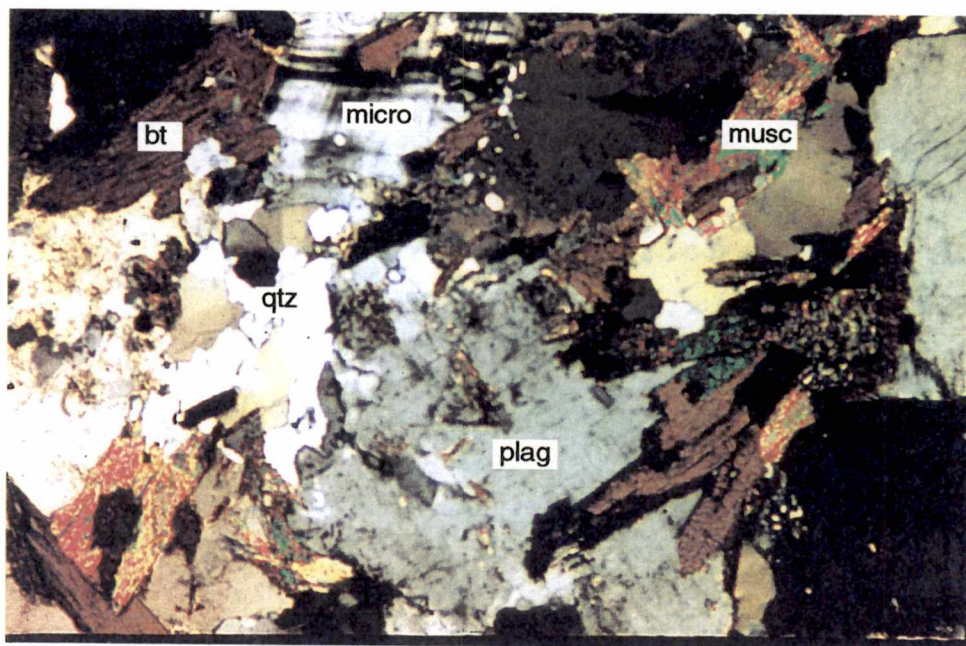


Figure 17. Photomicrograph of the megacrystic phase of the Rabun granodiorite. Field of view is 4.25 mm. From the Rabun Gap Quarry, Rabun Bald quadrangle. bt-biotite, qtz-quartz, musc-muscovite, plag-plagioclase, micro-microcline.

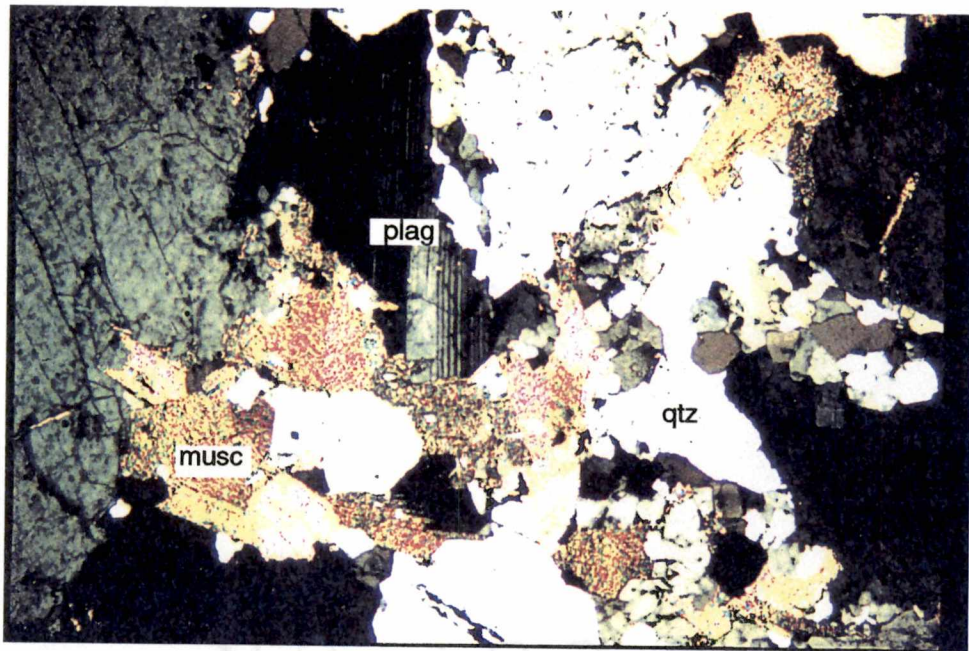


Figure 18. Photomicrograph of the equigranular phase of the Rabun granodiorite. Field of view is 1.70 mm. From the Rabun Gap Quarry, Rabun Bald quadrangle. qtz-quartz, musc-muscovite, plag-plagioclase.

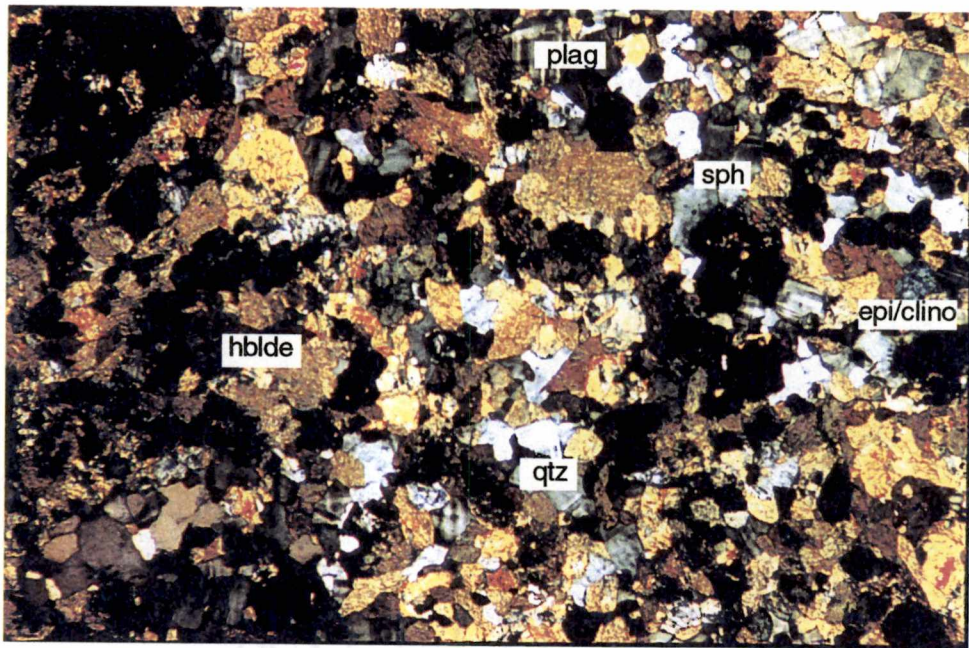


Figure 19. Photomicrograph of a calc-silicate quartzite from the Rabun granodiorite. Field of view is 4.25 mm. From along N.C. 106 near Scaly Mountain. qtz-quartz, plag-plagioclase, epi/clino-epidote/clinozoisite, hblde-hornblende, sph-sphene.

### *Pegmatite Bodies*

Numerous pegmatite dikes occur within the study area. They are primarily found within the Tallulah Falls Formation and the Rabun granodiorite and are relatively undeformed, indicating that these dikes were emplaced late in the crustal evolution of the Scaly Mountain geology. The pegmatites are composed primarily of plagioclase-quartz-microcline-hornblende with minor concentrations of epidote/clinozoisite, sphene, garnet, calcite, and opaques.

### *Calc-Silicate Bodies*

Calc-silicate "pods" occur on the Scaly Mountain quadrangle as irregularly shaped bodies that have been polydeformed. They primarily occur within the Rabun granodiorite pluton and in the Tallulah Falls Formation, near the contact with the Rabun granodiorite, which indicates that those in the granodiorite are probably country rock that has been incorporated by stopping into the pluton. These enclaves of calc-silicate rocks are found primarily near the southern end of the quadrangle (Plate 1). They have at least two different mineral assemblages: one is epidote/clinozoisite-hornblende-quartz-calcite with minor plagioclase ( $An_{10-20}$ ), sphene, garnet, and opaques. The other is epidote/clinozoisite-quartz-diopside-calcite-hornblende with minor plagioclase ( $An_{10-20}$ ), sphene, and opaques.

### *Amphibolite*

There are very few mappable amphibolites within the study area. They are found as small bodies in the lower part of the Tallulah Falls Formation (Plate 1) and are



polydeformed. Amphibolite is composed of hornblende-plagioclase (An<sub>10-20</sub>)-quartz-biotite with minor garnet, sphene, epidote/clinozoisite, zircon, and opaques. Another mineral assemblage is hornblende-plagioclase (An<sub>10-20</sub>)-quartz with minor garnet, calcite, epidote/clinozoisite, sphene, and opaques.

### *Quaternary Deposits*

Many of the valley floors and lower slopes on the Scaly Mountain quadrangle are covered by Quaternary colluvium and alluvium. These deposits are shown in Plate 3. The colluvium consists primarily of cobble-to boulder-size rocks derived from upslope. These rest unconformably on all of the map units within the Scaly Mountain quadrangle. Alluvium occurs immediately adjacent to streams and where the streams are on shallow to moderate gradients. It is composed of clays, cross-bedded sands, and coarser sediments, particularly in smaller streams.

## CHAPTER 3

### Structures within the Scaly Mountain Quadrangle

#### Mesoscopic Structures

Mapping of the Scaly Mountain quadrangle was performed at 1:12,000 scale and structural data were collected at 1333 stations (Plate 2). The structures observed include a second generation foliation ( $S_2$ ), direct observations of the Chattahoochee fault, passive and flexural flow folds, open folds that may be related to emplacement of the Blue Ridge thrust sheet, crenulations that may be related to the emplacement of the Chattahoochee thrust sheet, and tectonic and magmatic foliations observed at the same stations in the Rabun granodiorite. The structural data appear in Appendix A.

Within the Tallulah Falls Formation the primary foliation is defined by the parallel alignment of minerals within the rocks (primarily biotite gneiss). At some locations, such as the Cat Stairs on N.C. 106, an earlier foliation that is probably Taconic in origin is preserved in boudins. The dominant foliation is thought to be Acadian in origin since peak metamorphism is Acadian (Hopson et al., 1989).

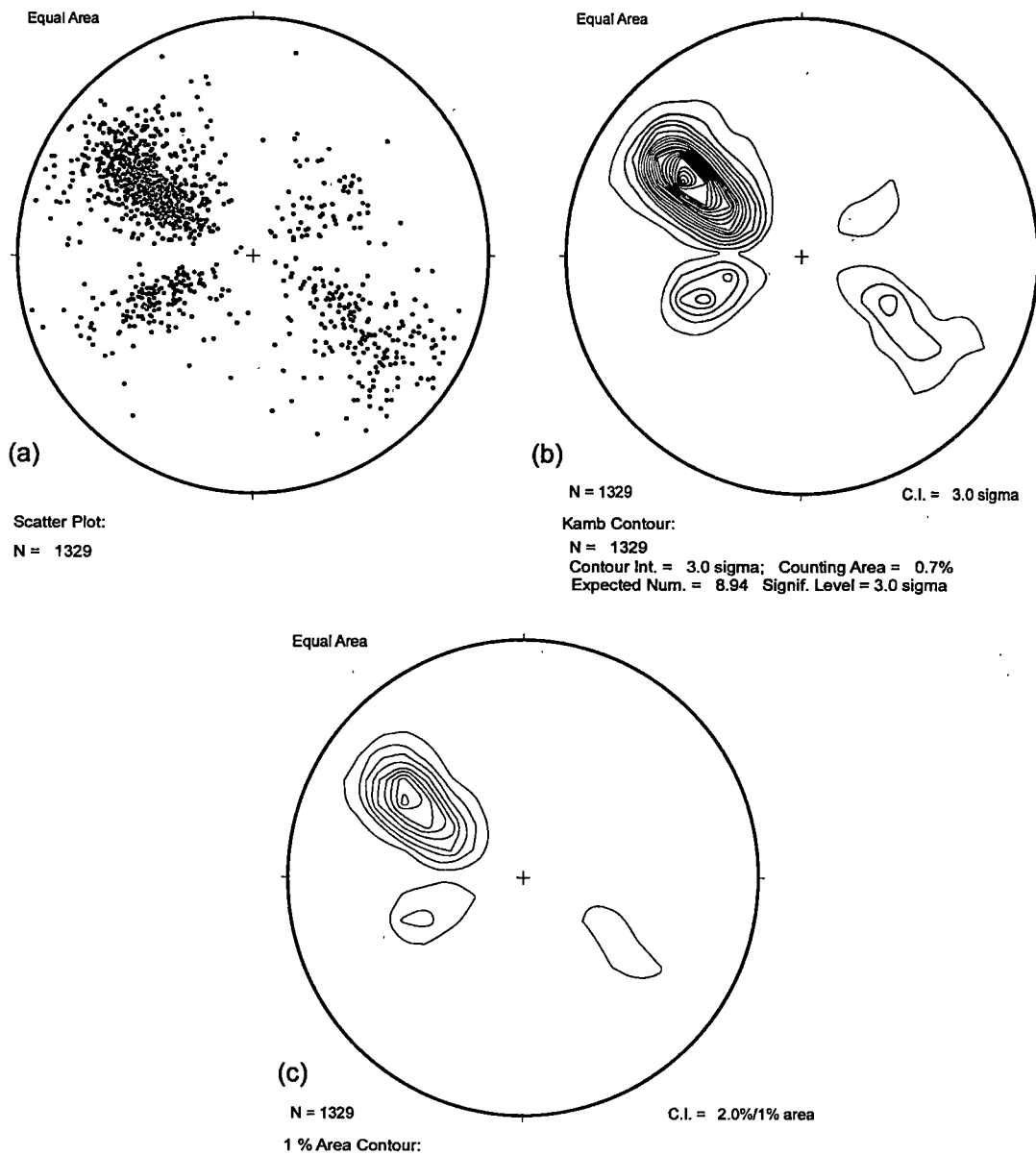
In the Otto Formation are two foliations and crenulations (Figure 9). The earlier  $F_1$  folding observed in boudins is probably Taconic in age. The  $F_2$  folding which deforms the  $F_1$  folds is probably Acadian in age. The southeast-dipping crenulations noted in Figure 9 are probably related to the emplacement of the Chattahoochee thrust sheet.

## **Map-Scale Structures**

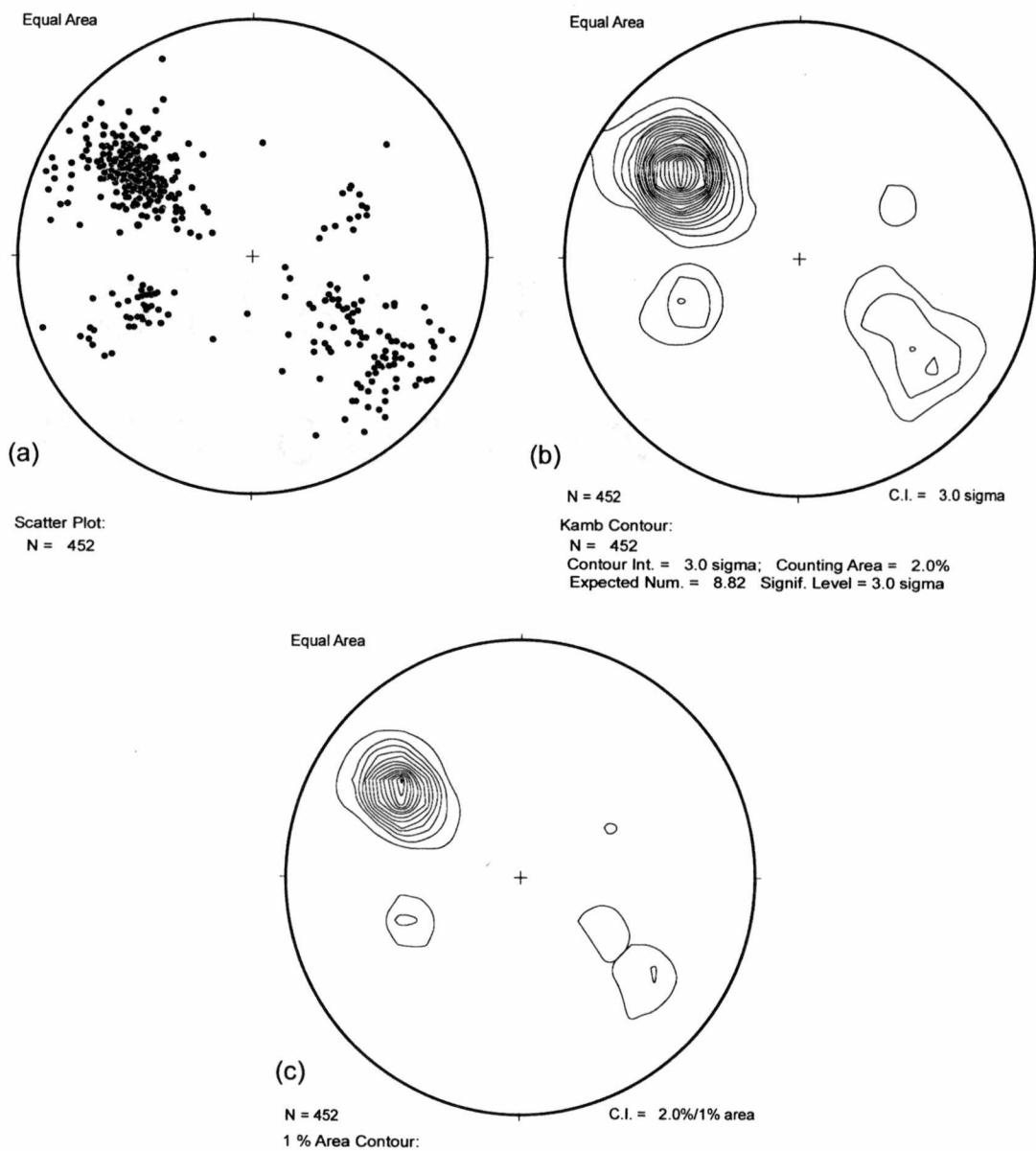
The geologic map of the Scaly Mountain quadrangle (Plate 1) shows that there have been multiple deformation events recorded in the observed map-scale structures. Figure 2 shows that to the south of the Scaly Mountain quadrangle fold interference patterns that have been mapped on the Satolah, Rabun Bald, and Dillard quadrangles may indicate earlier Taconic structures that have been refolded by Acadian deformation events.

Evidence for multiple deformation events can also be seen along the Chattahoochee fault. The fault deforms the Rabun granodiorite, therefore the fault postdates the granodiorite. The fault also truncates other earlier structures e.g., the dominant foliation in the rocks of the hanging wall and footwall. More evidence is that the fault itself is folded. Therefore, there have been at least two deformation events, and probably more, within the study area. Fabric diagrams (Figures 20-24) of the rock units occurring in the Scaly Mountain quadrangle show that the rocks have two distinct strike directions for foliations.

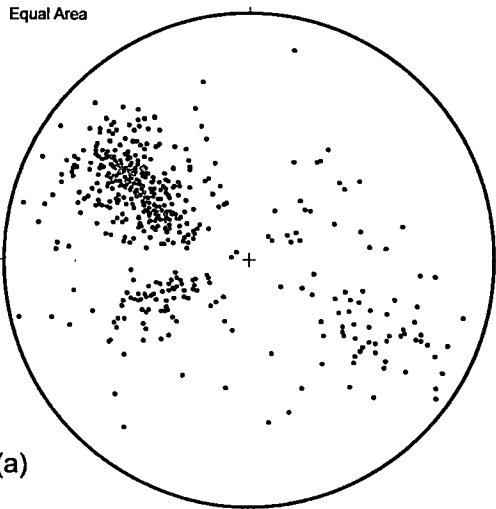
Further proof of multiple deformation events is given when the structural data for the Rabun granodiorite are plotted on equal-area projections (Fig. 23). The plot of poles to foliations for the Rabun granodiorite shows that the majority of the foliations strike to the northeast and dip to the southeast, although there are some that dip to the northwest. Also some (the minority) of the foliations strike to the northwest and dip to the northeast or southwest. The scatter plot of lineations (feldspar alignment) within the granodiorite are primarily northeast trending (Fig. 24). This would indicate that there have been multiple deformation events within the area. First the granodiorite would have been intruded into the surrounding country rock and later the tectonic foliation would have overprinted the magmatic foliation.



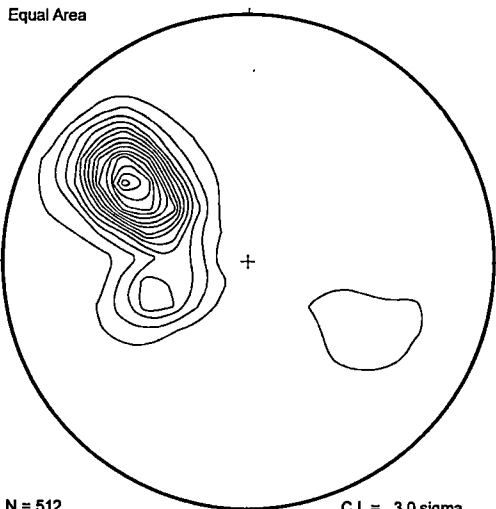
**Figure 20.** Scatter plot and fabric diagrams for all foliation measurements obtained in the study area. (a) Lower-hemisphere, equal-area scatter plot of 1,329 poles to foliation measurements. (b) Lower-hemisphere, equal-area Kamb contour diagram of 1,329 poles to foliation measurements. (c) Lower-hemisphere, equal-area two percent per one percent area contoured diagram of 1,329 poles to foliation measurements.



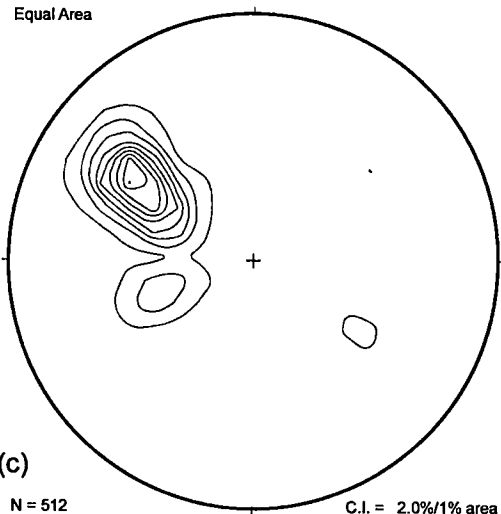
**Figure 21.** Scatter plot and fabric diagrams for foliation measurements obtained in the study area from the Otto Formation. (a) Lower-hemisphere, equal-area scatter plot of 452 poles to foliation measurements. (b) Lower-hemisphere, equal-area Kamb contour diagram of 452 poles to foliation measurements. (c) Lower-hemisphere, equal-area two percent per one percent area contoured diagram of 452 poles to foliation measurements.



Scatter Plot:  
N = 512

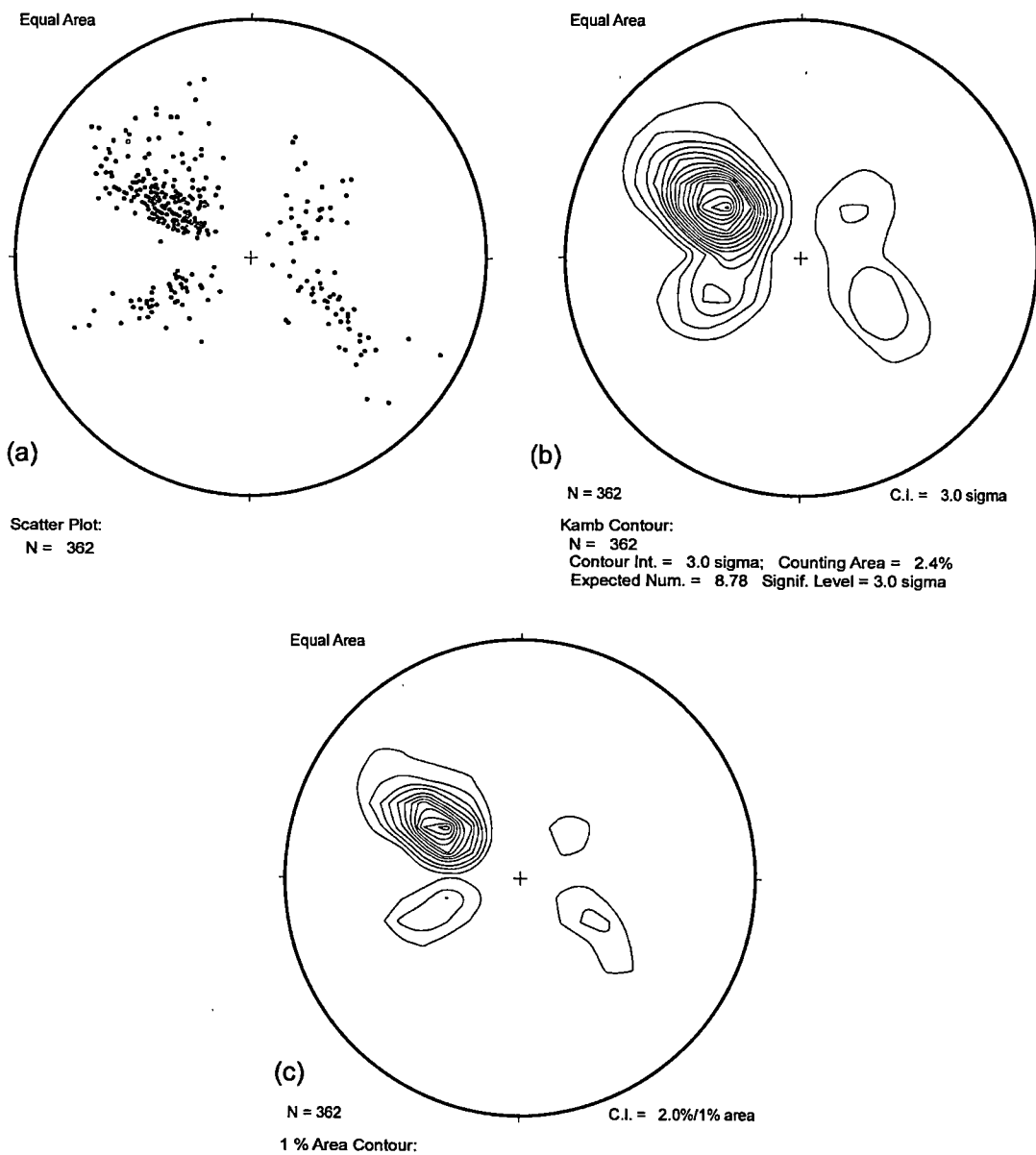


N = 512 C.I. = 3.0 sigma  
Kamb Contour:  
N = 512  
Contour Int. = 3.0 sigma; Counting Area = 1.7%  
Expected Num. = 8.84 Signif. Level = 3.0 sigma

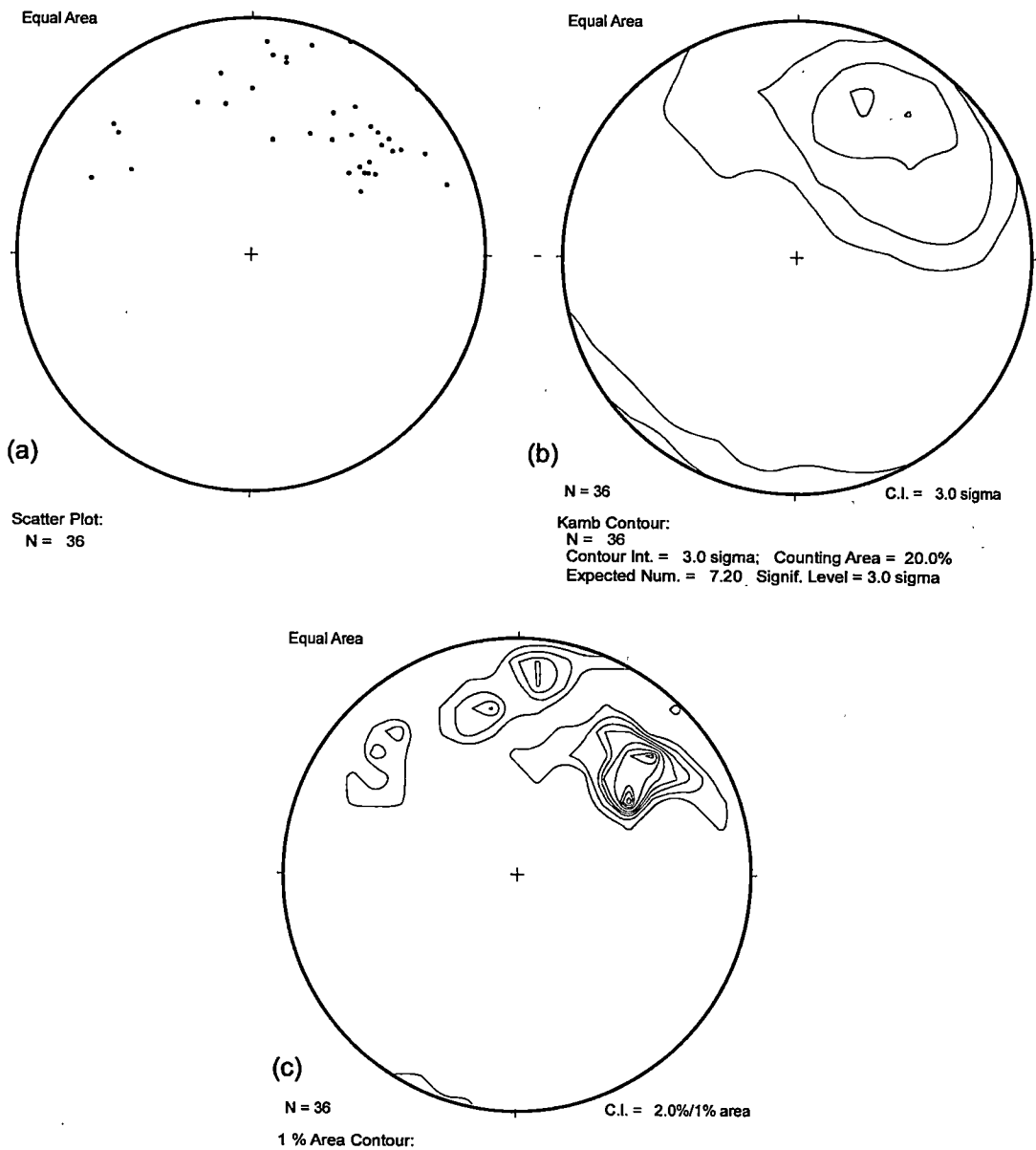


N = 512 C.I. = 2.0%/1% area  
1 % Area Contour:

**Figure 22.** Scatter plot and fabric diagrams for foliation measurements obtained from the Tallulah Falls Formation in the study area. (a) Lower-hemisphere, equal-area scatter plot of 512 poles to foliation measurements. (b) Lower-hemisphere, equal-area Kamb contour diagram of 512 poles to foliation measurements. (c) Lower-hemisphere, equal-area two percent per one percent area contoured diagram of 512 poles to foliation measurements.



**Figure 23.** Scatter plot and fabric diagrams for foliation measurements obtained in the Rabun granodiorite in the study area. (a) Lower-hemisphere, equal-area scatter plot of 362 poles to foliation measurements. (b) Lower-hemisphere, equal-area Kamb contour diagram of 362 poles to foliation measurements. (c) Lower-hemisphere, equal-area two percent per one percent area contoured diagram of 362 poles to foliation measurements.



**Figure 24.** Scatter plot and fabric diagrams for lineation measurements obtained in the Rabun granodiorite in the study area. (a) Lower-hemisphere, equal-area scatter plot of 36 poles to lineation measurements. (b) Lower-hemisphere, equal-area Kamb contour diagram of 36 poles to lineation measurements. (c) Lower-hemisphere, equal-area two percent per one percent area contoured diagram of 36 poles to lineation measurements.



This evidence would indicate that at least six to seven deformation events are recorded in the rocks occurring within the study area:

- 1) Early folding and formation of  $S_1$  foliation; development of the  $S_2$  foliation in the Tallulah Falls Formation, during Acadian folding and metamorphism.
- 2) The Rabun granodiorite intruded the country rock.
- 3) The granodiorite magmatic foliation was tectonically overprinted (may have occurred as part of 4 or 6).
- 4) The Chattahoochee fault became active.
- 5) A crenulation cleavage developed within the Dahlonega gold belts rocks, corresponding to the emplacement of the Chattahoochee thrust sheet.
- 6) The Chattahoochee fault was folded along with other features.
- 7) Arching of the Tallulah Falls dome occurred.

### **Tectonic Boundaries**

The eastern Blue Ridge is separated from the western Blue Ridge by the Hayesville fault and from the Inner Piedmont by the Brevard fault zone (Fig 2). The Hayesville fault separates the Blue Ridge into two distinct tectonostratigraphic terranes. The western Blue Ridge, west of the Hayesville fault, is predominantly rocks of the Great Smoky Group and Murphy belt that were deposited unconformably on Middle Proterozoic Grenville basement. Exposures of the Grenville basement are common in western North Carolina west of the Hayesville fault. The eastern Blue Ridge is characterized by one-mica, one-feldspar dominant metasediments and by abundant mafic and ultramafic rocks with rare exposures of Grenville basement (Hopson et al., 1989).

The Brevard fault zone contains numerous faults, its own stratigraphy, and separates the eastern Blue Ridge from the Inner Piedmont to the east. The Rosman fault forms the southeast boundary of the eastern Blue Ridge and northwest margin of the Brevard fault zone. It is characterized by a cataclastic zone up to 50 m thick (Hopson et al., 1989; Horton and McConnell, 1991; Hatcher, 2001).

Within the eastern Blue Ridge province at the latitude of and within the Scaly Mountain quadrangle are two main thrust faults: the Chattahoochee fault and the Soque River fault. Also occurring at the latitude of the Scaly Mountain quadrangle is the Shope Fork fault.

#### *Chattahoochee Fault*

The Chattahoochee fault separates rocks of the Dahlonega gold belt from the Tallulah Falls Formation. The trace of the Chattahoochee fault is marked by a sharp break from the migmatitic Tallulah Falls Formation rocks to non-migmatitic metasandstones and schists of the Otto Formation. Faulting is thought to be post metamorphic peak because migmatite is not observed in the Dahlonega gold belt (Hopson et al., 1989).

The Chattahoochee fault is folded and displacement along the fault occurred while the rocks were ductile. Evidence of ductility is the lack of cataclasis along the fault. Folding of the fault itself occurred after the fault was emplaced and provides evidence that the rocks were ductile the entire time that the Chattahoochee fault was being emplaced.

The Chattahoochee fault was emplaced late in the deformational and metamorphic history of the Scaly Mountain quadrangle. Evidence for this is found on the northwestern

flank of the Rabun pluton. The Tallulah Falls Formation rocks are faulted out near the southwest end of the pluton in the Dillard quadrangle (Acker and Hatcher, unpublished map). The rocks of the Otto Formation are also truncated by the fault. It is possible that the Chattahoochee fault is a strike-slip fault and not a thrust fault. The primary evidence for this is the alignment of foliation strikes on either side of the fault. The foliation strikes within both the Otto Formation and the Tallulah Falls Formation align almost uniformly with the fault plane. The northeast-trending mineral lineations could be stretching lineations indicating northeast or southwest directed strike slip.

#### *Shope Fork Fault*

The Shope Fork fault was originally named and recognized in the Prentiss quadrangle by Hatcher (1980). The Coweeta syncline (Hatcher, 1979) extends southwest from north of the North Carolina-Georgia border into the Hightower Bald quadrangle (Hatcher, 1979; Hopson et al., 1989). The southeast limb of the syncline is truncated by the Shope Fork fault that separates amphibolite-poor Coweeta Group from amphibolite-rich biotite gneiss and schist to the northwest (Hopson et al., 1989).

#### *Soque River Fault*

The Soque River fault separates rocks of the Dahlonge gold belt from rocks of the Coweeta Group. There is some debate as to whether the Soque River fault and the Shope Fork fault are the same fault. Gillon (1982) and Nelson (1982) correlated this fault with the Shope Fork fault. Hopson et al. (1989) refuted this because the Coweeta Group rocks that occur in the footwall of the Shope Fork fault are laterally continuous with correlative

rocks that occur in the hanging wall of the fault mapped by Gillon (1982). Hopson et al. (1989) also stated that the Shope Fork fault is pre- to synmetamorphic while the Soque River fault is post-metamorphic peak.

### **Metamorphism**

Metamorphic grade on the Scaly Mountain quadrangle ranges from staurolite-kyanite grade to sillimanite grade.

The biotite gneisses of the Tallulah Falls Formation were subjected to kyanite-sillimanite grade metamorphism. As seen in Table 3, the typical mineral assemblage is quartz-plagioclase-biotite-muscovite with minor constituents of microcline, garnet, epidote/clinozoisite, sphene, zircon and opaques. The rocks chosen for modal analysis do not contain kyanite or sillimanite, but both minerals were noted in the field.

The Rabun granodiorite was metamorphosed along with all of the adjacent rocks following emplacement (probably ~360 Ma, B. Bream, personal communication, 2001). Lack of a contact aureole indicates emplacement as a catazonal pluton into a crust that was already hot and near peak metamorphic conditions. Deformation of the Rabun granodiorite and the country rocks occurred after emplacement, producing one of the high temperature foliations in the Rabun granodiorite.

The Otto Formation rocks reach staurolite-kyanite grade metamorphism within the field area. The non-migmatitic nature of the Otto Formation indicates upper amphibolite facies metamorphic conditions.

Amphibolites, occurring within the other rock units as isolated bodies, reach metamorphic grades as high as sillimanite grade. There is quite a variation in the mineral

assemblages of the amphibolites (Table 3). The fact the hornblende is present indicates that these rocks reached amphibolite facies metamorphic conditions.

Calc-silicates also occur as isolated bodies within the other rock types in the area. The calc-silicate rocks underwent high-grade metamorphism. The fact that hornblende is present would indicate that the rocks reached amphibolite facies metamorphic conditions. There was a variation within the assemblages of the rocks that were chosen for modal analysis (Table 3).

The pegmatite dikes that crosscut the other rock units have undergone very little metamorphism.

### **Geomorphic expression of the Rabun granodiorite**

The Rabun granodiorite and the Tallulah Falls Formation rocks form the highest ridges in the Scaly Mountain quadrangle. The Otto Formation also forms ridges but at lower elevations. The aspect of the Rabun ridges that is different is that exfoliation surfaces are found on the south-southwest facing slopes. These exfoliation surfaces are due to sheeting within the pluton. The exfoliation surfaces loosen over time due to mechanical weathering processes and eventually break loose from the main body of rock. These exfoliation surfaces occur in both the megacrystic phase and the equigranular phase of the granodiorite. Sheeting joints form subparallel to surface topography and the spacing between the joints increases with depth into the crust (Hatcher, 1995). Sheeting is thought to form by unloading over long periods of time as erosion removes large quantities of overburden from a rock mass (Hatcher, 1995). The mass expands normal to the Earth's surface so that extension fractures form normal to the expansion direction and

parallel to the surface (Hatcher, 1995). The Tallulah Falls Formation and the Otto Formation ridges do not exhibit exfoliation surfaces on the slopes.

## CHAPTER 4

### The Rabun Granodiorite

#### Geology of the Rabun Granodiorite

The Rabun granodiorite pluton is comprised of two distinct types of granitic rock. The main body of the pluton is megacrystic granodiorite with large phenocrysts of microcline. On the northeast flank of the main pluton is a medium-grained, equigranular, leucocratic, granitic gneiss that can be mapped separately. Some map-scale folds occur within the pluton that become apparent when observing foliations at map-scale (Plate 1). It is possible that the Rabun granodiorite has been tilted on its side; however, this is a difficult hypothesis to prove when the entire pluton is considered. In the Scaly Mountain quadrangle there is a large portion of the medium-grained phase present on the northeast side of the pluton. However, at the Rabun Gap quarry on the Rabun Bald quadrangle to the south there is very little medium-grained granodiorite present on the northeast side of the pluton. Even further south on the Dillard quadrangle there is some of the medium-grained phase present; however, it occurs on the southwest flank of the pluton. More research will be needed to determine whether or not the pluton has been tilted.

#### Magmatic Flow Structures Versus Tectonic Flow Structures

At some places within the Rabun granodiorite it is possible to observe two distinct foliations (Figs 23 and 24). One of the foliations was concluded to be the product of magmatic flow, while the other was determined to have a tectonic origin. Evidence for magmatic flow foliations includes: the preferred orientation of primary igneous minerals

that show no evidence of plastic deformation or recrystallization; aligned crystals surrounded by anhedral, non-deformed quartz grains or non-aligned; anhedral aggregates of quartz; imbrication or "tiling" of crystals; preferred alignment of elongate microgranitoid enclaves; magmatic flow foliations deflected around xenoliths; schlieren layering; and absence of phenocrysts and enclaves at the intrusion contact (Paterson et al., 1989). Evidence of solid state flow (tectonic foliations) includes: microscopic evidence of plastic deformation within mineral grains (e.g. undulatory extinction); fractured or boudinaged strong minerals, such as feldspar and hornblende; the foliation commonly passes through enclaves; strain is commonly heterogeneous and mylonitic zones may develop; and evidence of pressure solution of crystals may be found (Paterson et al., 1989). Superposition of solid-state deformation (tectonic) on magmatic foliations can be inferred if the rocks have aligned igneous minerals, especially euhedral feldspars, but they also show evidence of recrystallization. If the feldspar crystal faces are preserved, a dominant magmatic flow component may be inferred (Paterson et al., 1989).

Within the Rabun granodiorite it is possible to see some of the above-mentioned criteria for the superposition of a tectonic foliation on magmatic flow foliation. The igneous minerals—especially the feldspar megacrysts—have a preferred alignment and the crystal faces are fairly well preserved, which would indicate a dominant magmatic flow foliation. Within the granitoid, however, is another foliation that trends differently than the magmatic flow foliation and is interpreted to be a tectonic overprinting foliation that is roughly parallel to the foliation in the enclosing country rocks (Figs. 20-23). The orientations of these foliations primarily trend to the northeast with some points trending to the northwest (Figs. 20-23).



The poles to foliations and a scatter plot of the feldspar lineation (magmatic foliation) were plotted on equal area stereonet projections (Figs. 23 and 24). These data indicate that these are indeed two distinct and separate structures within the Rabun granodiorite.

#### **Contacts of the Rabun granodiorite with the surrounding country rock.**

The Rabun granodiorite is in contact with the Tallulah Falls Formation on the eastern flank and on part of the western flank of the pluton, and is truncated by the Chattahoochee fault on another part of the western flank (Plate 1). No metamorphic aureole exists at the contacts of the pluton with the country rock; the contact is gradational of a scale of a few centimeters to as much as a meter and is relatively easily defined. The contact between the pluton and surrounding rock is folded. At the contacts with the Tallulah Falls Formation there is an increasing occurrence of pegmatite dikes.

#### **Relationship of the Rabun granodiorite with surrounding country rock.**

The Rabun granodiorite pluton intruded the Tallulah Falls Formation at approximately 375 Ma (Miller et al., 2000) and is presumed at one time to have been completely surrounded by the Tallulah Falls Formation rocks. At a later time a portion of the Tallulah Falls Formation and the pluton were faulted out by the Chattahoochee fault. This is evident in the southwestern portion of the Scaly Mountain quadrangle (Plate 1). The pluton and the surrounding rocks share at least some deformation events that are indicated by the folded contacts and by similar foliation trends within both rock units. An important observation is that the Tallulah Falls Formation rocks, however, contain

more deformation events than the pluton. An earlier foliation which has been truncated by the dominant  $S_2$  foliation exists at some locations in the Tallulah Falls Formation, such as the Cat Stairs on N.C. 106 where the earlier foliation is preserved in boudins.

### **Description and possible relationship of the pluton facies.**

After modal analyses were performed (Table 3) some trends were noted within each facies of the pluton. The plagioclase content is approximately the same for both facies. The microcline content increases in the megacrystic phase and is mostly found as phenocrysts. Miller (1997) noted that the potassium in this phase is located almost wholly within the microcline megacrysts. Quartz content is higher in the medium-grained phase. The relative abundances of biotite and muscovite are reversed in the two facies, with biotite more abundant in the megacrystic phase. This trend would indicate that potassium in the medium-grained phase went into muscovite and biotite, while potassium in the megacrystic phase went primarily into microcline and biotite with little muscovite forming. The megacrystic facies contains zircon and epidote while the medium-grained facies contains these minerals in lesser abundance. Although there are some differences in mineralogy between the two facies of the Rabun granodiorite, these differences are minor. The major difference is the presence or absence of the phenocrysts.

### **Chemistry of the Rabun granodiorite.**

The chemistry of the Rabun granodiorite pluton has been previously determined (Miller et al., 1997). Major and trace element chemistry were determined for seven samples

from the pluton and the analyses are presented in Table 4. The granodiorite has a distinct Nd crustal isotopic signature and high concentrations of incompatible elements. Isotopic diversity implies that a variety of materials were involved, which is consistent with crustal anatexis (Miller et al., 1997). Several constraints were placed on the types of source material, as concluded by Miller et al. (1997).

1. The U-Pb inheritance in zircons indicates involvement of relatively old, variable age crustal material, either *in situ* or as detrital fragments in sediment. Sr and Nd isotopic data support this conclusion, but suggest that most samples also include a more juvenile component. Inheritance is also demonstrated in the zircon studies by Miller et al. (2000) where 1.05 to 1.24 Ga cores were observed in zircons from the Rabun granodiorite.
2.  $\delta^{18}\text{O}$  values are typical of the crust—higher than those of mafic rocks, but lower than those of sedimentary rocks. A sedimentary component may have contributed to the melt, but it was probably not dominant.
3. The granodiorite is poor in heavy REEs, moderately rich in Sr, and has very small negative Eu anomalies. The residue of melting must have contained a heavy REE-concentrating phase, probably garnet, and probably was not dominated by feldspars.

**Table 4**  
**Elemental and Isotopic Data for Representative Samples from the Rabun Granodiorite**  
 Modified from Miller et al., 1997

(wt%)	R2	R4	R7	R9	R11	R14	R22A
SiO <sub>2</sub>	71.7	70.2	67.7	66.8	66.5	71.7	68.9
TiO <sub>2</sub>	0.20	0.22	0.41	0.33	0.44	0.16	0.37
Al <sub>2</sub> O <sub>3</sub>	15.5	14.9	15.6	16.1	16.4	16.1	15.1
Fe <sub>2</sub> O <sub>3</sub>	1.65	1.74	2.91	2.61	3.13	1.36	2.73
MnO	0.02	0.02	0.03	0.03	0.03	0.02	0.03
MgO	0.57	0.55	0.97	0.83	1.05	0.44	0.84
CaO	2.62	1.94	2.65	2.31	3.05	1.64	2.58
Na <sub>2</sub> O	5.24	4.34	4.60	4.39	4.74	5.85	4.49
K <sub>2</sub> O <sub>5</sub>	0.87	3.47	2.68	4.03	2.32	1.41	2.79
P <sub>2</sub> O <sub>5</sub>	0.12	0.07	0.14	0.13	0.17	0.05	0.12
LOI	1.54	0.62	0.62	0.47	0.54	1.39	0.70
Total	100.03	98.07	98.31	98.03	98.37	100.12	98.65
(ppm)							
Rb	39	80	108	105	76	53	77
Sr	385	426	732	497	825	673	431
Ba	110	840	940	1,330	850	340	690
Th	—	—	—	8.1	—	2.7	7.7
U	—	—	—	0.8	—	0.8	0.8
Zr	70	100	160	160	180	90	150
Hf	—	—	—	4.6	—	—	—
Ta	—	—	—	0.4	—	—	—
La	—	23.8	—	35	55	9.2	28
Ce	—	47.8	—	57.8	98.5	18	52
Nd	—	15.2	—	22.7	35	9	19
Sm	—	2.64	—	3.92	6.09	2	3.6
Eu	—	0.714	—	1.07	1.38	0.69	1.18
Tb	—	—	—	—	—	0.27	0.35
Dy	—	—	—	—	—	1.1	1.4
Yb	—	0.38	—	0.7	1.07	0.65	0.64
La	—	0.093	—	0.108	0.161	0.1	0.1
<sup>87</sup> Rb/ <sup>86</sup> Sr	0.295	0.542	0.642	0.613	0.37	0.228	0.518
<sup>87</sup> Sr/ <sup>86</sup> Sr <sub>meas</sub>	0.70849	0.70954	0.70956	0.70964	0.70851	0.70615	0.70868
<sup>87</sup> Sr/ <sup>86</sup> Sr <sub>400</sub>	0.7068	0.7065	0.7059	0.7061	0.7064	0.7049	0.7057
<sup>147</sup> Sm/ <sup>144</sup> Nd	—	—	—	0.0976	0.0937	—	—
<sup>143</sup> Nd/ <sup>144</sup> Nd <sub>meas</sub>	—	—	—	0.512303	0.51227	—	—
<sup>143</sup> Nd/ <sup>144</sup> Nd <sub>400</sub>	—	—	—	0.512047	0.512025	—	—
ε <sub>Nd, 400</sub>	—	—	—	-1.5	-1.9	—	—
<sup>206</sup> Pb/ <sup>204</sup> Pb <sub>dws</sub>	—	—	—	—	—	—	18.49
<sup>207</sup> Pb/ <sup>204</sup> Pb <sub>feld</sub>	—	—	—	—	—	—	15.63
<sup>208</sup> Pb/ <sup>204</sup> Pb <sub>feld</sub>	—	—	—	—	—	—	38.35
δ <sup>18</sup> O <sub>wr</sub>	9.1	—	8.4	8.9	8.8	6.5	8.7

4. High Ba and moderate K<sub>2</sub>O contents suggest that K-feldspar was not abundant in the residue. K-feldspar saturation would require higher potassium concentrations in coexisting melts, and abundant K-feldspar would result in partitioning of Ba into the residue (Miller et al., 1997).
5. <sup>87</sup>Sr/<sup>86</sup>Sr ratios indicate that the granodiorite has “normal” continent margin granitoid ratios (Miller et al., 1997), with a probable source in the continental crust.

The granodiorite source was probably mixed, comprising both Early to Middle Proterozoic and younger rocks indicated from zircon dating (Miller et al., 2000), and including both relatively felsic, perhaps sedimentary, crust and more depleted material. The granodiorite may also have been a hybrid between trondhjemitic and ancient felsic crust-derived magmas (Miller et al., 1997).

Miller et al. (1997) suggested the following scenario for the generation of the magma. Fragments of a primitive magmatic arc were emplaced tectonically as a consequence of convergence beneath the Blue Ridge crust. The thermal blanketing resulting from crustal thickening could ultimately have led to temperatures high enough to induce melting in the underaccreted mafic crust, up to 850°C or more, on a time scale of tens of millions of years to 100 m.y. The more ancient, felsic component could have been contributed by overlying crust that may have also exceeded its solidus, or it could have come from North America-derived sedimentary rocks that may have been part of the near-continent arc assemblage. Mafic and felsic rocks may have been interleaved depositionally, by intrusion of mafic rocks into a sedimentary sequence, or tectonically.

This hypothesis does not fit with current thinking that the eastern Blue Ridge basement is oceanic in nature. However, the  $^{87}\text{Sr}/^{86}\text{Sr}$  ratios are relatively high which indicates a component of continental crust derived material. This may indicate that the eastern Blue Ridge basement is not entirely derived from an oceanic source.

#### **Timing and possible modes of emplacement of the Rabun granodiorite.**

The Rabun granodiorite is the youngest of a series of mid-Devonian age plutons that were emplaced during the Acadian orogeny. The Rabun granodiorite has an ion probe U-Pb age of 375 Ma. (Miller et al., 2000) and is syntectonic. The Rabun is deformed and contains a second foliation, is concordant, and does not have a contact aureole. These facts also indicate it is probably early to synmetamorphic, and was intruded into a hot crust.

Miller et al. (1997) suggested that melting for the Rabun granodiorite magma took place at relatively great depths (> 30 km) within the tectonically thickened crust. After the magma was generated, it presumably ascended and was emplaced into the Tallulah Falls Formation, but still at depth because of the concordant nature of the contact and the lack of a contact aureole.

Different modes of emplacement and arguments for or against each, for the Rabun pluton, are presented in the following section. Previous attempts to describe emplacement mechanisms in different plutons by others are outlined in Table 5.

**Table 5**  
**Pluton Emplacement Mechanisms**  
**Proposed by Others**

<b>Researcher(s)</b>	<b>Emplacement Mechanism(s)</b>	<b>Relative Emplacement Depth</b>
Paterson and Fowler (1993)	Outward displacement of the Earth's surface. Lowering the Moho.	Upper Crust. Middle or Lower Crust.
Johnson, Alibertz, and Paterson (2001)	Dike feeding.	Upper to Middle Crust.
Hutton (1997)	Principle of effective stress.	Upper to Middle Crust.
John and Stunitz (1997)	Magmatic fracturing and small-scale melt segregation.	Upper Crust.
Ramsay (1989) McBirney (1993)	Diapirism.	Middle to Lower Crust.

### *Emplacement of the pluton along the Chattahoochee fault.*

This emplacement mechanism is unlikely. The pluton is truncated by the Chattahoochee fault indicating it was emplaced before the fault formed. This agrees with previous work that has suggested that the Chattahoochee fault is post-emplacement.

### *Stoping*

Evidence for this a component of this emplacement mechanism is apparent within both facies of the pluton. Within the medium-grained facies are small xenoliths of the surrounding Tallulah Falls Formation biotite gneiss. Within the megacrystic facies are xenoliths of calc-silicate rocks and xenoliths and schlieren of Tallulah Falls biotite gneiss. This mechanism can account for at least a small part of the emplacement history of the Rabun pluton.

### *Diapirism*

Diapirism is the most likely emplacement mechanism for the Rabun pluton. If the two pluton facies are considered as separate magma pulses, it is possible that the medium-grained facies was emplaced and at least partially solidified when the megacrystic facies was emplaced. In this scenario part of the medium-grained phase was incorporated into the megacrystic phase and only remnants of the medium-grained phase (on the flanks of the megacrystic phase) survived.

However, the gradational contact between the two phases of the pluton would indicate that they were probably liquids when in contact and that there is a possibility of some mixing between the two phases.

Further evidence for diapirism as an emplacement mechanism is obtained when the magmatic orientation of the microcline megacrysts is considered. The megacrysts



have a preferred alignment that is roughly parallel to the pluton's margins. This would indicate that megacrysts were aligned by magmatic flow while the pluton was ascending through the crust.

#### *Outward displacement of the Earth's surface*

Paterson and Fowler (1993) suggested this as one of their two emplacement mechanisms; the other mechanism they suggested is lowering the Moho. Evidence of the outward displacement of the Earth's surface is not readily available, however it is unlikely due to the nature of the Rabun pluton. The pluton was emplaced deep within the Earth's crust (>30 km) and would probably not have exerted force to displace the Earth's surface.

#### *Principle of effective stress*

Hutton (1997) suggested that the principle of effective stress may be important for the emplacement of plutons in contractional tectonic settings. This mechanism requires that forces within the magma become incorporated into the overall regional stress field. This would allow the magma to overcome the compressional forces within the contractional zone. This mechanism is a difficult hypothesis to test. The pluton is clearly syntectonic, in a convergent setting.

#### *Dike-feeding of the pluton*

Johnson et al. (2001) put forth dike-feeding as a pluton emplacement mechanism. The overall shape of the Rabun pluton (pencil-like) could have arisen from emplacement by this mechanism. However, Johnson et al. (2001) state that there should be evidence of brittle deformation of the country rock. This brittle deformation is not found around the Rabun pluton. The formation of dikes usually occurs at shallow depths where brittle

deformation style is dominant. It is unlikely that this mechanism played a part in the emplacement of the Rabun pluton.

## CHAPTER 5

### Conclusions

Conclusions drawn from this study are:

- 1) The Scaly Mountain quadrangle contains three tectonic units: the Chattahoochee thrust sheet, the Dahlonga gold belt, and the Shope Fork thrust sheet.
- 2) The rocks present in the Scaly Mountain quadrangle are: the Tallulah Falls Formation (graywacke-schist member), the Rabun granodiorite, the Otto Formation, the Coweeta Group (Coleman River Formation), calc-silicate rocks, amphibolites, and pegmatites. In addition there are surficial deposits of colluvium, alluvium, and ancient landslides.
- 3) There are six to seven deformation events represented in the rocks in the Scaly Mountain quadrangle.
- 4) Evidence for multiple deformation events can be seen along the trace of the Chattahoochee fault. The fault deforms the Rabun granodiorite, truncates structures in the surrounding country rock, and is itself folded. Evidence for multiple deformation events can also be seen in the surrounding country rock. There is an early foliation that is preserved in boudins. There are at least two generations of folding as well.
- 5) The Chattahoochee fault postdates the Rabun granodiorite. Evidence for this is the deformation of the Rabun by the Chattahoochee fault.
- 6) The Rabun granodiorite consists of a medium-grained phase and a megacrystic phase.

- 7) The Rabun granodiorite contains a magmatic flow foliation and an overprinting tectonic foliation.
- 8) The Rabun granodiorite was emplaced primarily by diapirism. Stoping may have played a minor role in the emplacement of the pluton.

This research is the first detailed structural study of the Rabun granodiorite and provides some insight into the histories of similar plutons occurring within the eastern Blue Ridge. This research also provides new data supporting findings from previous studies of the regional geology of the eastern Blue Ridge province of the southern Appalachians.

**REFERENCES CITED**

## REFERENCES CITED

- Acker, L.L., Unpublished data, Dillard and Rabun Bald quadrangles, North Carolina, Scale 1/24,000.
- Eckert, J.O., Unpublished data, Corbin Knob and Franklin quadrangles, North Carolina, Scale 1/24,000.
- Fernandez, C., Castro, A., and De La Rosa, J. D., 1997, Rheological aspects of magma transport inferred from rock structures, *in* Bouchez, J. L. et al. editors, *Granite: from segregation of melt to emplacement*, Kluwer Academic Publishers, p. 75-91.
- Fullagar, P. D., Hatcher, R. D., Jr., and Merschat, C. E., 1979, 1200 m.y. old gneisses in the Blue Ridge Province of North and South Carolina: *Southeastern Geology*, v. 20, p. 69-77.
- Fullagar, P. D., Goldberg, S. A., and Butler, J. R., 1997, Nd and Sr isotopic characterization of crystalline rocks from the southern Appalachian Piedmont and Blue Ridge, North and South Carolina, *in* Sinha, A. K., Whalen, J. B., and Hogan, J. P., eds., *The nature of magmatism in the Appalachian Orogen*: Boulder, Colorado, Geological Society of America Memoir 191, p. 165-179.
- Gillon, K. A., 1982, Stratigraphy, structural, and metamorphic geology of portions of the Cowrock and Helen, Georgia 71/2 minute quadrangles [Unpublished M.S. thesis]: Athens, University of Georgia, 236 p.
- Hatcher, R. D., Jr., 1971, The geology of Rabun and Habersham counties, Georgia: The Geological Survey of Georgia, Department of Mines, Mining and Geology, Bulletin 83, 51 p.
- Hatcher, R. D., Jr., 1974, An introduction to the Blue Ridge tectonic history of northeast Georgia: The Georgia Geological Survey, Guidebook 13-A, 60 p.
- Hatcher, R. D., Jr., 1976, Introduction to the geology of the eastern Blue Ridge of the Carolinas and nearby Georgia: Carolina Geological Society, Field Trip Guidebook, 53 p.
- Hatcher, R. D., Jr., 1978, Tectonics of the western Piedmont and Blue Ridge, southern Appalachians: Review and speculation: *American Journal of Science*, v. 278, p. 276-304.
- Hatcher, R. D., Jr., 1979, The Coweeta Group and Coweeta syncline: Major features of the North Carolina-Georgia Blue Ridge: *Southeastern Geology*, v. 21, p. 17-29.

- Hatcher, R. D., Jr., 1980, Geologic map and mineral resources of the Prentiss quadrangle, North Carolina: North Carolina Geological Survey, GM 167-SW, scale 1/24,000.
- Hatcher, R. D., Jr., 1989, Tectonic synthesis of the U. S. Appalachians, *in* Hatcher, R. D., Jr., Thomas, W. A., and Viele, G. W., eds., *The Appalachian-Ouachita Orogen in the United States*: Boulder, Colorado, Geological Society of America, *The Geology of North America*, v. F-2, p. 511-535.
- Hatcher, R. D., Jr., and Goldberg, S. A., 1991, The Blue Ridge geologic province, *in* Horton, J. W. and Zullo, V. A., eds., *The Geology of the Carolinas-Carolina Geological Society 50th Anniversary Volume*: Knoxville, TN, The University of Tennessee Press, p. 11-35.
- Hatcher, R. D., Jr., 1995, *Structural Geology: Principles, concepts, and problems*, 2<sup>nd</sup> ed., Prentiss-Hall, Inc., Englewood Cliffs, New Jersey, p. 525.
- Hatcher, R. D., Jr., 1999, Digital map of the eastern Blue Ridge in northeastern Georgia, northwestern South Carolina, and southwestern North Carolina: *Geological Society of America Abstracts with Programs (SE Section)*, v. 31, p. A-20.
- Hatcher, R. D., Jr., 2001, Rheological partitioning during multiple reactivation of the Palaeozoic Brevard fault zone, southern Appalachians, USA, *in* Holdsworth, R.E., Strachan, R.A., Magloughlin, J.F., and Knipe, R.J., eds., *The nature and tectonic significance of fault zone weakening*: Geological Society, London, *Special Publications*, 186, p. 255-268.
- Hopson, J. L., Hatcher, R. D., Jr., and Stieve, A. L., 1989, Geology of the eastern Blue Ridge, northeastern Georgia and the adjacent Carolinas, *in* Fritz, W. J., Hatcher, R. D., Jr., and Hopson, J. L., eds., *Geology of the eastern Blue Ridge of northeast Georgia and the adjacent Carolinas*: Georgia Geological Society Guidebooks, v. 9, p. 1-40.
- Hopson, J. L., 1994, *Geology of part of the eastern Blue Ridge, northeast Georgia and the adjacent Carolinas* [Ph.D. dissertation]: Knoxville, University of Tennessee, 350 p.
- Horton, J. W., Jr., and McConnell, K. I., 1991, The western Piedmont, *in* Horton, J. W. and Zullo, V. A., eds., *The Geology of the Carolinas-Carolina Geological Society 50th Anniversary Volume*: Knoxville, TN, The University of Tennessee Press, p. 36-58.
- Hutton, D. H. W., 1997, Syntectonic granites and the principle of effective stress: A general solution to the space Problem?, *in* Bouchez, J. L., et al., eds., *Granite: From segregation of melt to emplacement fabrics*, Kluwer Academic Publishers, p. 189-197.

- John, B. E. and Stunitz, H., 1997, Magmatic fracturing and small-scale melt segregation during pluton emplacement: Evidence from the Adamello Massif (Italy), *in* Bouchez, J. L., et al., eds., Granite: From segregation of melt to emplacement fabrics, Kluwer Academic Publishers, p. 55-74.
- Johnson, S. E., Alibert, M., and Paterson, S. R., 2001, Growth rates of dike-fed plutons: Are they compatible with observations in the middle and upper crust?, *Geology*, v.29, no.8, p. 727-730.
- McBirney, A. R., 1993, *Igneous Petrology*, 2<sup>nd</sup> ed., Jones and Bartlett Publishers, Boston, Massachusetts, p. 508.
- Miller, C. F., Fullagar, P. D., Sando, T. W., Russell, G. S., Kish, S. A., Soloman, G. C., and Wood, L. F., 1990, Plutonism in the Blue Ridge of southwest North Carolina and northeast Georgia: Geological Society of America Abstracts with Programs, v. 22, p. 26.
- Miller, C. F., Fullagar, P. D., Sando, T. W., Kish, S. A., Soloman, G. C., Russell, G. S., and Wood Steltenpohl, L. F., 1997, Low-potassium, trondhjemitic to granodioritic plutonism in the eastern Blue Ridge, southwestern North Carolina-northeastern Georgia, *in* Sinha, A. K., Whalen, J. B., and Hogan, J. P., eds., The nature of magmatism in the Appalachian Orogen: Boulder, Colorado, Geological Society of America Memoir 191, p. 235-254.
- Miller, C. F., Hatcher, R. D., Jr., Ayers, J. C., Coath, C. D., and Harrison, T. M., 2000, Age and zircon inheritance of eastern Blue Ridge plutons, southwestern North Carolina and northeastern Georgia, with implications for magma history and evolution of the southern Appalachian Orogen: *American Journal of Science*, v. 300, p. 142-172.
- Nelson, A. E., 1982, Geologic map of the Tray Mountain Roadless Area, northern Georgia: U.S. Geological Survey Miscellaneous Field Studies Map MF-1347-A, scale 1:30,000.
- Paterson, S. R., Vernon, R. H., and Tobisch, O. T., 1989, A review of criteria for the identification of magmatic and tectonic foliations in granitoids: *Journal of Structural Geology*, v. 11, p. 349-363.
- Paterson, S. R. and Fowler, K. T., 1993, Re-examining pluton emplacement processes: *Journal of Structural Geology*, v. 15, p. 191-206.
- Ramsay, J. G., 1989, Emplacement kinematics of a granite diapir: The Chindamora batholith, Zimbabwe: *Journal of Structural Geology*, v. 11, p. 191-209.



- Speer, J. A., McSween, H. Y., and Gates, A. E., 1994, Generation, segregation, ascent, and emplacement of Alleghanian plutons in the southern Appalachians: *The Journal of Geology*, v. 102, p. 249-267.
- Stieve, A. L., 1989, The structural evolution and metamorphism of the southern portion of the Tallulah Falls Dome, northeast Georgia [Ph.D. dissertation]: Columbia, University of South Carolina, 206 p.
- Teague, K. H. and Furcron, A. S., 1948, Geology and mineral resources of Rabun and Habersham counties, Georgia: Georgia Dept. of Mines, Mining and Geology, scale 1/125,000.
- Yurkovich, S., Unpublished geologic map of Corbin Knob quadrangle, North Carolina, scale 1/24,000.

## **APPENDICES**

**APPENDIX A**

**STRUCTURAL DATA FOR THE SCALY MOUNTAIN QUADRANGLE**

**NOTE:** Structural measurements are presented in quadrant format. Abbreviations in the lithologic unit column refer to: tf-Tallulah Falls Formation, rg-Rabun granodiorite, op-Otto Formation pelitic schist, oss-Otto Formation metasandstone, cr-Coleman River Formation. All Scaly Mountain data were collected as part of this study.

Station	Foliation		Feldspar Lineation		Fold Axis		Axial Surface		Lithologic Unit
	Strike	Dip	Plunge	Trend	Plunge	Trend	Strike	Dip	
SM1	N 63 E	30 SE							tf
SM2	N 75 E	54 NW							tf
SM3	N 67 E	47 NW							tf
SM4	N 30 W	18 SW							tf
SM5	N 22 E	22 SE							tf
SM6	N 56 W	15 NE							tf
SM7	N 14 W	39 SW							tf
SM8	N 03 E	68 SE							tf
SM9	N 05 E	60 NW							tf
SM10	N 51 E	50 SE							tf
SM11	N 35 E	20 SE							tf
SM12	N 06 W	41 SW							tf
SM13	N 38 E	35 SE							tf
SM14	N 13 E	28 SE							tf
SM15	N 40 E	48 SE							rg
SM16	N 20 E	08 NW							rg
SM17	N 50 E	32 SE							rg
SM18	N 10 E	32 SE							rg
SM19	N 65 E	42 SE							rg
SM21	N 30 E	31 SE							rg
SM22	N 30 E	58 SE							rg
SM23	N 29 E	36 SE							rg
SM24	N 15 W	24 SW							op
SM25	N 65 E	30 NW							op
SM26	N 45 E	34 NW							op
SM27	N 48 E	32 SE							op
SM28	N 20 E	23 SE							op
SM29	N 44 E	48 SE							op
SM30	N 40 W	64 SW							op
SM31	N 50 E	55 SE							op
SM32	N 10 E	41 NW							op
SM33	N 30 E	16 SE							op
SM34	N 30 E	54 SE							op
SM35	N 50 E	46 SE							op
SM36	N 60 E	46 SE							op
SM37	N 45 E	39 SE							op
SM38	N 52 E	44 SE							op
SM39	N 40 E	80 SE							op
SM40	N 24 E	30 SE							op
SM41	N 56 E	64 SE							op
SM42	N 50 E	74 NW							op
SM43	N 52 E	56 SE							op
SM44	N 65 E	82 SE							op
SM45	N 61 E	50 NW							op
SM46	N 45 E	81 SE							op
SM47	N 20 E	40 SE							op
SM48	N 20 W	43 SW							op
SM49	N 50 E	62 NW							op
SM50	N 52 E	70 NW							op
SM51	N 25 E	46 SE							op
SM52	N 34 E	84 SE							op
SM53	N 16 E	66 NW							op
SM54	N 26 E	85 SE							op
SM55	N 50 E	40 NW							op
SM56	N 30 E	15 NW							op
SM57	N 22 E	42 NW							op
SM58	N 54 E	37 NW							op
SM59	N 42 E	46 NW							op
SM60	N 44 E	22 SE							op
SM61	N 26 E	30 NW							op
SM62	N 45 E	68 SE							op
SM63	N 28 E	56 SE							op

Station	Foliation		Feldspar Lineation		Fold Axis		Axial Surface		Lithologic Unit
	Strike	Dip	Plunge	Trend	Plunge	Trend	Strike	Dip	
SM64	N 42 E	48 SE							op
SM65	N 34 E	58 SE							op
SM66	N 26 E	76 NW							op
SM67	N 32 E	49 SE							op
SM68	N 29 E	78 NW							op
SM69	N 28 E	28 SE							op
SM70	N 19 E	54 NW							op
SM71	N 30 E	64 NW							op
SM72	N 35 E	76 SE							op
SM73	N 20 E	42 SE							op
SM74	N 20 E	70 NW							op
SM75	N 41 E	38 NW							op
SM76	N 35 E	50 NW							op
SM77	N 34 E	63 NW							op
SM78	N 35 E	64 NW							op
SM79	N 36 E	45 NW							op
SM80	N 52 E	45 SE							op
SM81	N 50 E	60 SE							op
SM82	N 45 W	66 NE							tf
SM83	N 68 E	20 SE							tf
SM84	N 25 E	20 SE							tf
SM85	N 30 W	15 NE							tf
SM86	N 25 E	65 NW							tf
SM87	N 22 E	72 SE							tf
SM88	N 30 E	72 SE							tf
SM89	N 60 E	20 SE							tf
SM90	N 35 E	84 SE							tf
SM91	N 10 E	77 SE							tf
SM92	N 65 E	20 SE							tf
SM93	N 10 E	48 SE							tf
SM94	N 36 E	45 NW							tf
SM95	N 21 E	60 SE							tf
SM96	N 35 E	50 SE							tf
SM97	N 28 E	70 SE							tf
SM98	N 75 E	67 SE							rg
SM99	N 64 E	40 SE							rg
SM100	N 60 E	25 NW							rg
SM101	N 45 E	54 NW							rg
SM102	N 30 E	24 SE							tf
SM103	N 40 E	50 SE							tf
SM104	N 50 E	50 SE							tf
SM105	N 30 E	32 SE							tf
SM106	N 26 E	30 SE							tf
SM107	N 36 W	40 SW							tf
SM108	N 40 E	54 SE							tf
SM109	N 30 E	44 SE							tf
SM110	N 35 E	46 SE							tf
SM111	N 55 W	40 SW							tf
SM112	N 40 E	48 SE							tf
SM113	N 40 E	46 SE							tf
SM114	N 20 E	54 SE							tf
SM115	N 10 E	40 SE							tf
SM116	N 40 E	45 SE							tf
SM117	N 50 E	70 SE							tf
SM118	N 20 E	52 SE							tf
SM119	N 25 E	26 SE							tf
SM120	N 50 E	31 SE							tf
SM121	N 30 E	25 NW	23	350					rg
SM122	N 30 E	20 NW	49	010					rg
SM123	N 60 E	26 NW	30	360					rg
SM124	N 50 W	16 SW	08	016					rg
SM125	N 30 E	24 SE	16	006					rg

Station	Foliation		Feldspar Lineation		Fold Axis		Axial Surface		Lithologic Unit
	Strike	Dip	Plunge	Trend	Plunge	Trend	Strike	Dip	
SM126	N 28 E	20 SE	18	010					rg
SM127	N 20 W	24 NE	16	010					rg
SM128	N 26 E	24 NW	10	004					rg
SM129	N 30 E	40 NW							rg
SM130	N 11 E	24 NW	31	030					rg
SM131	N 31 E	18 SE	40	035					rg
SM132	N 26 E	41 SE	39	055					rg
SM133	N 70 W	43 SW	26	046					rg
SM134	N 30 E	31 NW	26	043					rg
SM135	N 26 E	84 SE							tf
SM136	N 25 E	69 SE							tf
SM137	N 33 E	36 NW	28	050					rg
SM138	N 28 E	39 SE	45	050					rg
SM139	N 40 E	36 NW							rg
SM140	N 45 W	20 SW	34	040					rg
SM141	N 20 W	27 NE							tf
SM142					20	060	N 20 E	15 SE	tf
SM143	N 21 W	29 NE							tf
SM144	N 10 W	25 NE							tf
SM145	N 20 E	51 NW							op
SM146	N 49 E	61 SE							op
SM147	N 24 E	74 SE							op
SM148	N 21 E	80 SE							op
SM149	N 18 E	81 SE							op
SM150	N 35 E	53 SE							op
SM151	N 38 E	80 SE							op
SM152	N 28 E	69 SE							op
SM153	N 15 E	74 SE							op
SM154	N 16 E	71 SE							op
SM155	N 27 E	76 SE							op
SM156	N 32 E	73 SE							op
SM157	N 34 E	71 NW							op
SM158	N 22 E	85 SE							op
SM159	N 49 E	60 SE							op
SM160	N 24 E	82 SE							op
SM161	N 57 E	78 NW							op
SM162	N 60 E	66 SE							oss
SM163	N 18 E	54 NW							oss
SM164	N 35 E	81 NW							oss
SM165	N 10 W	44 NE							op
SM166	N 54 E	65 NW							op
SM167	N 85 W	20 NE							op
SM168	N 30 E	73 SE							op
SM169	N 35 W	42 SW							op
SM170	N 21 W	27 SW							op
SM171	N 19 W	84 NE							op
SM172	N 20 E	72 SE							op
SM173	N 40 E	70 NW							op
SM174	N 50 E	78 NW							op
SM175	N 45 E	24 SE							op
SM176	N 23 E	46 SE							op
SM177	N 45 E	70 NW							op
SM178	N 34 E	82 NW							op
SM179	N 38 E	38 SE							tf
SM180	N 16 W	24 NE							tf
SM181	N 32 W	15 SW							tf
SM182	N 45 E	57 SE							tf
SM183	N 22 E	45 NW							tf
SM184	N 24 E	39 SE							tf
SM185	N 37 E	67 SE							tf
SM186	N 15 E	37 SE							tf
SM187	N 60 W	25 SW							rg

Station	Foliation		Feldspar Lincation		Fold Axis		Axial Surface		Lithologic Unit
	Strike	Dip	Plunge	Trend	Plunge	Trend	Strike	Dip	
SM188	N 48 W	16 NE							rg
SM189	N 25 W	15 NE							rg
SM190	N 25 W	25 NE							rg
SM191	N 40 E	66 SE							rg
SM192	N 39 E	77 SE							rg
SM193	N 24 E	34 NW							rg
SM194	N 37 E	65 SE	25	295					rg
SM195	N 24 E	37 SE							rg
SM196	N 23 E	36 SE							rg
SM197	N 29 E	17 SE							rg
SM198	N 30 E	40 SE	36	052					rg
SM199	N 28 E	64 SE	24	050					rg
SM200	N 33 E	32 NW	26	054					rg
SM201	N 45 W	35 SW	40	051					rg
SM202	N 25 E	47 SE	23	055					rg
SM203	N 32 W	33 SW							rg
SM204	N 20 W	15 SW	40	054					rg
SM205	N 39 E	34 SE							rg
SM206	N 39 E	73 SE							tf
SM207	N 31 W	30 NE							rg
SM208	N 45 E	79 SE							tf
SM209	N 55 E	54 SE							tf
SM210	N 35 E	66 SE							tf
SM211	N 30 E	49 SE							tf
SM212	N 39 E	54 SE							tf
SM213	N 31 E	45 SE							tf
SM214	N 32 E	60 SE							tf
SM215	N 40 E	37 SE							tf
SM216	N 20 E	62 NW							tf
SM217	N 23 E	29 SE							tf
SM218	N 80 W	44 NE							tf
SM219	N 44 E	38 SE							tf
SM220	N 50 E	40 SE							tf
SM221	N 36 E	49 SE							tf
SM222	N 44 E	50 SE							tf
SM223	N 37 E	52 SE							tf
SM224					25	010	N 25 E	35 SE	tf
SM225	N 41 E	51 SE							tf
SM226	N 52 E	50 SE							tf
SM227	N 29 E	40 SE							tf
SM228	N 29 E	44 SE							tf
SM229	N 46 E	56 SE							tf
SM230	N 48 E	53 SE							tf
SM231	N 44 E	60 SE							tf
SM232	N 34 E	53 SE							tf
SM233	N 19 E	56 SE							tf
SM234	N 43 E	35 SE							tf
SM235	N 36 E	56 SE							tf
SM236	N 34 E	49 SE							tf
SM237	N 34 E	64 SE							tf
SM238	N 15 E	48 SE							tf
SM239	N 24 E	33 SE							tf
SM240	N 38 E	34 SE							tf
SM241	N 28 E	40 SE							tf
SM242	N 17 E	47 SE							tf
SM243	N 22 E	52 SE							tf
SM244	N 35 E	39 NW							tf
SM245	N 21 E	64 SE							tf
SM246	N 16 E	45 SE							tf
SM247	N 15 E	61 SE							tf
SM248	N 24 E	49 SE							tf
SM249	N 26 E	50 SE							tf



Station	Foliation		Feldspar Lineation		Fold Axis		Axial Surface		Lithologic Unit
	Strike	Dip	Plunge	Trend	Plunge	Trend	Strike	Dip	
SM250	N 30 W	55 NE							tf
SM251	N 36 E	67 SE							tf
SM252	N 30 E	35 NW							tf
SM253	N 20 E	33 SE							tf
SM254	N 24 E	57 SE							tf
SM255	N 33 E	39 SE							tf
SM256	N 27 E	55 SE							tf
SM257	N 25 W	24 NE							tf
SM258	N 46 E	34 SE							tf
SM259	N 28 E	05 SE							tf
SM260	N 22 E	34 SE							tf
SM261	N 37 E	34 SE							tf
SM262	N 18 E	74 SE							tf
SM263	N 76 E	32 NW							tf
SM264	N 10 E	43 SE							tf
SM265	N 25 E	44 SE							tf
SM266	N 32 E	34 SE							tf
SM267	N 15 E	80 NW							tf
SM268	N 23 W	31 SW							tf
SM269	N 23 E	49 SE							tf
SM270	N 05 E	66 NW							tf
SM271	N 12 W	54 SW							tf
SM272	N 30 E	55 NW							tf
SM273	N 14 W	87 NE							tf
SM274	N 04 E	63 SE							tf
SM275	N 75 E	64 SE							tf
SM276	N 27 E	75 NW							tf
SM277	N 14 W	25 NE							tf
SM278	N 26 E	21 SE							tf
SM279	N 25 W	20 NE							tf
SM280	N 06 E	35 SE							tf
SM281	N 26 E	48 SE							tf
SM282	N 68 W	22 NE							tf
SM283	N 20 W	34 NE							tf
SM284	N 52 W	18 NE							tf
SM285	N 17 E	38 SE							tf
SM286	N 24 E	31 SE							tf
SM287	N 20 W	18 SW							tf
SM288	N 39 W	10 SW							tf
SM289	N 10 E	06 SE							tf
SM290	N 15 E	52 NW							tf
SM291	N 18 E	29 SE							tf
SM292	N 33 E	52 NW							tf
SM293	N 10 E	29 SE							tf
SM294	N 31 W	33 NE							tf
SM295	N 18 E	23 SE							tf
SM296	N 60 E	43 SE							tf
SM297	N 30 W	56 NE							tf
SM298	N 19 E	46 SE							tf
SM299	N 13 E	54 SE							tf
SM300	N 10 E	30 SE							tf
SM301	N 12 E	26 SE							tf
SM302	N 15 E	23 SE							tf
SM303	N 20 E	29 NW							op
SM304	N 32 E	32 SE							op
SM305	N 25 E	38 SE							op
SM306	N 21 E	32 NW							op
SM307	N 25 E	50 SE							op
SM308	N 22 E	36 SE							op
SM309	N 31 E	40 SE							op
SM310	N 18 E	12 NW							op
SM311	N 25 E	40 NW							op

Station	Foliation		Feldspar Lineation		Fold Axis		Axial Surface		Lithologic Unit
	Strike	Dip	Plunge	Trend	Plunge	Trend	Strike	Dip	
SM312	N 10 E	64 SE							oss
SM313	N 20 E	20 SE							oss
SM314	N 25 W	30 NE							oss
SM315	N 35 W	36 NE							op
SM316	N 64 E	40 SE							op
SM317	N 48 E	40 SE							op
SM318	N 40 E	28 NW							op
SM319	N 50 E	45 SE							oss
SM320	N 28 E	32 NW							oss
SM321	N 40 E	26 NW							oss
SM322	N 10 E	48 SE							op
SM323	N 20 E	28 SE							op
SM324	N 12 E	34 SE							tf
SM325	N 10 E	21 SE							tf
SM326	N 45 E	36 NW							tf
SM327	N 32 W	24 NE							tf
SM328	N 26 E	59 NW							tf
SM329	N 24 E	46 SE							tf
SM330					05	015	N 30 E	10 NW	tf
SM331	N 70 E	34 SE							tf
SM332	N 45 E	48 SE							tf
SM333	N 16 E	39 SE							tf
SM334	N 40 E	69 SE							tf
SM335	N 41 W	25 SW							tf
SM336	N 55 W	15 NE							tf
SM337	N 50 W	10 SW							tf
SM338	N 12 E	22 NW							tf
SM339	N 18 E	63 SE							tf
SM340	N 30 E	37 SE							tf
SM341	N 20 E	36 SE							tf
SM342	N 35 E	61 SE							tf
SM343	N 20 W	40 NE							tf
SM344	N 30 W	25 NE							tf
SM345	N 42 E	25 SE							tf
SM346	N 40 E	56 SE							tf
SM347	N 50 W	20 NE							tf
SM348	N 14 E	85 SE							tf
SM349	N 20 E	20 SE							tf
SM350	N 33 E	47 SE							tf
SM351	N 77 W	24 NE							tf
SM352	N 65 W	36 SW							tf
SM353	N 60 E	20 SE							rg
SM354	N 40 E	30 SE							rg
SM355	N 70 E	55 SE							tf
SM356	N 38 E	36 SE							tf
SM357	N 52 E	45 SE							rg
SM358	N 55 W	10 SW							rg
SM359	N 25 E	15 NW							rg
SM360	N 25 E	38 SE							op
SM361	N 41 E	74 SE							op
SM362	N 15 E	42 SE							op
SM363	N 40 E	34 SE							op
SM364	N 10 E	77 SE							oss
SM365	N 34 E	74 SE							op
SM366	N 31 E	49 SE							oss
SM367	N 30 E	70 SE							op
SM368	N 20 E	32 NW							op
SM369	N 35 W	39 SW							op
SM370	N 36 W	43 SW							op
SM371	N 23 W	44 SW							op
SM372	N 85 W	40 SW							op
SM373	N 30 W	44 SW							oss

Station	Foliation		Feldspar Lineation		Fold Axis		Axial Surface		Lithologic Unit
	Strike	Dip	Plunge	Trend	Plunge	Trend	Strike	Dip	
SM374	N 46 E	63 NW							oss
SM375	N 65 W	32 NE							oss
SM376	N 50 E	18 NW							oss
SM377	N 30 E	37 NW							op
SM378	N 25 E	74 NW							oss
SM379	N 60 E	69 NW							op
SM380	N 36 E	78 NW							op
SM381	N 57 E	40 NW							op
SM382	N 50 E	42 NW							op
SM383	N 38 E	78 NW							op
SM384	N 75 E	42 NW							op
SM385	N 50 E	44 NW							op
SM386	N 47 E	73 NW							op
SM387	N 37 E	48 SE							op
SM388	N 70 E	70 NW							op
SM389	N 34 E	82 NW							tf
SM390	N 28 E	74 SE							tf
SM391	N 36 E	54 NW							tf
SM392	N 30 E	54 SE							tf
SM393	N 28 E	69 SE							tf
SM394	N 30 E	81 NW							tf
SM395	N 35 E	59 NW							oss
SM396	N 22 E	82 NW							oss
SM397	N 50 E	60 NW							oss
SM398	N 41 E	73 SE							oss
SM399	N 32 E	40 NW							oss
SM400	N 42 E	72 NW							oss
SM401	N 31 E	45 SE							oss
SM402	N 34 E	66 SE							oss
SM403	N 50 E	67 NW							rg
SM404	N 20 W	30 NE							rg
SM405	N 20 W	20 NE							tf
SM406	N 35 E	27 SE							rg
SM407	N 15 W	13 NE							rg
SM408	N 23 W	30 NE							rg
SM409	N 15 E	21 SE							tf
SM410	N 30 E	22 SE							rg
SM411	N 28 E	24 NW							tf
SM412	N 25 E	58 SE							rg
SM413	N 34 E	36 SE							tf
SM414	N 40 E	32 NW							tf
SM415	N 35 E	70 SE							rg
SM416	N 10 E	30 NW							rg
SM417	N 15 W	51 NE							rg
SM418	N 62 W	35 SW							rg
SM419	N 50 W	22 SW	12	070					rg
SM420	N 32 W	20 NE							rg
SM421	N 45 W	21 NE							rg
SM422	N 55 E	29 SE	24	035					rg
SM423	N 48 E	24 SE	42	026					rg
SM424	N 40 E	40 SE	20	313					rg
SM425	N 25 E	20 SE	37	305					rg
SM426	N 20 W	36 SW							rg
SM427	N 25 E	25 SE	35	350					rg
SM428	N 20 E	25 SE	32	340					rg
SM429	N 25 W	20 SW	15	060					rg
SM430	N 23 E	26 SE	37	057					rg
SM431	N 32 E	20 SE	24	312					rg
SM432	N 36 E	15 SE							rg
SM433	N 52 E	30 SE							rg
SM434	N 53 E	34 SE							rg
SM435									rg

Station	Foliation		Feldspar Lineation		Fold Axis		Axial Surface		Lithologic Unit
	Strike	Dip	Plunge	Trend	Plunge	Trend	Strike	Dip	
SM436	N 65 E	27 SE							rg
SM437	N 62 E	57 SE							rg
SM437(B)	N 50 E	25 SE							rg
SM438	N 60 E	40 SE							rg
SM439	N 54 E	41 SE	45	060					rg
SM440	N 50 E	66 SE							rg
SM441	N 70 E	60 SE							rg
SM442	N 70 E	67 SE							rg
SM443	N 50 E	28 SE							rg
SM444	N 35 E	20 SE							rg
SM445	N 45 E	45 NW	0	025					rg
SM446	N 45 W	30 NE	0	045					rg
SM447	N 60 W	34 NE							rg
SM448	N 55 E	38 SE							rg
SM449	N 25 W	25 NE							rg
SM450	N 35 E	20 NW							rg
SM451	N 45 E	65 SE							rg
SM452	N 45 E	25 SE							rg
SM453	N 60 W	38 SW							rg
SM454	N 40 W	25 SW							rg
SM455	N 35 E	27 NW							rg
SM456	N 40 W	42 SW							rg
SM457	N 45 E	52 SE							rg
SM458	N 45 E	30 SE							rg
SM459	N 45 W	28 SW							rg
SM460	N 20 W	20 SW							rg
SM461	N 35 W	30 SW							rg
SM462	N 25 W	21 SW							rg
SM463	N 35 E	39 NW							rg
SM464	N 30 W	28 SW							rg
SM465	N 37 E	34 SE							rg
SM466	N 26 E	36 SE							rg
SM467	N 41 E	31 SE							rg
SM468	N 20 E	20 SE							rg
SM469	N 37 E	35 SE							rg
SM470	N 72 E	50 SE							rg
SM471	N 39 E	44 SE							rg
SM472	N 30 E	50 SE							rg
SM473	N 40 E	74 SE							rg
SM474	N 33 E	41 NW							rg
SM475	N 26 E	37 SE							rg
SM476	N 20 E	25 SE							rg
SM477	N 45 E	38 SE							rg
SM478	N 30 E	32 SE							rg
SM479	N 44 E	68 SE							tf
SM480	N 83 E	56 NW							tf
SM481	N 30 E	55 SE							tf
SM482	N 29 E	51 SE							tf
SM483	N 49 W	26 SW							tf
SM484	N 44 E	50 NW							tf
SM485	N 30 W	20 NE							tf
SM486	N 60 W	45 NE							tf
SM487	N 35 W	46 SW							tf
SM488	N 30 E	35 SE							tf
SM489	N 30 W	34 NE							tf
SM490	N 37 W	32 NE							tf
SM491	N 49 E	56 SE							rg
SM492	N 56 E	44 SE							rg
SM493	N 74 E	36 SE							rg
SM494	N 21 E	35 SE							rg
SM495	N 16 W	73 NE							tf
SM496	N 54 W	41 SW							tf

Station	Foliation		Feldspar Lineation		Fold Axis		Axial Surface		Lithologic Unit
	Strike	Dip	Plunge	Trend	Plunge	Trend	Strike	Dip	
SM497	N 40 E	14 NW							tf
SM498	N 53 W	74 NE							tf
SM499	N 18 E	34 NW							tf
SM499B	N 53 E	61 SE							tf
SM499C	N 24 E	32 NW							tf
SM500					16	042	N 44 E	41 NW	tf
SM501	N 42 E	53 SE							tf
SM502	N 48 E	63 SE							tf
SM503	N 52 E	57 SE							tf
SM504	N 56 E	46 SE							tf
SM505	N 33 E	44 SE							tf
SM506	N 27 E	35 SE							tf
SM507	N 37 W	54 NE							tf
SM508	N 54 W	46 SW							tf
SM509	N 29 W	32 NE							tf
SM510	N 34 E	47 SE							tf
SM511	N 08 E	41 SE							tf
SM512	N 39 E	60 SE							tf
SM513	N 38 E	60 NW							tf
SM514	N 36 E	50 SE							tf
SM515	N 15 E	61 NW							tf
SM516	N 28 E	20 NW							tf
SM517	N 05 E	68 SE							tf
SM518	N 18 E	39 SE							tf
SM519	N 56 E	36 SE							tf
SM520	N 58 E	39 SE							tf
SM521	N 46 E	54 SE							tf
SM522	N 44 E	71 SE							tf
SM523	N 68 E	26 SE							tf
SM524	N 36 E	85 NW							tf
SM525	N 44 E	35 SE							tf
SM526	N 30 E	43 SE							tf
SM527	N 38 W	26 SW							tf
SM528	N 62 W	18 SW							tf
SM529	N 24 E	60 SE							tf
SM530	N 37 E	40 NW							tf
SM531	N 57 E	37 SE							tf
SM532	N 53 E	65 SE							tf
SM533	N 23 E	78 NW							tf
SM534	N 20 W	26 NE							tf
SM535	N 40 W	32 NE							tf
SM536	N 41 E	35 SE							rg
SM537	N 36 E	27 SE							rg
SM538	N 16 W	24 SW							rg
SM539	N 48 E	26 SE							rg
SM540	N 70 W	45 SW							rg
SM541	N 30 E	61 SE							rg
SM542	N 23 W	38 NE							rg
SM543	N 36 E	43 NW							rg
SM544	N 30 E	24 SE							rg
SM545	N 29 W	20 NE							rg
SM546	N 05 E	15 NW							rg
SM547	N 28 E	32 SE							tf
SM548	N 30 E	20 SE							tf
SM549	N 29 E	28 SE							tf
SM550	N 24 E	32 NW							rg
SM551	N 36 E	56 NW							rg
SM552	N 60 E	25 SE							rg
SM553	N 38 E	32 SE							rg
SM554	N 45 E	63 SE							rg
SM555	N 31 E	35 SE							rg
SM556	N 40 E	40 SE							tf

Station	Foliation		Feldspar Lineation		Fold Axis		Axial Surface		Lithologic Unit
	Strike	Dip	Plunge	Trend	Plunge	Trend	Strike	Dip	
SM557	N 27 E	53 SE							tf
SM558	N 78 W	76 SW							tf
SM559	N 21 E	25 SE							
SM560	N 36 E	33 SE							rg
SM561	N 41 E	34 SE							rg
SM562	N 23 E	21 NW							rg
SM563	N 20 E	26 NW							rg
SM564	N 21 W	26 NE							rg
SM565	N 52 E	54 SE							rg
SM566	N 33 W	40 SW							rg
SM567	N 18 E	34 SE							tf
SM568	N 34 E	40 SE							tf
SM569	N 51 E	62 SE							tf
SM570	N 42 E	32 SE							tf
SM571	N 27 W	28 NE							tf
SM572	N 45 E	41 SE							tf
SM573	N 39 E	46 SE							tf
SM574	N 23 E	32 NW							
SM575	N 43 E	25 SE							rg
SM576	N 29 E	39 SE							rg
SM577	N 60 E	32 SE							rg
SM578	N 34 E	48 SE							rg
SM579	N 28 E	41 SE							tf
SM580	N 34 E	39 SE							tf
SM581	N 24 E	34 SE							rg
SM582	N 60 E	58 SE							rg
SM583	N 34 E	62 SE							tf
SM584	N 25 E	39 SE							tf
SM585	N 38 E	47 SE							tf
SM586	N 29 E	36 SE							tf
SM587	N 21 E	64 SE							tf
SM588	N 24 E	34 SE							tf
SM589	N 18 E	44 SE							tf
SM590	N 24 E	73 SE							tf
SM591	N 47 E	35 SE							tf
SM592	N 46 E	52 SE							tf
SM593	N 23 W	15 SW							tf
SM594	N 26 W	38 NE							tf
SM595	N 20 W	19 NE							tf
SM596	N 23 W	34 NE							tf
SM597	N 57 E	64 SE							rg
SM598	N 38 E	46 SE							tf
SM599	N 43 E	52 SE							rg
SM600	N 27 E	43 SE							rg
SM601	N 60 E	51 SE							rg
SM602	N 56 E	62 SE							rg
SM603	N 21 E	36 SE							tf
SM604	N 35 E	47 SE							tf
SM605	N 27 E	40 SE							tf
SM606	N 31 E	52 SE							tf
SM607	N 42 E	67 SE							tf
SM608	N 70 E	43 SE							tf
SM609	N 20 W	15 NE							tf
SM610	N 30 E	27 SE							tf
SM611	N 25 E	38 SE							tf
SM612	N 32 E	50 SE							tf
SM613	N 17 E	33 SE							tf
SM614	N 29 E	40 SE							tf
SM615	N 39 E	42 SE							tf
SM616	N 32 E	42 SE							tf
SM617	N 34 E	44 SE							tf
SM618	N 40 E	38 SE							tf

Station	Foliation		Feldspar Lineation		Fold Axis		Axial Surface		Lithologic Unit
	Strike	Dip	Plunge	Trend	Plunge	Trend	Strike	Dip	
SM619	N 47 E	65 NW							tf
SM620	N 48 E	60 SE							tf
SM621	N 37 E	17 SE							tf
SM622	N 34 E	65 SE							tf
SM623	N 43 W	37 NE							tf
SM624	N 42 E	49 NW							tf
SM625	N 36 E	62 SE							tf
SM 625B	N 35 E	68 NW							tf
SM626	N 38 E	35 SE							tf
SM627	N 32 E	42 SE							tf
SM628	N 21 E	51 NW							tf
SM629	N 41 E	70 SE							tf
SM630	N 54 E	43 NW							tf
SM631	N 28 E	55 NW							tf
SM632	N 25 E	67 NW							tf
SM633	N 10 W	62 NE							tf
SM634	N 15 E	76 SE							tf
SM635									tf
SM636	N 51 E	56 NW							tf
SM637	N 27 E	38 NW							tf
SM638	N 40 W	40 SW							tf
SM639	N 70 E	48 SE							tf
SM640	N 20 W	37 NE							tf
SM641	N 35 E	41 SE							tf
SM642	N 30 E	45 SE							tf
SM643	N 40 E	43 SE							tf
SM644	N 37 E	49 SE							tf
SM645	N 43 E	39 SE							tf
SM646	N 38 E	42 SE							tf
SM647	N 35 E	40 SE							tf
SM648	N 20 W	26 NE							tf
SM649	N 28 W	21 NE							tf
SM650	N 24 W	15 NE							tf
SM651	N 31 W	32 NE							tf
SM652	N 30 E	40 SE							tf
SM653	N 20 W	37 NE							tf
SM654	N 31 W	42 NE							tf
SM655	N 26 W	31 NE							tf
SM656	N 21 E	40 NW							tf
SM657	N 36 E	27 SE							tf
SM658	N 25 E	34 SE							tf
SM659	N 27 W	39 NE							tf
SM660	N 42 W	40 NE							tf
SM661	N 38 E	41 NW							tf
SM662	N 25 E	31 SE							tf
SM663	N 43 E	29 SE							tf
SM664	N 27 E	36 SE							tf
SM665	N 21 E	40 SE							tf
SM666	N 27 E	38 SE							tf
SM667	N 24 E	43 SE							tf
SM668	N 20 E	40 SE							tf
SM669	N 15 W	31 NE							tf
SM670	N 21 W	27 NE							tf
SM671	N 17 W	28 NE							tf
SM672	N 23 E	37 SE							tf
SM673	N 26 E	31 SE							tf
SM674	N 18 W	37 NE							tf
SM675	N 20 W	35 NE							tf
SM676	N 37 W	45 NE							tf
SM677	N 29 E	37 SE							tf
SM678	N 34 E	46 SE							tf
SM679	N 29 E	34 SE							tf

Station	Foliation		Feldspar Lineation		Fold Axis		Axial Surface		Lithologic Unit
	Strike	Dip	Plunge	Trend	Plunge	Trend	Strike	Dip	
SM680	N 31 E	31 SE							tf
SM681	N 21 E	59 SE							rg
SM682	N 46 E	74 NW							rg
SM683	N 27 E	54 SE							rg
SM684	N 34 E	64 SE							rg
SM685	N 18 W	57 NE							tf
SM686	N 10 E	50 SE							tf
SM687	N 30 W	32 NE							tf
SM688	N 50 E	60 SE							tf
SM689	N 14 W	32 NE							tf
SM690	N 05 W	40 NE							tf
SM691	N 33 E	70 SE							tf
SM692	N 30 E	70 SE							tf
SM693	N 42 E	65 SE							tf
SM694	N 31 E	65 SE							tf
SM695	N 44 E	71 SE							tf
SM696	N 18 W	42 NE							tf
SM697	N 36 E	60 SE							tf
SM698	N 39 E	47 SE							tf
SM699	N 36 E	64 SE							tf
SM700	N 24 W	49 NE							tf
SM701	N 15 W	43 NE							tf
SM702	N 20 W	46 NE							tf
SM703	N 30 E	53 SE							tf
SM704	N 36 E	59 SE							tf
SM705	N 34 E	54 SE							tf
SM706	N 30 E	47 SE							tf
SM707	N 17 W	39 NE							tf
SM708	N 29 E	39 SE							tf
SM709	N 31 E	30 SE							tf
SM710	N 25 E	35 SE							tf
SM711	N 21 E	30 SE							tf
SM712	N 20 W	40 NE							tf
SM713	N 18 W	45 NE							tf
SM714	N 10 W	40 NE							tf
SM715	N 60 E	30 SE							tf
SM716	N 56 E	59 SE							tf
SM717	N 35 E	41 SE							tf
SM718	N 20 W	67 NE							tf
SM719	N 08 E	43 SE							tf
SM720	N 60 E	25 SE							tf
SM721	N 34 E	45 SE							tf
SM722	N 20 W	39 NE							tf
SM723	N 34 E	20 SE							rg
SM724	N 45 E	43 SE							rg
SM725	N 34 E	21 SE							rg
SM726	N 44 E	47 NW							rg
SM727	N 50 E	24 SE							rg
SM728	N 24 W	26 NE							rg
SM729	N 29 E	35 SE							rg
SM730	N 34 E	40 SE							rg
SM731	N 30 E	30 SE							rg
SM732	N 42 E	37 SE							rg
SM733	N 31 E	27 SE							rg
SM734	N 35 E	24 SE							rg
SM735	N 28 E	20 SE							rg
SM736	N 32 E	23 SE							rg
SM737	N 34 E	41 SE							rg
SM738	N 31 E	39 SE							rg
SM739	N 39 E	33 SE							rg
SM740	N 20 W	45 NE							rg
SM741	N 24 W	40 NE							rg



Station	Foliation		Feldspar Lineation		Fold Axis		Axial Surface		Lithologic Unit
	Strike	Dip	Plunge	Trend	Plunge	Trend	Strike	Dip	
SM742	N 36 E	37 SE							rg
SM743	N 32 E	22 SE							rg
SM744	N 34 E	64 SE							rg
SM745	N 35 W	29 SW							rg
SM746	N 30 E	30 SE							rg
SM747	N 36 E	20 SE							rg
SM748	N 22 W	70 NE							rg
SM749	N 39 E	53 NW							rg
SM750	N 35 E	24 SE							rg
SM751	N 30 E	25 SE							rg
SM752	N 18 W	30 NE							rg
SM753	N 30 E	47 SE							rg
SM754	N 25 E	50 SE							rg
SM755	N 35 E	60 SE							rg
SM756	N 31 E	64 SE							rg
SM757	N 36 E	64 SE							rg
SM758	N 27 E	55 SE							rg
SM759	N 32 E	21 SE							rg
SM760	N 28 W	25 NE							rg
SM761	N 25 W	29 NE							rg
SM762	N 30 E	27 SE							rg
SM763	N 33 E	22 SE							rg
SM764	N 30 E	29 SE							rg
SM765	N 35 E	26 SE							rg
SM766	N 28 E	30 SE							rg
SM767	N 24 E	28 SE							rg
SM768	N 29 E	31 SE							rg
SM769	N 32 E	26 SE							rg
SM770	N 34 E	28 SE							rg
SM771	N 18 W	38 NE							op
SM772	N 24 W	42 NE							op
SM773	N 20 E	53 SE							op
SM774	N 38 E	51 SE							op
SM775	N 36 E	67 SE							tf
SM776	N 20 W	37 NE							rg
SM777	N 31 E	40 NW							rg
SM778	N 29 W	27 SW							rg
SM779	N 36 E	41 SE							rg
SM780	N 32 E	38 SE							rg
SM781	N 27 W	31 NE							rg
SM782	N 36 E	43 NW							rg
SM783	N 26 E	34 NW							op
SM784	N 31 E	30 NW							op
SM785	N 28 E	38 NW							op
SM786	N 21 W	40 SW							op
SM787	N 29 E	42 SE							op
SM788	N 35 E	40 SE							oss
SM789	N 31 E	44 SE							oss
SM790	N 36 E	51 SE							tf
SM791	N 35 E	56 SE							tf
SM792	N 23 W	40 NE							rg
SM793	N 17 W	36 NE							rg
SM794	N 30 W	42 NE							rg
SM795	N 35 E	48 NW							rg
SM796	N 34 E	51 NW							rg
SM797	N 19 W	60 NE							rg
SM798	N 23 W	64 NE							rg
SM799	N 33 E	54 SE							tf
SM800	N 15 W	35 NE							tf
SM801	N 27 E	36 SE							tf
SM802	N 36 E	59 NW							tf
SM803	N 30 E	41 SE							tf

Station	Foliation		Feldspar Lineation		Fold Axis		Axial Surface		Lithologic
	Strike	Dip	Plunge	Trend	Plunge	Trend	Strike	Dip	Unit
SM804	N 34 E	50 NW							tf
SM805	N 39 E	46 SE							tf
SM806	N 34 W	42 NE							tf
SM807	N 40 E	37 SE							tf
SM808	N 31 E	40 SE							tf
SM809	N 27 W	51 NE							tf
SM810	N 36 E	47 SE							rg
SM811	N 39 E	40 SE							rg
SM812	N 33 E	49 SE							rg
SM813	N 15 E	40 NW							tf
SM814	N 05 W	47 SW							tf
SM815	N 30 E	36 SE							rg
SM816	N 27 E	30 SE							rg
SM817	N 35 E	50 SE							rg
SM818	N 33 E	42 SE							rg
SM819	N 36 E	39 SE							rg
SM820	N 31 E	38 SE							rg
SM821	N 33 E	35 SE							rg
SM822	N 40 E	29 SE							rg
SM823	N 30 E	30 SE							rg
SM824	N 39 E	31 SE							rg
SM825	N 36 E	42 SE							rg
SM826	N 24 E	38 SE							rg
SM827	N 29 E	41 SE							rg
SM828	N 37 E	50 SE							tf
SM829	N 30 E	57 SE							tf
SM830	N 35 E	53 SE							tf
SM831	N 31 E	47 SE							tf
SM832	N 36 E	53 SE							tf
SM833	N 41 E	48 SE							tf
SM834	N 32 E	49 SE							tf
SM835	N 36 E	55 SE							tf
SM836	N 29 E	60 SE							tf
SM837	N 37 E	62 SE							tf
SM838	N 41 E	56 SE							tf
SM839	N 39 E	52 SE							tf
SM840	N 32 E	61 SE							tf
SM841	N 27 W	52 NE							rg
SM842	N 33 E	40 SE							rg
SM843	N 29 E	37 NW							rg
SM844	N 31 W	30 NE							rg
SM845	N 39 E	40 SE							rg
SM846	N 37 E	49 NW							rg
SM847	N 41 E	53 NW							rg
SM848	N 31 E	40 NW							op
SM849	N 27 E	36 SE							oss
SM850	N 30 E	46 SE							oss
SM851	N 35 E	43 SE							oss
SM852	N 32 E	40 SE							oss
SM853	N 37 E	56 SE							tf
SM854	N 21 W	42 NE							rg
SM855	N 26 W	39 NE							rg
SM856	N 23 W	45 NE							rg
SM857	N 37 E	42 SE							op
SM858	N 41 E	61 SE							oss
SM859	N 33 E	52 SE							oss
SM860	N 44 E	49 SE							op
SM861	N 21 W	37 NE							oss
SM862	N 15 W	40 NE							oss
SM863	N 36 E	40 SE							oss
SM864	N 31 E	48 SE							oss
SM865	N 26 E	41 SE							op

Station	Foliation		Feldspar Lineation		Fold Axis		Axial Surface		Lithologic Unit
	Strike	Dip	Plunge	Trend	Plunge	Trend	Strike	Dip	
SM866	N 30 E	41 SE							op
SM867	N 37 E	36 SE							op
SM868	N 20 W	47 NE							oss
SM869	N 25 W	42 NE							oss
SM870	N 33 E	39 SE							oss
SM871	N 35 E	44 SE							oss
SM872	N 36 E	39 SE							oss
SM873	N 26 W	40 NE							op
SM874	N 30 W	51 NE							oss
SM875	N 28 W	46 NE							oss
SM876	N 33 W	44 NE							oss
SM877	N 31 E	50 SE							oss
SM878	N 40 E	47 SE							oss
SM879	N 35 E	54 SE							oss
SM880	N 31 E	67 SE							oss
SM881	N 39 E	54 SE							oss
SM882	N 28 E	49 SE							oss
SM883	N 25 E	42 SE							op
SM884	N 31 E	50 SE							oss
SM885	N 35 E	36 SE							oss
SM886	N 30 E	39 SE							oss
SM887	N 39 E	40 SE							oss
SM888	N 28 E	41 SE							oss
SM889	N 30 E	44 SE							oss
SM890	N 40 E	42 SE							oss
SM891	N 15 W	52 NE							oss
SM892	N 21 W	37 SW							oss
SM893	N 31 E	48 SE							oss
SM894	N 36 E	49 SE							oss
SM895	N 35 E	47 SE							oss
SM896	N 34 E	47 SE							oss
SM897	N 43 E	51 SE							oss
SM898	N 32 E	41 SE							oss
SM899	N 37 E	41 SE							oss
SM900	N 31 E	49 SE							oss
SM901	N 39 E	53 SE							oss
SM902	N 40 E	41 SE							oss
SM903	N 38 E	46 SE							oss
SM904	N 30 E	31 SE							oss
SM905	N 32 E	29 SE							oss
SM906	N 36 E	34 SE							oss
SM907	N 33 E	30 SE							op
SM908	N 25 E	54 SE							oss
SM909	N 20 W	43 NE							oss
SM910	N 31 E	46 SE							oss
SM911	N 26 E	36 SE							oss
SM912	N 24 E	45 SE							oss
SM913	N 21 E	59 SE							oss
SM914	N 30 E	51 SE							oss
SM915	N 24 E	46 SE							oss
SM916	N 29 E	49 SE							oss
SM917	N 35 E	40 SE							oss
SM918	N 21 E	38 SE							rg
SM919	N 33 E	50 SE							oss
SM920	N 20 E	27 SE							rg
SM921	N 31 E	25 SE							rg
SM922	N 27 E	80 NW							rg
SM923	N 15 W	26 NE							rg
SM924	N 10 W	26 NE							rg
SM925	N 23 E	27 NW							rg
SM926	N 29 E	21 SE							rg
SM927	N 22 E	24 SE							rg

Station	Foliation		Feldspar Lineation		Fold Axis		Axial Surface		Lithologic Unit
	Strike	Dip	Plunge	Trend	Plunge	Trend	Strike	Dip	
SM928	N 17 W	25 NE							rg
SM929	N 23 E	29 SE							rg
SM930	N 35 E	30 SE							rg
SM931	N 26 E	30 SE							rg
SM932	N 29 E	26 SE							rg
SM933	N 28 E	27 SE							rg
SM934	N 21 E	31 SE							rg
SM935	N 24 E	25 SE							rg
SM936	N 13 W	27 NE							rg
SM937	N 16 W	21 NE							rg
SM938	N 27 E	29 SE							rg
SM939	N 23 E	33 SE							rg
SM940	N 16 W	27 NE							rg
SM941	N 21 E	33 SE							rg
SM942	N 20 E	48 SE							oss
SM943	N 25 E	30 SE							rg
SM944	N 20 E	27 SE							rg
SM945	N 24 E	28 SE							rg
SM946	N 23 E	25 SE							rg
SM947	N 20 E	29 SE							rg
SM948	N 26 E	30 SE							rg
SM949	N 21 E	29 SE							rg
SM950	N 23 E	35 SE							rg
SM951	N 30 E	33 SE							rg
SM952	N 27 E	38 SE							rg
SM953	N 35 E	43 SE							rg
SM954	N 21 E	29 SE							tf
SM955	N 20 E	51 SE							tf
SM956	N 24 E	59 NW							tf
SM957	N 25 E	60 NW							tf
SM958	N 29 E	64 SE							tf
SM959	N 21 E	60 SE							tf
SM960	N 30 E	43 SE							rg
SM961	N 30 E	41 SE							rg
SM962	N 33 E	45 SE							rg
SM963	N 27 E	47 SE							rg
SM964	N 25 E	40 SE							rg
SM965	N 31 E	25 NW							rg
SM966	N 34 W	20 SW							rg
SM967	N 20 E	31 SE							rg
SM968	N 26 E	35 SE							rg
SM969	N 39 E	47 SE							rg
SM970	N 32 E	40 SE							rg
SM971	N 35 E	50 SE							rg
SM972	N 20 E	55 SE							tf
SM973	N 24 E	50 SE							tf
SM974	N 21 E	56 SE							tf
SM975	N 26 E	59 SE							tf
SM976	N 30 E	42 SE							rg
SM977	N 26 E	31 NW							rg
SM978	N 25 E	40 SE							rg
SM979	N 20 E	61 SE							tf
SM980	N 25 E	70 NW							tf
SM981	N 23 E	66 NW							tf
SM982	N 27 E	70 SE							tf
SM983	N 30 E	47 SE							op
SM984	N 21 E	50 SE							op
SM985	N 28 E	60 SE							op
SM986	N 26 E	51 SE							op
SM987	N 35 E	47 SE							rg
SM988	N 29 E	40 SE							rg
SM989	N 21 E	44 SE							rg

Station	Foliation		Feldspar Lineation		Fold Axis		Axial Surface		Lithologic Unit
	Strike	Dip	Plunge	Trend	Plunge	Trend	Strike	Dip	
SM990	N 24 E	37 SE							rg
SM991	N 30 E	29 SE							rg
SM992	N 27 E	33 SE							rg
SM993	N 30 E	30 NW							rg
SM994	N 26 E	41 NW							rg
SM995	N 25 E	29 SE							rg
SM996	N 31 E	35 SE							rg
SM997	N 29 E	46 SE							rg
SM998	N 30 E	25 SE							rg
SM999	N 26 E	29 SE							rg
SM1000	N 21 E	37 SE							rg
SM1001	N 35 E	51NW							rg
SM1002	N 25 W	43 NE							rg
SM1003	N 31 E	40 SE							rg
SM1004	N 27 E	51 SE							rg
SM1005	N 20 W	37 NE							rg
SM1006	N 29 W	40 NE							rg
SM1007	N 20 E	30 SE							tf
SM1008	N 25 E	34 NW							rg
SM1009	N 35 W	29 NE							rg
SM1010	N 31 E	55 SE							tf
SM1011	N 26 E	50 SE							tf
SM1012	N 35 E	54 SE							tf
SM1013	N 27 E	40 SE							tf
SM1014	N 24 E	57 SE							tf
SM1015	N 30 E	51 SE							tf
SM1016	N 32 E	54 SE							tf
SM1017	N 39 E	52 SE							tf
SM1018	N 36 E	57 SE							tf
SM1019	N 29 E	54 SE							tf
SM1020	N 31 E	49 SE							tf
SM1021	N 37 E	59 SE							tf
SM1022	N 33 E	51 SE							tf
SM1023	N 34 E	56 SE							tf
SM1024	N 38 E	52 SE							tf
SM1025	N 34 E	58 SE							tf
SM1026	N 40 E	64 SE							tf
SM1027	N 39 E	71 SE							op
SM1028	N 30 E	50 SE							tf
SM1029	N 33 E	47 SE							tf
SM1030	N 29 E	54 SE							tf
SM1031	N 30 E	50 SE							tf
SM1032	N 36 E	58 SE							tf
SM1033	N 28 E	55 SE							tf
SM1034	N 25 W	47 NE							tf
SM1035	N 31 E	52 SE							tf
SM1036	N 42 E	67 SE							tf
SM1037	N 40 E	64 SE							tf
SM1038	N 45 E	68 SE							tf
SM1039	N 41 E	60 SE							tf
SM1040	N 40 E	55 SE							tf
SM1041	N 44 E	65 SE							tf
SM1042	N 35 E	47 SE							tf
SM1043	N 31 E	57 SE							tf
SM1044	N 26 E	70 SE							tf
SM1045	N 21 E	76 NW							op
SM1046	N 35 E	61 SE							oss
SM1047	N 39 E	65 SE							oss
SM1048	N 34 E	57 SE							op
SM1049	N 37 E	65 SE							op
SM1050	N 36 E	57 SE							op
SM1051	N 41 E	68 SE							oss

Station	Foliation		Feldspar Lineation		Fold Axis		Axial Surface		Lithologic Unit
	Strike	Dip	Plunge	Trend	Plunge	Trend	Strike	Dip	
SM1052	N 40 E	60 SE							oss
SM1053	N 45 E	62 SE							oss
SM1054	N 34 E	66 NW							oss
SM1055	N 36 E	55 SE							oss
SM1056	N 29 E	67 NW							oss
SM1057	N 38 E	64 NW							oss
SM1058	N 39 E	51 SE							oss
SM1059	N 41 E	60 SE							oss
SM1060	N 36 E	57 SE							op
SM1061	N 42 E	65 SE							op
SM1062	N 39 E	54 SE							op
SM1063	N 43 E	57 SE							op
SM1064	N 41 E	62 SE							op
SM1065	N 37 E	65 NW							oss
SM1066	N 42 E	50 SE							oss
SM1067	N 26 W	41 NE							oss
SM1068	N 29 W	45 NE							oss
SM1069	N 31 E	57 SE							oss
SM1070	N 29 E	62 SE							oss
SM1071	N 20 W	40 NE							op
SM1072	N 27 E	45 SE							op
SM1073	N 27 E	41 SE							op
SM1074	N 31 E	48 SE							op
SM1075	N 35 E	60 SE							op
SM1076	N 28 E	51 SE							op
SM1077	N 25 E	49 SE							op
SM1078	N 21 W	38 NE							op
SM1079	N 33 E	44 SE							op
SM1080	N 37 E	51 SE							op
SM1081	N 29 E	41 NW							oss
SM1082	N 33 E	49 SE							oss
SM1083	N 38 E	47 SE							oss
SM1084	N 34 E	46 SE							oss
SM1085	N 39 E	57 SE							oss
SM1086	N 41 E	62 SE							op
SM1087	N 42 E	60 NW							op
SM1088	N 37 E	61 NW							op
SM1089	N 30 E	57 NW							op
SM1090	N 40 E	62 NW							op
SM1091	N 35 E	51 SE							op
SM1092	N 42 E	57 SE							op
SM1093	N 39 E	48 SE							op
SM1094	N 36 E	52 SE							op
SM1095	N 40 E	61 NW							op
SM1096	N 38 E	50 SE							op
SM1097	N 35 W	62 NE							op
SM1098	N 36 E	52 SE							op
SM1099	N 45 E	67 SE							op
SM1100	N 31 E	57 SE							op
SM1101	N 40 E	50 SE							op
SM1102	N 38 E	54 SE							oss
SM1103	N 36 E	50 SE							oss
SM1104	N 42 E	47 SE							oss
SM1105	N 39 E	53 SE							oss
SM1106	N 33 E	49 SE							oss
SM1107	N 37 E	57 SE							op
SM1108	N 43 E	62 NW							op
SM1109	N 40 E	60 NW							op
SM1110	N 36 E	59 SE							op
SM1111	N 41 E	55 SE							op
SM1112	N 30 E	53 NW							op
SM1113	N 35 E	60 SE							op

Station	Foliation		Feldspar Lineation		Fold Axis		Axial Surface		Lithologic Unit
	Strike	Dip	Plunge	Trend	Plunge	Trend	Strike	Dip	
SM1114	N 27 W	67 NE							op
SM1115	N 25 W	64 NE							op
SM1116	N 39 E	61 SE							op
SM1117	N 37 E	58 SE							op
SM1118	N 37 E	60 SE							op
SM1119	N 39 E	57 NW							op
SM1120	N 45 E	61 SE							op
SM1121	N 32 E	57 SE							op
SM1122	N 43 E	50 SE							op
SM1123	N 36 E	54 SE							op
SM1124	N 41 E	67 SE							op
SM1125	N 38 E	47 SE							op
SM1126	N 43 E	39 SE							op
SM1127	N 30 E	47 SE							op
SM1128	N 28 E	36 SE							op
SM1129	N 33 E	46 SE							op
SM1130	N 36 E	52 SE							op
SM1131	N 35 E	56 SE							op
SM1132	N 31 E	50 SE							op
SM1133	N 40 E	61 SE							op
SM1134	N 42 E	56 SE							op
SM1135	N 39 E	50 NW							oss
SM1136	N 36 E	49 NW							oss
SM1137	N 38 E	52 SE							oss
SM1138	N 45 E	60 SE							oss
SM1139	N 36 E	51 SE							oss
SM1140	N 40 E	49 SE							oss
SM1141	N 37 E	60 SE							oss
SM1142	N 44 E	57 SE							oss
SM1143	N 27 W	42 NE							op
SM1144	N 30 W	45 NE							op
SM1145	N 36 E	52 SE							op
SM1146	N 40 E	51 SE							oss
SM1147	N 38 E	60 SE							oss
SM1148	N 29 W	67 NE							oss
SM1149	N 34 W	65 NE							oss
SM1150	N 41 E	57 SE							oss
SM1151	N 39 E	44 SE							oss
SM1152	N 41 E	50 SE							oss
SM1153	N 27 W	49 NE							oss
SM1154	N 39 E	54 SE							op
SM1155	N 42 E	60 SE							op
SM1156	N 40 E	54 SE							op
SM1157	N 30 W	38 NE							op
SM1158	N 38 E	42 SE							op
SM1159	N 42 E	51 SE							op
SM1160	N 30 E	61 NW							op
SM1161	N 37 E	60 NW							op
SM1162	N 31 E	59 NW							op
SM1163	N 40 E	60 SE							oss
SM1164	N 49 E	70 SE							oss
SM1165	N 39 E	54 SE							oss
SM1166	N 45 E	60 SE							oss
SM1167	N 55 E	64 NW							oss
SM1168	N 45 E	60 NW							op
SM1169	N 49 E	65 NW							oss
SM1170	N 41 E	59 SE							oss
SM1171	N 44 E	49 SE							oss
SM1172	N 39 E	48 SE							op
SM1173	N 45 E	50 SE							op
SM1174	N 34 E	46 SE							op
SM1175	N 31 W	49 NE							op

Station	Foliation		Feldspar Lineation		Fold Axis		Axial Surface		Lithologic Unit
	Strike	Dip	Plunge	Trend	Plunge	Trend	Strike	Dip	
SM1176	N 36 W	40 NE							op
SM1177	N 30 E	60 SE							op
SM1178	N 35 E	50 SE							oss
SM1179	N 39 E	57 SE							oss
SM1180	N 41 E	49 SE							oss
SM1181	N 35 E	45 SE							oss
SM1182	N 40 E	49 SE							oss
SM1183	N 36 E	52 SE							oss
SM1184	N 39 E	49 SE							oss
SM1185	N 45 E	55 SE							oss
SM1186	N 29 E	35 SE							rg
SM1187	N 33 E	39 SE							rg
SM1188	N 30 E	27 SE							rg
SM1189	N 41 E	33 SE							rg
SM1190	N 37 E	42 SE							rg
SM1191	N 40 E	31 SE							rg
SM1192	N 45 E	29 SE							rg
SM1193	N 27 W	37 NE							rg
SM1194	N 31 W	31 NE							rg
SM1195	N 40 W	39 NE							rg
SM1196	N 38 W	45 SW							rg
SM1197	N 25 W	31 SW							rg
SM1198	N 31 E	46 SE							rg
SM1199	N 39 E	57 SE							rg
SM1200	N 36 E	50 SE							rg
SM1201	N 43 E	61 SE							rg
SM1202	N 37 E	49 NW							tf
SM1203	N 31 E	27 SE							tf
SM1204	N 30 E	30 SE							tf
SM1205	N 19 W	41 NE							tf
SM1206	N 25 E	37 SE							tf
SM1207	N 35 E	32 SE							tf
SM1208	N 15 W	27 NE							tf
SM1209	N 20 W	24 NE							tf
SM1210	N 21 E	29 SE							tf
SM1211	N 27 E	65 NW							rg
SM1212	N 20 E	51 SE							rg
SM1213	N 24 E	56 SE							rg
SM1214	N 30 E	50 SE							rg
SM1215	N 20 W	31 NE							tf
SM1216	N 25 W	40 NE							tf
SM1217	N 35 E	40 SE							tf
SM1218	N 31 E	29 SE							tf
SM1219	N 27 E	50 SE							rg
SM1220	N 31 E	59 SE							rg
SM1221	N 30 E	50 SE							tf
SM1222	N 35 E	47 SE							tf
SM1223	N 27 E	38 SE							tf
SM1224	N 33 E	37 SE							tf
SM1225	N 20 W	35 NE							tf
SM1226	N 31 E	42 NW							tf
SM1227	N 41 E	47 SE							tf
SM1228	N 38 E	45 SE							tf
SM1229	N 25 W	51 NE							tf
SM1230	N 39 E	49 NW							tf
SM1231	N 36 E	40 SE							tf
SM1232	N 27 E	45 SE							tf
SM1233	N 31 E	59 SE							rg
SM1234	N 27 E	42 SE							rg
SM1235	N 26 W	40 NE							rg
SM1236	N 29 W	45 NE							rg
SM1237	N 30 E	49 SE							rg



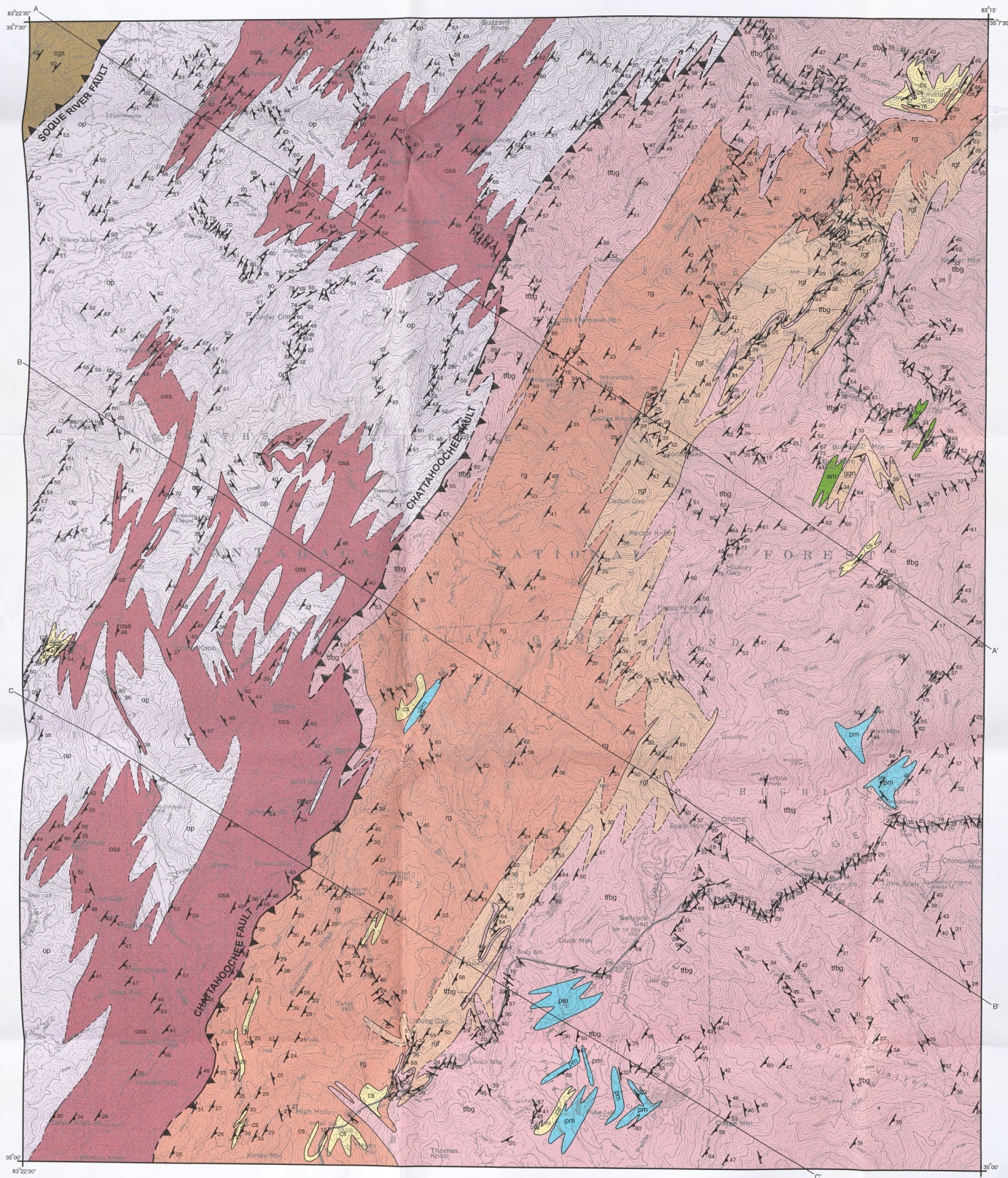
Station	Foliation		Feldspar Lineation		Fold Axis		Axial Surface		Lithologic Unit
	Strike	Dip	Plunge	Trend	Plunge	Trend	Strike	Dip	
SM1238	N 34 E	40 SE							rg
SM1239	N 31 E	38 SE							rg
SM1240	N 32 E	50 SE							rg
SM1241	N 27 E	53 SE							rg
SM1242	N 36 E	43 SE							rg
SM1243	N 29 W	40 NE							rg
SM1244	N 31 E	46 SE							rg
SM1245	N 35 E	40 SE							rg
SM1246	N 38 E	50 SE							tf
SM1247	N 21 E	37 NW							tf
SM1248	N 29 E	47 NW							tf
SM1249	N 34 E	57 SE							tf
SM1250	N 20 E	51 SE							op
SM1251	N 15 W	60 NE							op
SM1252	N 24 W	65 NE							op
SM1253	N 30 E	61 SE							op
SM1254	N 32 E	55 SE							op
SM1255	N 36 E	51 SE							op
SM1256	N 30 E	52 SE							op
SM1257	N 25 W	43 SW							op
SM1258	N 21 W	40 SW							op
SM1259	N 15 W	37 SW							op
SM1260	N 29 E	35 NW							op
SM1261	N 30 E	49 SE							op
SM1262	N 27 E	51 SE							op
SM1263	N 34 E	50 SE							op
SM1264	N 38 E	64 NW							op
SM1265	N 25 W	70 NE							op
SM1266	N 20 W	31 SW							op
SM1267	N 33 E	42 NW							op
SM1268	N 29 E	57 SE							op
SM1269	N 31 E	50 SE							op
SM1270	N 35 E	57 SE							op
SM1271	N 28 E	51 SE							op
SM1272	N 20 W	42 NE							op
SM1273	N 21 W	36 NE							op
SM1274	N 17 W	41 NE							op
SM1275	N 27 E	51 SE							op
SM1276	N 35 E	47 NW							op
SM1277	N 30 E	57 SE							op
SM1278	N 31 E	60 SE							op
SM1279	N 37 E	53 SE							op
SM1280	N 31 E	52 SE							op
SM1281	N 29 E	50 SE							op
SM1282	N 27 E	42 NW							op
SM1283	N 35 E	50 SE							op
SM1284	N 31 E	45 SE							op
SM1285	N 37 E	50 NW							cr
SM1286	N 30 E	47 NW							cr
SM1287	N 31 E	57 SE							op
SM1288	N 39 E	51 SE							op
SM1289	N 35 E	60 SE							op
SM1290	N 30 E	54 SE							op
SM1291	N 37 E	50 SE							op
SM1292	N 27 E	61 SE							op
SM1293	N 33 E	43 SE							op
SM1294	N 20 W	51 NE							op
SM1295	N 29 E	57 SE							op
SM1296	N 26 W	50 NE							op
SM1297	N 37 E	51 SE							op
SM1298	N 31 E	60 SE							op
SM1299	N 36 E	50 SE							op

Station	Foliation		Feldspar Lineation		Fold Axis		Axial Surface		Lithologic Unit
	Strike	Dip	Plunge	Trend	Plunge	Trend	Strike	Dip	
SM1300	N 30 E	57 SE							op
SM1301	N 29 E	51 SE							oss
SM1302	N 35 E	55 SE							oss
SM1303	N 33 E	50 SE							oss
SM1304	N 31 E	57 SE							oss
SM1305	N 29 E	59 SE							oss
SM1306	N 34 E	61 SE							oss
SM1307	N 31 E	54 SE							op
SM1308	N 28 E	52 SE							op
SM1309	N 34 E	57 SE							op
SM1310	N 34 E	51 SE							op
SM1311	N 27 E	62 SE							op
SM1312	N 31 E	58 SE							op
SM1313	N 29 E	54 SE							tf
SM1314	N 31 E	61 SE							tf
SM1315	N 30 E	51 SE							tf
SM1316	N 35 E	50 SE							tf
SM1317	N 33 E	50 SE							tf
SM1318	N 37 E	67 SE							op
SM1319	N 34 E	61 SE							op
SM1320	N 30 E	65 SE							op
SM1321	N 36 E	68 SE							op
SM1322	N 33 E	61 SE							op
SM1323	N 35 E	64 SE							op
SM1324	N 39 E	59 SE							op
SM1325	N 31 E	64 SE							op
SM1326	N 36 E	69 SE							op
SM1327	N 34 E	63 SE							op
SM1328	N 29 E	58 SE							op
SM1329	N 32 E	66 SE							op
SM1330	N 38 E	61 SE							op
SM1331	N 34 E	54 SE							op
SM1332	N 35 E	58 SE							op
SM1333	N 32 E	55 SE							op

## VITA

Dwight D. Lamb was born in Princeton Kentucky but spent most of his youth on a small tobacco and cattle farm in Lyon County, Kentucky. As a boy Dwight developed an interest in the various rocks, minerals, and fossils that he found on the family farm. In June 1980, Dwight graduated from Lyon County High School and chose to attend college classes at Mississippi State University where he majored in biochemistry and chemical engineering. There, he also played basketball for MSU and worked in the biochemistry department through the University work-study program. Spring 1981, Dwight left MSU to return to work on the family farm. In 1984, Dwight decided to return to college at a location closer to his Kentucky home. June 1988, Dwight earned his Bachelor's degree in biology with a minor in geology from the University of Tennessee-Martin. One year later Dwight returned to UT-Martin where he earned a Bachelor's degree in geology. In the fall, 1992, Dwight entered the masters program in geological sciences at The University of Tennessee-Knoxville. There, he worked as a graduate teaching assistant and later as an intern at Hazardous Waste Remedial Action Programs. Following his internship, Dwight accepted a full time position for an environmental firm, which slowed his goal of obtaining a Masters degree. Dwight obtained his Masters degree in December 2001. Today, Dwight remains in Knoxville where he and his wife are expecting their second child.

# Plate 1: Geologic map and cross sections, Scaly Mountain 7.5 minute quadrangle, North Carolina



## MAP UNITS

OTTO FORMATION		COWEETA GROUP			
Middle or Late Proterozoic	op	Biotite-muscovite schist with minor metagraywackes	Middle or Late Proterozoic	cgs	Coleman River Formation -metasandstones
	oss	Metagraywacke with minor biotite-muscovite schist			
RABUN GRANODIORITE		TALLULAH FALLS FORMATION			
Middle or Late Proterozoic	rg	Megacrystic granodiorite	Middle or Late Proterozoic	ftbg	Biotite gneiss and metagraywackes
	rgf	Equigranular granodiorite			
Middle or Late Proterozoic	cs	Calc-silicate quartzite	Middle or Late Proterozoic	am	Amphibolite
	p	Pegmatite			
				cs	Calc-silicate quartzite
				p	Pegmatite

## DESCRIPTION OF ROCK UNITS

- OTTO FORMATION**
- op** BIOTITE-MUSCOVITE SCHIST - Pelitic schist with minor amounts of metagraywacke. Schist is light gray to dark gray/black (fresh) and fine- to coarse-grained containing muscovite, quartz, plagioclase, biotite, +/- garnet, +/- staurolite, +/- epidote/clinozoisite, +/- tourmaline, and +/- microcline with opaques (ilmenite & magnetite?) locally abundant. Locally abundant garnet and staurolite. Schistose outcrops weather tan to orange.
  - oss** METAGRAYWACKE - Metagraywacke with minor amounts of biotite-muscovite schist. Metagraywackes are light- to dark-gray and fine- to medium-grained containing quartz, plagioclase, microcline, biotite, and muscovite, +/- garnet, +/- epidote/clinozoisite, and +/- zircon. Metagraywackes are locally gneissic. Metagraywackes and schists are interlayered with thin layers of schist within metagraywacke.
- RABUN GRANODIORITE**
- rg** MEGACRYSTIC PHASE - Megacrystic granodiorite white to light gray, porphyritic and trachytic texture, containing plagioclase, microcline, quartz, and +/- biotite, muscovite, zircon, and calcite. Phenocrysts are microcline. Outcrops commonly display a magmatic flow foliation and an overprinting tectonic foliation.
  - rgf** EQUIGRANULAR PHASE - Medium-grained granodiorite, white to light gray, subhedral texture, containing plagioclase, microcline, quartz, and +/- biotite, muscovite, and calcite.
  - am** AMPHIBOLITE - Dark green to black, fine- to medium-grained, containing amphibole, plagioclase, quartz, biotite, and +/- hornblende, garnet, sphene, microcline, epidote/clinozoisite, and zircon.
  - pm** PEGMATITE - White to tan, coarse grained containing plagioclase, quartz, microcline, amphibole, hornblende, and +/- epidote/clinozoisite, sphene, garnet, and calcite.
- TALLULAH FALLS FORMATION**
- ftbg** BIOTITE GNEISS AND METAGRAYWACKE - Biotite gneiss and metagraywacke are medium to dark gray to black and fine to medium grained containing quartz, plagioclase, biotite, calcite, hornblende, and +/- microcline, garnet, epidote/clinozoisite, sphene, and zircon.
  - am** AMPHIBOLITE - Dark green to black, fine- to medium-grained, containing amphibole, plagioclase, quartz, biotite, and +/- hornblende, garnet, sphene, microcline, epidote/clinozoisite, and zircon.
  - cs** CALC-SILICATE QUARTZITE - Light green, fine-grained, containing amphibole, plagioclase, quartz, diopside, quartz, calcite, hornblende, and +/- plagioclase, microcline, sphene, garnet, and zircon.
  - pm** PEGMATITE - White to tan, coarse grained containing plagioclase, quartz, microcline, amphibole, hornblende, and +/- epidote/clinozoisite, sphene, garnet, and calcite.
- COLEMAN RIVER FORMATION**
- cgs** METASANDSTONES - Metasandstones are typically dark gray to black, fine to medium grained, and inequigranular containing quartz, feldspar (plagioclase?), biotite, and +/- garnet.

### STRUCTURAL FEATURES AND SYMBOLS

**CONTACTS**

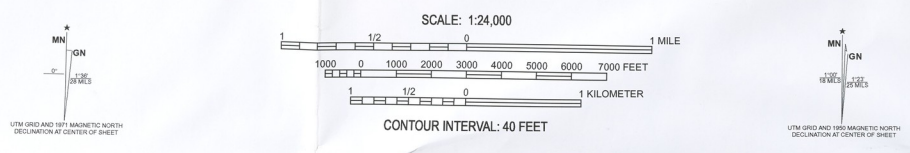
- Lithologic contact, dashed where approximately located, solid where exact.
- Thrust fault, dashed where approximately located, solid where exact. Teeth on hanging wall.

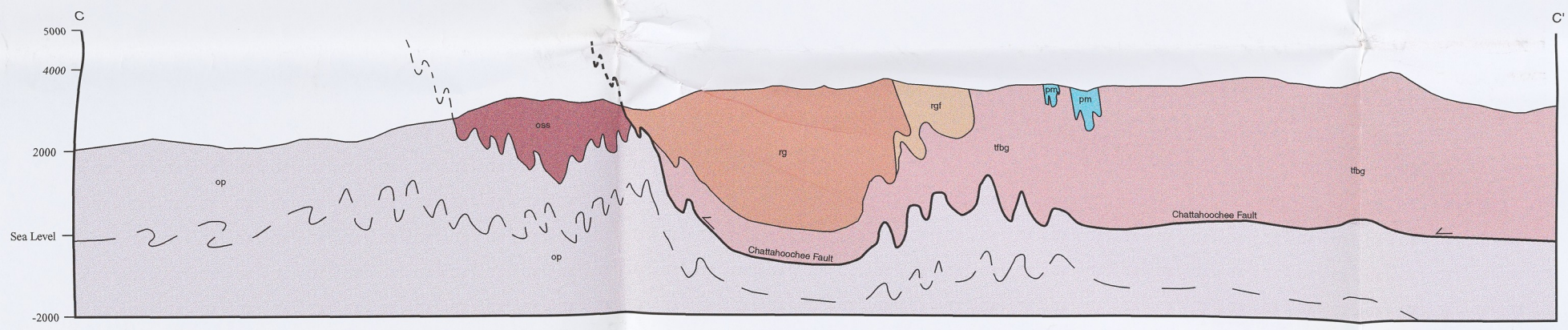
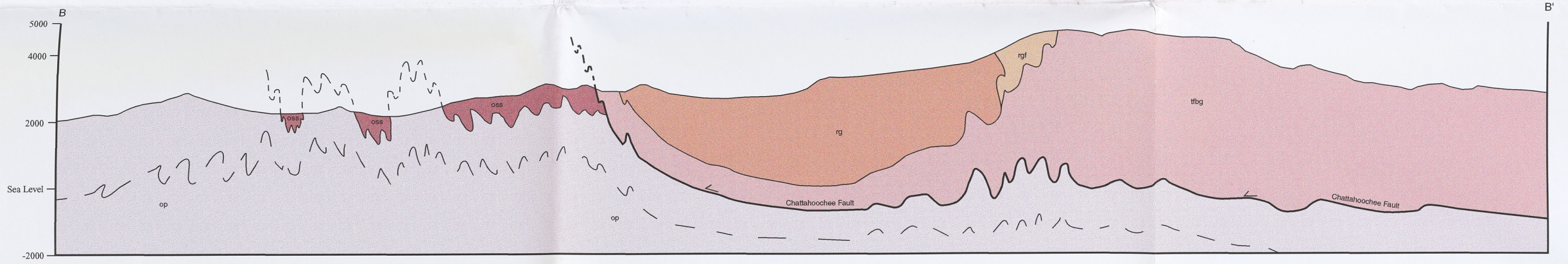
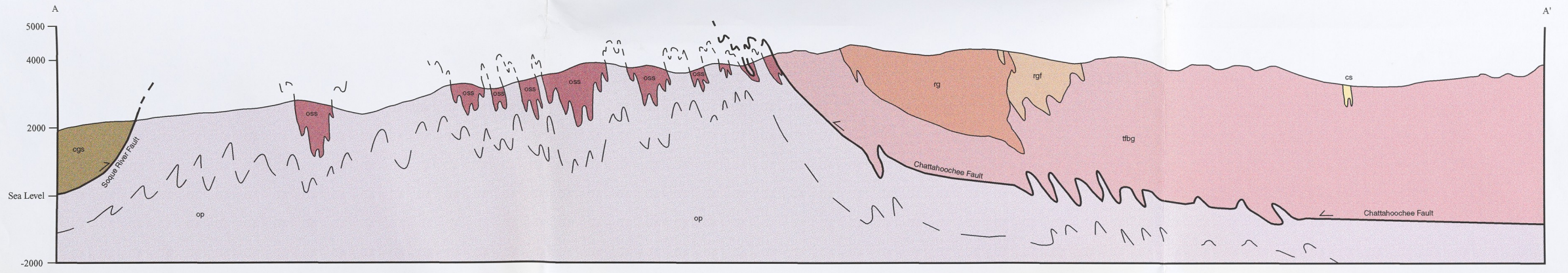
**PLANAR STRUCTURES**

- Strike and dip of foliation; inclined, vertical

**LINEAR STRUCTURES**

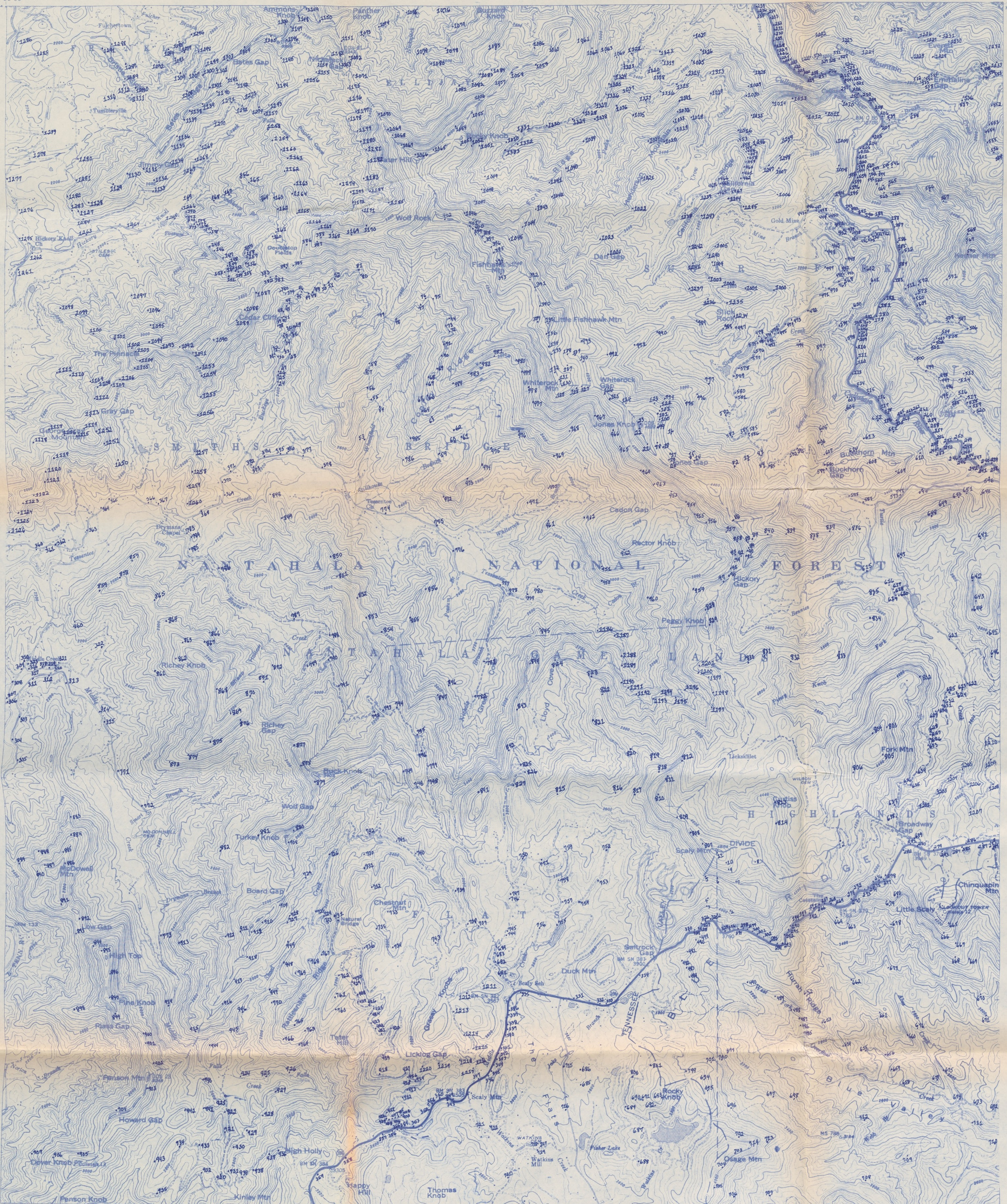
- Trend and plunge of mineral lineation



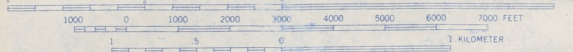


Thesis  
2001  
137

Plate 2  
Data Station Map,  
Scaly Mountain 7.5 Minute Quadrangle,  
North Carolina



SCALE 1:24 000



CONTOUR INTERVAL 40 FEET NATIONAL GEODETIC VERTICAL DATUM OF 1929

# Plate 3: Quaternary surficial deposits, Scaly Mountain 7.5 minute quadrangle, North Carolina



**MAP UNITS**

**SURFICIAL DEPOSITS**

Quaternary

- Qal Alluvium
- Qc Colluvium
- Qcal Alluvium and Colluvium, undivided

**DESCRIPTION OF UNITS**

**SURFICIAL DEPOSITS**

- Qal **ALLUVIUM** - Variably sorted deposits of clay, silt, sand, pebbles, cobbles, and boulders present in stream valleys.
- Qc **COLLUVIUM** - Hillslope deposits of unconsolidated clay, silt, sand, pebbles, cobbles, and boulders present in areas of high relief.
- Qcal **ALLUVIUM AND COLLUVIUM, UNDIVIDED** - Variably sorted deposits of clay, silt, sand, pebbles, cobbles, and boulders present on hillslopes and stream valleys.

SCALE: 1:24,000

MN  
GN  
1°20'  
28 MILES

UTM GRID AND 1971 MAGNETIC NORTH DECLINATION AT CENTER OF SHEET

1 1/2 0 1 MILE

1000 0 1000 2000 3000 4000 5000 6000 7000 FEET

1 1/2 0 1 KILOMETER

CONTOUR INTERVAL: 40 FEET

MN  
GN  
1°20'  
28 MILES

UTM GRID AND 1960 MAGNETIC NORTH DECLINATION AT CENTER OF SHEET